TUM–HEP–490/02
hep–ph/0403054
February 1, 2008

Systematic study of the impact of CP–violating phases of the MSSM on leptonic high–energy observables

Seong Youl Choi[1], Manuel Drees[2] and Benedikt Gaissmaier[2]

[1] *Department of Physics, Chonbuk National University, Chonju 561-756, Korea*
[2] *Physik Dept., TU München, James Franck Str., D–85748 Garching, Germany*

Abstract

Low-energy results from measurements of leptonic dipole moments are used to derive constraints on the CP–violating phases of the dimensionful parameters of the minimal supersymmetric extension of the standard model (MSSM). We use these (known) bounds to investigate the impact of these phases on CP–even cross sections at high–energy e^+e^- and e^-e^- colliders. To that end we define two measures of the significance with which the existence of non–vanishing phases could be deduced from the measurements of these cross sections. We find that highly significant evidence for deviations from the CP–conserving MSSM could be obtained at the next e^+e^- collider even if the electric dipole moment of the electron is very small or zero. We also analyze a CP–odd final state polarization, which can be large when two different charginos or neutralinos are produced. Finally, we study correlations between the phase–sensitive observables.

1 Introduction

CP violation was observed first in the neutral kaon system [1], and has recently been found in $B-$meson decays [2]. In addition, CP violation constitutes one of the conditions for a dynamical generation of the cosmological baryon asymmetry [3]. In the Standard Model (SM), which contains only one physical neutral Higgs boson and assumes neutrinos to be massless, the only source of CP violation is the complex phase of the quark mixing matrix [4].*

Supersymmetry (SUSY) is now widely regarded to be the most plausible extension of the SM; among other things, it stabilizes the gauge hierarchy [6] and allows the grand unification of all known gauge interactions [7]. Of course, supersymmetry most be (softly) broken to be phenomenologically viable. In general this introduces a large number of unknown parameters, many of which can be complex [8]. In the most general minimal supersymmetric standard model (MSSM) 44 phases cannot be removed by suitable redefinitions of fields and remain as "physical" phases in the model. For example, they have a direct impact on the mass spectra as they enter most mass matrices in the Lagrangian. Of course, one can use more specific assumptions on the soft breaking terms and/or an underlying GUT theory to get simpler versions of the MSSM with a smaller number of parameters, but the price for doing so is the loss of generality.

CP-violating phases associated with sfermions of the first and, to a lesser extent, second generation, and with the chargino/neutralino sector, are severely constrained by bounds on the electric dipole moments of the electron, neutron and muon. However, as emphasized in [9, 10, 11, 12] cancellations between different diagrams allow some combinations of these phases to be rather large even for a sfermion mass spectrum accessible at the expected center–of–mass energy of a possible next linear e^+e^- collider (LC). Even in models with universal boundary conditions for soft breaking mass at some very high energy scale, the relative phase between the supersymmetric Higgsino mass parameter μ and the universal trilinear soft breaking parameter A_0 can be $\mathcal{O}(1)$ [13]. If universality is not assumed, the relative phase between the $U(1)_Y$ and $SU(2)$ gaugino masses may also be large.

In the past few years a lot of effort has been devoted to analyses of the physics output that can be expected from experiments at the LC, including a possible e^-e^- option [14]. Work towards the design of such a device has also made great progress. Today it is assumed that it will (initially) have a center–of–mass energy $\sqrt{s}$ in the range between 500 GeV and 1 TeV, an integrated luminosity of at least several hundred fb^{-1}, and adjustable polarization for both beams. Detailed analyses [14, 15] have established that sparticles with mass $\lesssim \sqrt{s}/2$ can easily be discovered at an LC. Moreover, many of their properties (masses, spins, some couplings) can be measured precisely.

Unfortunately most of these analyses [15] show the dangerous tendency to neglect phases, which are actually free parameters of the model and are not necessarily negligibly small. Note

*The observation [5] of neutrino flavor oscillations opens the possibility that the neutrino mass matrix contains non–trivial CP–violating phases, but this has not yet been confirmed experimentally. In principle CP could also be violated in the SM by the QCD $\theta-$term, but bounds on the electric dipole moment of the neutron force $|\theta_{\rm QCD}|$ to be $\lesssim 10^{-10}$.

that both masses and couplings depend on these phases, which will hence have a direct impact on sparticle production cross sections and decays. Neglecting non-vanishing phases when determining real parameters from experimental data could thus lead to wrong inputs for attempts to reconstruct the underlying theory at the unification scale. On the other hand, the construction of sizable and experimentally accessible CP–violating observables is rather difficult in most of the production channels at e^+e^- colliders, as at least one secondary decay has to be included in the analysis. At the tree level nonzero CP–odd asymmetries can only result if the decaying particle has nonzero spin, which should be at least partly reconstructed from its decay products.

We therefore first perform a rather general analysis of the impact of non–vanishing CP–odd phases on CP–even cross sections. We work in the framework of the MSSM with non–vanishing CP phases. We assume flavor universality for soft breaking terms associated with sfermions of the first and second generation, but we do not assume any specific model for SUSY breaking. Our free parameters are specified at the typical energy scale of an LC. The basic idea of this work is to take today's low energy data, such as lower mass bounds and bounds on leptonic dipole moments (d_e and a_μ), as constraints for a parameter space scan. We then use the resulting, low energy compatible points to check whether high energy experiments at an LC (in either the e^+e^- or the e^-e^- mode) could provide additional information on phases. We restrict ourselves to the following total, unpolarized cross sections:

$$e^+e^- \to \tilde{\chi}_i^0 \tilde{\chi}_j^0 \qquad i,j = 1,\ldots,4; \tag{1.1a}$$

$$e^+e^- \to \tilde{\chi}_i^- \tilde{\chi}_j^+ \qquad i,j = 1,2; \tag{1.1b}$$

$$e^+e^- \to \tilde{e}_i^- \tilde{e}_j^+ \qquad i,j = 1,2; \tag{1.1c}$$

$$e^-e^- \to \tilde{e}_i^- \tilde{e}_j^- \qquad i,j = 1,2. \tag{1.1d}$$

There is a complementarity between the leptonic dipole operators and the high energy production amplitudes. Since several diagrams involving neutralinos as well as charginos contribute coherently to the low–energy observables, they can only give bounds on *combinations* of phases. In contrast, high energy observables can be used to investigate the different sectors of the theory separately. As our aim is to study the impact of low energy compatible, non–vanishing phases on the cross sections, we assign a significance $\mathcal{S}(f_1 f_2)$ to each final state, defined as difference in production rates between a CP–conserving point (CPC–point: real parameters, all phases identical to zero or π) in parameter space and a CP–violating point (CPV–point: same absolute values of parameters, but non–vanishing phases) normalized to the statistical error of the cross section in the CPC–point. Since the phase dependence of a given cross section might partly arise from kinematical effects (kinematical masses depend on the phases), we also introduce a second significance $\bar{\mathcal{S}}(f_1 f_2)$, where the CPV–point is chosen such that the masses of two neutralinos and one chargino coincide with the CPC–point; this can be achieved by adjusting the absolute values of the relevant dimensionful input parameters.

We find that these significances can be very large for some reactions of the types (1.1a) and (1.1d), but are usually small for (1.1b) once the low–energy constraints have been taken into account. Moreover, if the absolute values of the input parameters, or three chargino/neutralino masses, are kept fixed while the phases are varied randomly, there is no visible correlation

between these high–energy significances and d_e. On the other hand, in most cases sizable high–energy significances are strongly correlated with each other, and slightly less strongly correlated with a_μ.

Strictly speaking these significances only measure deviations from the CP–conserving version of the MSSM. These deviations might also be explained by some extension of the MSSM without invoking new sources of CP violation. If some deviation from the CP–conserving MSSM is observed, a more direct probe for CP violation in the production and decay of superparticles thus becomes important. We therefore compute the CP–odd polarization of charginos and neutralinos that is normal to the production plane, and find that in all cases considered, it can be sizable for neutralinos; a large CP–odd polarization of charginos is possible only at large $|\mu|$ and small $\tan\beta$. In contrast to earlier, related work [16, 17] we emphasize a detailed semi–analytical understanding of the observed effects; isolate the measurements that hold the most promise; and analyze the correlations between various phase sensitive observables.

The remainder of this paper is organized as follows. In Section 2 we briefly review the mass spectra and mixing patterns of the sleptons, charginos and neutralinos. This section also contains an overview of the relevant parameters. After summarizing the relevant parts of the MSSM Lagrangian in Section 3, we present in Section 4 the analytical expressions for the SUSY contributions to d_e and a_μ, and discuss briefly possible scenarios for suppressing these leptonic dipole moments while keeping some phases sizable. This Section also discusses numerical constraints on these phases in three benchmark scenarios where selectrons as well as the lighter neutralino and chargino eigenstates can be produced at a 500 GeV e^+e^- collider. Section 5 summarizes the well–known results for total cross sections of the production channels (1.1). We also give results for the components of polarization vectors for reactions (1.1a,b). The significances are introduced in Section 6. In Section 7 we show the most important results of our detailed numerical analysis of the high energy observables. Section 8 completes our work with a brief summary of our findings and some conclusions.

2 Particle mixing

2.1 Slepton mixing

As mentioned in the Introduction, we will assume that flavor mixing is negligible in the slepton sector. This can e.g. be motivated by the very tight experimental constraints on branching ratios for lepton flavor violating decays like $\mu \to e\gamma$, $\mu \to 3e$ etc. The simplest way to satisfy these bounds on flavor changing processes is to assume that soft SUSY breaking parameters in the slepton sector are the same for the first and second generation, as is the case in most models that attempt to describe SUSY breaking by a small number of parameters (which are usually defined at a high energy scale). The only relevant mixing in the slepton sector then occurs between $SU(2)$ doublet sleptons $\tilde{l}_L$ and singlets $\tilde{l}_R$. The squared mass matrix $\mathcal{M}^2_{\tilde{l}}$ in the

basis $(\tilde{l}_L, \tilde{l}_R)$ is given by [18]

$$\mathcal{M}^2_{\tilde{l}} = \begin{pmatrix} X_{\tilde{l}} & Z_{\tilde{l}} \\ Z^\star_{\tilde{l}} & Y_{\tilde{l}} \end{pmatrix}. \tag{2.1}$$

The elements of this matrix are defined as

$$X_{\tilde{l}} = m_l^2 + m^2_{\tilde{l}_L} + \frac{1}{2}\left(M_Z^2 - 2M_W^2\right)\cos 2\beta, \tag{2.2a}$$

$$Y_{\tilde{l}} = m_l^2 + m^2_{\tilde{l}_R} + \left(M_W^2 - M_Z^2\right)\cos 2\beta, \tag{2.2b}$$

$$|Z_{\tilde{l}}| = m_l |A_l^\star + \mu \tan\beta|, \tag{2.2c}$$

$$\arg(Z^\star_{\tilde{l}}) = \phi_{\tilde{l}} = \arg\left(-A_l - \mu^\star \tan\beta\right), \tag{2.2d}$$

where m_l is the mass of the charged lepton l, $m^2_{\tilde{l}_{L,R}}$ and A_l are soft SUSY breaking parameters, which we assume to be the same for the first and second generation, μ is the Higgsino mass parameter, and $\tan\beta$ is the ratio of vacuum expectation values (vevs) of the two neutral Higgs fields. In general, $\mu \equiv |\mu| e^{i\phi_\mu}$ and $A_l \equiv |A_l| e^{i\phi_A}$ can be complex, while all other parameters appearing in eqs.(2.2) are real.

$\mathcal{M}^2_{\tilde{l}}$ can be diagonalized by a unitary transformation

$$U^\dagger_{\tilde{l}} \mathcal{M}^2_{\tilde{l}} U_{\tilde{l}} = \mathrm{diag}\left(m^2_{\tilde{l}_1}, m^2_{\tilde{l}_2}\right), \tag{2.3}$$

with the mass ordering $m^2_{\tilde{l}_1} \leq m^2_{\tilde{l}_2}$ by convention. The diagonalization matrix $U_{\tilde{l}}$ can be parameterized as

$$U_{\tilde{l}} = \begin{pmatrix} \cos\theta_{\tilde{l}} & -\sin\theta_{\tilde{l}} e^{-i\phi_{\tilde{l}}} \\ \sin\theta_{\tilde{l}} e^{i\phi_{\tilde{l}}} & \cos\theta_{\tilde{l}} \end{pmatrix}, \tag{2.4}$$

where $-\pi/2 \leq \theta_{\tilde{l}} \leq \pi/2$ and $0 \leq \phi_{\tilde{l}} \leq 2\pi$. Defining

$$\bar{M}^2_{\tilde{l}} \equiv \frac{m^2_{\tilde{l}_2} + m^2_{\tilde{l}_1}}{2} = \frac{X_{\tilde{l}} + Y_{\tilde{l}}}{2}, \tag{2.5a}$$

$$\Delta_{\tilde{l}} \equiv m^2_{\tilde{l}_2} - m^2_{\tilde{l}_1} = \sqrt{(X_{\tilde{l}} - Y_{\tilde{l}})^2 + 4|Z_{\tilde{l}}|^2}, \tag{2.5b}$$

the slepton mass eigenvalues and mixing angles are given as

$$m^2_{\tilde{l}_{1,2}} = \bar{M}^2_{\tilde{l}} \mp \frac{\Delta_{\tilde{l}}}{2}; \tag{2.6a}$$

$$\sin 2\theta_{\tilde{l}} = -2\frac{|Z_{\tilde{l}}|}{\Delta_{\tilde{l}}}; \qquad \cos 2\theta_{\tilde{l}} = \frac{X_{\tilde{l}} - Y_{\tilde{l}}}{\Delta_{\tilde{l}}}. \tag{2.6b}$$

Eqs.(2.6b) and (2.2c) show that slepton left-right mixing is suppressed by the corresponding lepton mass, but is enhanced for large $\tan\beta$ and large $|\mu|$.

As sneutrinos are only present as components of left handed superfields in the MSSM, there is no partner to mix with and the mass simply reads

$$m^2_{\tilde{\nu}_l} = m^2_{\tilde{l}_L} + \frac{1}{2}\cos 2\beta M_Z^2. \tag{2.7}$$

2.2 Chargino mixing

The Dirac mass matrix for charginos mixes the $SU(2)$ gaugino $\tilde{w}^{\pm}$ and the charged Higgsinos $\tilde{h}^{\pm}$. In the basis $(\tilde{w}^{-}, \tilde{h}^{-})$ it is given by [18]

$$\mathcal{M}_C = \begin{pmatrix} M_2 & \sqrt{2} M_W \cos\beta \\ \sqrt{2} M_W \sin\beta & \mu \end{pmatrix}, \tag{2.8}$$

where the soft breaking mass parameter M_2 for $SU(2)$ gauginos is taken to be real and positive; this can be achieved without loss of generality by appropriate field redefinitions. This complex mass matrix is asymmetric and hence has to be diagonalized by a biunitary transformation

$$U_R \mathcal{M}_C U_L^{\dagger} = \mathrm{diag}\left(m_{\tilde{\chi}_1^{\pm}}, m_{\tilde{\chi}_2^{\pm}} \right), \tag{2.9}$$

with the mass ordering $m_{\tilde{\chi}_1^{\pm}} \leq m_{\tilde{\chi}_2^{\pm}}$ as convention. The mixing matrices may be written as [19]

$$U_L = \begin{pmatrix} \cos\phi_L & \sin\phi_L e^{-i\beta_L} \\ -\sin\phi_L e^{i\beta_L} & \cos\phi_L \end{pmatrix}, \tag{2.10a}$$

$$U_R = \begin{pmatrix} e^{i\gamma_1} & 0 \\ 0 & e^{i\gamma_2} \end{pmatrix} \begin{pmatrix} \cos\phi_R & \sin\phi_R e^{-i\beta_R} \\ -\sin\phi_R e^{i\beta_R} & \cos\phi_R \end{pmatrix}, \tag{2.10b}$$

with $-\pi/2 \leq \phi_{L,R} \leq \pi/2$ and $0 \leq \gamma_{1,2}, \beta_{L,R} \leq 2\pi$. γ_1 and γ_2 denote two possible Dirac phases which have to be introduced to ensure that the mass eigenvalues of $\mathcal{M}_C$ are positive and real. The parameters of U_L and U_R can be determined from $\mathcal{M}_C^{\dagger}\mathcal{M}_C$ and $\mathcal{M}_C\mathcal{M}_C^{\dagger}$, respectively. Introducing the quantity

$$\begin{aligned} \Delta_C &= \left\{ \left(M_2^2 - |\mu|^2 \right)^2 + 4M_W^4 \cos^2(2\beta) + 4M_W^2 \left(M_2^2 + |\mu|^2 \right) + 8M_W^2 |\mu| \cos\phi_\mu M_2 \sin 2\beta \right\}^{1/2} \\ &= m^2_{\tilde{\chi}_2^{\pm}} - m^2_{\tilde{\chi}_1^{\pm}}, \end{aligned} \tag{2.11}$$

the squared mass eigenvalues are:

$$m^2_{\tilde{\chi}_{1,2}^{\pm}} = \frac{1}{2} \left(M_2^2 + |\mu|^2 + 2M_W^2 \mp \Delta_C \right), \tag{2.12}$$

while the mixing angles can be computed from

$$\cos 2\phi_L = \frac{-M_2^2 + |\mu|^2 + 2M_W^2 \cos 2\beta}{\Delta_C}, \tag{2.13a}$$

$$\sin 2\phi_L = \frac{-2\sqrt{2} M_W}{\Delta_C} \left(M_2^2 \cos^2\beta + |\mu|^2 \sin^2\beta + M_2 |\mu| \cos\phi_\mu \sin 2\beta \right)^{1/2}, \tag{2.13b}$$

$$\cos 2\phi_R = \frac{-M_2^2 + |\mu|^2 - 2M_W^2 \cos 2\beta}{\Delta_C}, \tag{2.13c}$$

$$\sin 2\phi_R = \frac{-2\sqrt{2} M_W}{\Delta_C} \left(M_2^2 \sin^2\beta + |\mu|^2 \cos^2\beta + M_2 |\mu| \cos\phi_\mu \sin 2\beta \right)^{1/2}, \tag{2.13d}$$

and the phases are

$$\tan\beta_L = \frac{-|\mu|\sin\phi_\mu}{|\mu|\cos\phi_\mu + \cot\beta M_2}; \tag{2.14a}$$

$$\tan\beta_R = \frac{|\mu|\sin\phi_\mu}{|\mu|\cos\phi_\mu + \tan\beta M_2}; \tag{2.14b}$$

$$\cot\gamma_1 = \frac{M_W^2|\mu|\cos\phi_\mu \sin 2\beta + M_2\left(m^2_{\tilde{\chi}_1^\pm} - |\mu|^2\right)}{M_W^2|\mu|\sin\phi_\mu \sin 2\beta}; \tag{2.14c}$$

$$\cot\gamma_2 = -\frac{|\mu|\cos\phi_\mu\left(m^2_{\tilde{\chi}_2^\pm} - M_2^2\right) + M_W^2 M_2 \sin 2\beta}{|\mu|\sin\phi_\mu\left(m^2_{\tilde{\chi}_2^\pm} - M_2^2\right)}. \tag{2.14d}$$

2.3 Neutralino mixing

The neutralino mass matrix $\mathcal{M}_N$ mixes the neutral components of both Higgsinos $\tilde{h}^0_{u,d}$ with hypercharge $\pm 1/2$, the $U(1)_Y$ gaugino $\tilde{B}$ and the neutral $SU(2)$ gaugino $\tilde{W}_3$. The mass matrix in the basis $(\tilde{B}, \tilde{W}_3, \tilde{h}^0_d, \tilde{h}^0_u)$ reads [18]

$$\mathcal{M}_N = \begin{pmatrix} M_1 & 0 & -M_Z\cos\beta\sin\theta_W & M_Z\sin\beta\sin\theta_W \\ 0 & M_2 & M_Z\cos\beta\cos\theta_W & -M_Z\sin\beta\cos\theta_W \\ -M_Z\cos\beta\sin\theta_W & M_Z\cos\beta\cos\theta_W & 0 & -\mu \\ M_Z\sin\beta\sin\theta_W & -M_Z\sin\beta\cos\theta_W & -\mu & 0 \end{pmatrix}. \tag{2.15}$$

The $U(1)_Y$ gaugino mass parameter $M_1 \equiv |M_1|e^{i\phi_1}$ is in general complex. This symmetric mass matrix is diagonalized by a unitary transformation

$$N^T \mathcal{M}_N N = \mathrm{diag}(m_{\tilde{\chi}_1^0}, m_{\tilde{\chi}_2^0}, m_{\tilde{\chi}_3^0}, m_{\tilde{\chi}_4^0}), \tag{2.16}$$

i.e. the $n-$th mass eigenstate* is given by the complex conjugate of the $n-$th column of N. Although the neutralino mass matrix can be diagonalized analytically even for complex parameters [20], the general expressions are too lengthy to reproduce here. Of course, a numerical computation of N is straightforward. However, in order to qualitatively understand mixing in the neutralino sector, a perturbative diagonalization of the mass matrix (2.15) is often sufficient. Here M_Z is considered to be a small parameter compared to $|M_1|$, M_2 and $|\mu|$. Keeping all terms up to first order in M_Z, as well as a few $\mathcal{O}(M_Z^2)$ terms that will be important later, one finds for the masses and eigenvectors:

$$m_{\tilde{\chi}_1^0} \simeq |M_1| + \delta m_1, \;\; \tilde{\chi}_1^0 \simeq e^{i\phi_1/2}\left(1,\, \delta_{12},\, \delta_{13},\, \delta_{14}\right)/N_1; \tag{2.17a}$$

$$m_{\tilde{\chi}_2^0} \simeq M_2 + \delta m_2, \quad \tilde{\chi}_2^0 \simeq \left(\delta_{21},\, 1,\, \delta_{23},\, \delta_{24}\right)/N_2; \tag{2.17b}$$

*When written as a row vector $\tilde{\chi}_n^0$ in the $(\tilde{B}, \tilde{W}_3, \tilde{h}^0_d, \tilde{h}^0_u)$ basis, the mass eigenstate satisfies $\mathcal{M}_N(\tilde{\chi}_n^0)^\dagger = m_{\tilde{\chi}_n^0}(\tilde{\chi}_n^0)^T$ (no sum over n), i.e. it is not an eigenvector of $\mathcal{M}_N$ in the usual sense.

$$m_{\tilde{\chi}_3^0} \simeq |\mu|, \quad \tilde{\chi}_3^0 \simeq \frac{e^{i(\phi_\mu+\pi)/2}}{\sqrt{2}} \left(\delta_{31},\, \delta_{32},\, 1,\, 1\right); \tag{2.17c}$$

$$m_{\tilde{\chi}_4^0} \simeq |\mu|, \quad \tilde{\chi}_4^0 \simeq \frac{e^{i\phi_\mu/2}}{\sqrt{2}} \left(\delta_{41},\, \delta_{42},\, 1,\, -1\right). \tag{2.17d}$$

In eqs.(2.17) we have assumed the ordering $|M_1| < M_2 < |\mu|$. If these three mass parameters are ordered differently, the eigenstates in eqs.(2.17) are no longer labeled in order of increasing mass. Note that the eigenvalues do not receive $\mathcal{O}(M_Z)$ corrections. However, mixing between gauginos and Higgsinos is generated at this order, and $\tilde{B} - \tilde{W}_3$ mixing is generated at order M_Z^2. These mixings are described by the complex quantities δ_{ij} in eqs.(2.17); they are given by:

$$\delta_{12} = -\frac{M_Z^2 \sin\theta_W \cos\theta_W \left[|M_1|^2 + M_1^* M_2 + \sin(2\beta)\left(\mu^* M_1^* + M_2\mu\right)\right]}{\left(M_2^2 - |M_1|^2\right)\left(|\mu|^2 - |M_1|^2\right)}; \tag{2.18a}$$

$$\delta_{13} = \frac{M_Z \sin\theta_{\rm W}\left(M_1^* \cos\beta + \mu \sin\beta\right)}{|\mu|^2 - |M_1|^2}; \tag{2.18b}$$

$$\delta_{14} = -\frac{M_Z \sin\theta_{\rm W}\left(M_1^* \sin\beta + \mu \cos\beta\right)}{|\mu|^2 - |M_1|^2}; \tag{2.18c}$$

$$\delta_{21} = \frac{M_Z^2 \sin\theta_W \cos\theta_W \left[M_2^2 + M_1 M_2 + \sin(2\beta)\left(M_2\mu^* + M_1\mu\right)\right]}{\left(M_2^2 - |M_1|^2\right)\left(|\mu|^2 - M_2^2\right)}; \tag{2.18d}$$

$$\delta_{23} = -\frac{M_Z \cos\theta_{\rm W}\left(M_2 \cos\beta + \mu \sin\beta\right)}{|\mu|^2 - M_2^2}; \tag{2.18e}$$

$$\delta_{24} = \frac{M_Z \cos\theta_{\rm W}\left(M_2 \sin\beta + \mu \cos\beta\right)}{|\mu|^2 - M_2^2}; \tag{2.18f}$$

$$\delta_{31} = \frac{M_Z \sin\theta_{\rm W}(\sin\beta - \cos\beta)}{\left(|\mu|^2 - |M_1|^2\right)}\left(M_1 - \mu^*\right); \tag{2.18g}$$

$$\delta_{32} = \frac{M_Z \cos\theta_{\rm W}(\sin\beta - \cos\beta)}{\left(|\mu|^2 - M_2^2\right)}\left(\mu^* - M_2\right); \tag{2.18h}$$

$$\delta_{41} = -\frac{M_Z \sin\theta_{\rm W}(\sin\beta + \cos\beta)}{\left(|\mu|^2 - |M_1|^2\right)}\left(M_1 + \mu^*\right); \tag{2.18i}$$

$$\delta_{42} = \frac{M_Z \cos\theta_{\rm W}(\sin\beta + \cos\beta)}{\left(|\mu|^2 - M_2^2\right)}\left(\mu^* + M_2\right). \tag{2.18j}$$

$N_1,\ N_2$ in eqs.(2.17a,b) are normalization constants, which differ from unity at $\mathcal{O}(M_Z^2)$. Note that the phases of the 0−th order eigenstates have been factored out in eqs.(2.17); this gives more symmetric looking expressions for the δ_{ij}. Finally, the $\mathcal{O}(M_Z^2)$ mass shifts of the gaugino–like states are given by

$$\delta m_1 = -\frac{M_Z^2 \sin^2\theta_W}{|\mu|^2 - |M_1|^2}\left[|M_1| + |\mu| \sin 2\beta \cos(\phi_1 + \phi_\mu)\right]; \tag{2.19a}$$

$$\delta m_2 = -\frac{M_Z^2 \cos^2\theta_W}{|\mu|^2 - M_2^2}\left[M_2 + |\mu|\sin 2\beta\cos\phi_\mu\right]. \tag{2.19b}$$

Eqs.(2.18) and (2.19) show that the expansion will break down if $|\mu| - |M_1|$ or $|\mu| - M_2$ becomes close to M_Z in absolute value. In other words, even if the unknown dimensionful parameters in the mass matrix (2.15) are all $\gg M_Z$, there can still be strong Higgsino–gaugino mixing if some of these parameters have similar absolute values.

2.4 Relevant parameters

The mixing patterns in the part of the SUSY spectrum which will be relevant for the remainder of our work depend on 10 SUSY parameters (plus some SM parameters whose values are already known accurately). Some of these parameters ($m_{\tilde{l}_L},\ m_{\tilde{l}_R},\ |A_l|,\ \phi_A,\ |M_1|,\ \phi_1$) only enter in a single sector (sleptons and neutralinos, respectively), while M_2 appears in both the chargino and neutralino mass matrices, and $|\mu|,\ \phi_\mu$ and $\tan\beta$ affect all three sectors. Therefore the mixing patterns in the separate sectors are partly correlated to each other. In particular, choosing the parameters of the neutralino mass matrix completely determines the chargino mass matrix as well. Moreover, increasing $|\mu|$ suppresses gaugino–Higgsino mixing, but enhances $\tilde{l}_L - \tilde{l}_R$ mixing. Finally, taking $\tan\beta \gg 1$ again enhances $\tilde{l}_L - \tilde{l}_R$ mixing, but reduces the impact of all phases on the physical masses.

3 Interaction Lagrangian

In order to make our paper self–contained, and to fix the notation, this section is devoted to a short collection of the relevant pieces of the interaction Lagrangian expressed in terms of physical mass eigenstates.

3.1 Interactions involving SM gauge bosons

First of all, the well–known SM coupling between charged leptons and gauge bosons is given by

$$\mathcal{L}_{l\bar{l}\gamma,Z} = e\bar{l}\gamma^\mu\left(A_\mu Q_\gamma^{\alpha,l} P_\alpha + Z_\mu Q_Z^{\alpha,l} P_\alpha\right) l, \tag{3.1}$$

where e is the QED coupling constant, and $P_\alpha,\ \alpha \in \{+,-\} \equiv \{R,L\}$, are standard chirality projection operators, defined as

$$P_\pm = \frac{1 \pm \gamma_5}{2}. \tag{3.2}$$

The linear charges $Q_{\gamma,Z}^{\alpha,l}$ in eq.(3.1) are

$$Q_\gamma^{+,l} = Q_\gamma^{-,l} = 1; \tag{3.3a}$$

$$Q_Z^{-,l} = \frac{-1}{\sin\theta_{\rm W}\cos\theta_{\rm W}}\left(\sin^2\theta_{\rm W} - \frac{1}{2}\right); \tag{3.3b}$$

$$Q_Z^{+,l} = -\tan\theta_{\rm W}. \tag{3.3c}$$

Slepton $L-R$ mixing does not affect the couplings between sleptons and photons. Moreover, in case of selectrons $L-R$ mixing can safely be neglected for high–energy applications. The vertices with two charged sleptons and one gauge boson are defined via the momentum–space Lagrangian

$$\mathcal{L}_{\tilde{l}_i\tilde{l}_j\gamma,Z} = e\left(A_\mu Q_\gamma^{\tilde{l},ij} + Z_\mu Q_Z^{\tilde{l},ij}\right)(k_i+k_j)^\mu \tilde{l}_i(k_i)\tilde{l}_j(k_j)^\star, \tag{3.4}$$

where $i,j \in \{R,L\}$. The corresponding linear charges $Q_{\gamma,Z}^{\tilde{l},ij}$ are

$$Q_\gamma^{\tilde{l},ij} = \delta_{ij}; \tag{3.5a}$$

$$Q_Z^{\tilde{l},ij} = -\delta_{ij}\left[\tan\theta_{\rm W} - \frac{1}{2\cos\theta_{\rm W}\sin\theta_{\rm W}}\delta_{iL}\right]. \tag{3.5b}$$

The couplings between physical Majorana neutralinos and the Z boson are given by

$$\mathcal{L}_{\tilde{\chi}_i^0\tilde{\chi}_j^0 Z} = \frac{e}{2\cos\theta_{\rm W}\sin\theta_{\rm W}} Z_\mu \overline{\tilde{\chi}_i^0}\gamma^\mu Q_{\tilde{\chi}^0}^{\alpha,ij} P_\alpha \tilde{\chi}_j^0, \tag{3.6}$$

where the linear charges $Q_{\tilde{\chi}^0}^{\alpha,ij}$ are defined as

$$Q_{\tilde{\chi}^0}^{+,ij} = -(Q_{\tilde{\chi}^0}^{-,ij})^\star = \frac{1}{2}\left(N_{3i}N_{3j}^\star - N_{4i}N_{4j}^\star\right) \equiv Z_{ij}. \tag{3.7}$$

The first equality in eq.(3.7) follows from the Majorana nature of the neutralinos. Of course there is no neutralino–photon coupling.

Finally, the interactions between neutral gauge bosons and charginos are given by

$$\mathcal{L}_{\tilde{\chi}_i^\pm\tilde{\chi}_j^\mp\gamma,Z} = e\overline{\tilde{\chi}_i^-}\gamma^\mu\left(Q_{\tilde{\chi}^\pm,\gamma}^{\alpha,ij}P_\alpha A_\mu + Q_{\tilde{\chi}^\pm,Z}^{\alpha,ij}P_\alpha Z_\mu\right)\tilde{\chi}_j^-, \tag{3.8}$$

with

$$Q_{\tilde{\chi}^\pm,\gamma}^{-,ij} = Q_{\tilde{\chi}^\pm,\gamma}^{+,ij} = \delta_{ij}; \tag{3.9a}$$

$$Q_{\tilde{\chi}^\pm,Z}^{\pm,ij} = \frac{-1}{\cos\theta_{\rm W}\sin\theta_{\rm W}}\left(\sin^2\theta_{\rm W}\delta_{ij} - (W_\pm)_{ij}\right). \tag{3.9b}$$

The matrices $(W_\pm)_{ij}$ can be obtained from the chargino mixing matrices via

$$(W_\pm)_{ij} = (U_\pm)_{i1}(U_\pm)_{j1}^\star + \frac{1}{2}(U_\pm)_{i2}(U_\pm)_{j2}^\star \quad [+,-=R,L] \quad , \tag{3.10}$$

and read explicitly in terms of chargino mixing angles and phases as

$$(W_-) = \begin{pmatrix} \frac{3}{4}+\frac{1}{4}\cos 2\phi_L & -\frac{1}{4}\sin 2\phi_L e^{-i\beta_L} \\ -\frac{1}{4}\sin 2\phi_L e^{i\beta_L} & \frac{3}{4}-\frac{1}{4}\cos 2\phi_L \end{pmatrix}; \tag{3.11a}$$

$$(W_+) = \begin{pmatrix} \frac{3}{4}+\frac{1}{4}\cos 2\phi_R & -\frac{1}{4}\sin 2\phi_R e^{i(\gamma_1-\beta_R-\gamma_2)} \\ -\frac{1}{4}\sin 2\phi_R e^{-i(\gamma_1-\beta_R-\gamma_2)} & \frac{3}{4}-\frac{1}{4}\cos 2\phi_R \end{pmatrix}. \tag{3.11b}$$

3.2 Slepton interactions with a chargino or neutralino

The neutralino–slepton–lepton vertices receive contributions from both gauge and Yukawa interactions:

$$\mathcal{L}_{\tilde{l}l\tilde{\chi}_i^0} = \frac{e}{\sqrt{2}\sin\theta_{\rm W}} \bar{l}\left(G_{ij}^{\alpha} + Y_{ij}^{\alpha}\right) P_{\alpha} \tilde{\chi}_i^0 \tilde{l}_j + h.c., \tag{3.12}$$

with

$$G_{ij}^{-} = -2\tan\theta_{\rm W} N_{1i} (U_{\tilde{l}})_{2j}; \tag{3.13a}$$

$$G_{ij}^{+} = \left(\tan\theta_{\rm W} N_{1i}^{\star} + N_{2i}^{\star}\right) (U_{\tilde{l}})_{1j}; \tag{3.13b}$$

$$Y_{ij}^{-} = -\sqrt{2} Y_l N_{3i} (U_{\tilde{l}})_{1j}; \tag{3.13c}$$

$$Y_{ij}^{+} = -\sqrt{2} Y_l N_{3i}^{\star} (U_{\tilde{l}})_{2j}. \tag{3.13d}$$

Here the dimensionless, rescaled Yukawa coupling Y_l is given by

$$Y_l = \frac{m_l}{\sqrt{2} M_W \cos\beta}. \tag{3.14}$$

Note that we have to keep terms $\propto Y_l$, as well as a non–trivial sleptonic mixing matrix $U_{\tilde{l}}$, when computing leptonic dipole moments. On the other hand, for high–energy applications Y_e can be set to zero, which implies $Y_{ij}^{\pm} = 0$ in case of selectrons. In the same limit $L-R$ mixing can be neglected, in which case the gauge contributions $G_{ij}^{\pm}$ simplify to

$$G_{ij}^{-} = -2\tan\theta_{\rm W} N_{1i} \delta_{Rj}; \tag{3.15a}$$

$$G_{ij}^{+} = \left(\tan\theta_{\rm W} N_{1i}^{\star} + N_{2i}^{\star}\right) \delta_{Lj}. \tag{3.15b}$$

The couplings between chargino, sneutrino and lepton also receive gauge and Yukawa contributions:

$$\mathcal{L}_{\tilde{\nu}_l l \tilde{\chi}_i^{\pm}} = \frac{e}{\sin\theta_{\rm W}} \overline{\tilde{\chi}_i^{-}} N_{\alpha,i} P^{\alpha} l \tilde{\nu}_l^{\star} + h.c.; \tag{3.16}$$

where

$$N_{\alpha,i} = -\delta_{\alpha L} (U_R)_{i1} + \delta_{\alpha R} (U_L)_{i2} Y_l. \tag{3.17}$$

As before, the term $\propto Y_e$ in eq.(3.17) can be dropped in collider physics applications, but it has to be kept when computing the leptonic dipole moments.

4 Low energy constraints

4.1 Experimental constraints

In this paper we are only interested in purely leptonic processes. We therefore ignore the (quite stringent) experimental constraints on the electric dipole moments of the neutron and mercury atom. The main reason for this choice is that leptonic processes suffer much less

from uncertainties due to non–perturbative strong interactions. For example, ref.[21] finds that different models relating electric dipole moments of quarks to that of the neutron or Hg atom differ by typically a factor of two. Since large phases in the hadronic sector can be tolerated if there are cancellations between different contributions, which have different hadronic matrix elements, a conservative interpretation of the experimental bounds on d_n tends to give [11] significantly weaker constraints on model parameters than the bound on the electric dipole moment of the electron does, even if one assumes some connection between the CP–violating phases in the squark and slepton sectors. The only CP–violating (more exactly, T–violating) low–energy quantity of relevance to us is therefore the electric dipole moment of the electron d_e. Given our assumption of flavor universality of the soft breaking terms in the slepton sector, at least as far as the first and second generation are concerned, the bound on the electric dipole moment of the muon [22] need not be considered separately: since $(d_l)_{\rm SUSY} \propto m_l$, all combinations of parameters that satisfy the constraint on the SUSY contribution to d_e will be at least five orders of magnitude below the maximal allowed SUSY contribution to d_μ.

On the other hand, our assumption of universal sleptonic soft breaking terms for the first two generations also implies [23] that the measurement [24] of the anomalous magnetic moment of the muon, $a_\mu \equiv (g_\mu - 2)/2$, gives a *tighter* constraint on SUSY parameters than the anomalous magnetic moment of the electron does. The reason is that for universal soft breaking masses the SUSY contribution to these leptonic magnetic moments is essentially proportional to the squared mass of the lepton, and the experimental errors satisfy [22, 24] $\delta a_\mu/m_\mu^2 < \delta a_e/m_e^2$. The second low–energy quantity of relevance to us is therefore a_μ. Note that the SUSY contributions to a_μ and d_e show very similar dependences on the absolute values of the relevant parameters; however, d_e receives nonvanishing contributions only in the presence of nontrivial phases, while the contribution to $|a_\mu|$ becomes maximal if all phases are zero or π.

The SM prediction for d_e is negligible. The current experimental measurement [22]

$$(d_e)_{\rm exp} = (0.069 \pm 0.074) \times 10^{-26}\ e \cdot {\rm cm} \tag{4.1}$$

can therefore directly be translated into a 2σ range for the supersymmetric contribution to d_e:

$$-0.079 \times 10^{-26}\ e \cdot {\rm cm} \leq (d_e)_{\rm SUSY} \leq 0.217 \times 10^{-26}\ e \cdot {\rm cm}. \tag{4.2}$$

The interpretation of the most recent measurement [24] of a_μ,

$$(a_\mu)_{\rm exp} = (11659208 \pm 6) \times 10^{-10}, \tag{4.3}$$

is less clear. The reason is that non–perturbative hadronic terms do contribute to a_μ, at about the 10^{-8} level. In principle this contribution can be calculated from experimental data using dispersion relations [25, 26]. Unfortunately calculations based on different data do not quite agree, although the discrepancy has become smaller after the recent release of corrected data by the CMD–2 collaboration [27]. Using e^+e^- annihilation data as input tends to give an SM prediction which falls a little short of the experimental value (4.3). A recent analysis which includes all existing e^+e^- data [28] finds

$$(a_\mu)_{\rm SM} = (11659180.9 \pm 8.0) \times 10^{-10}. \tag{4.4}$$

Adding all errors in quadrature, this gives a $\sim 2.7\sigma$ discrepancy. On the other hand, using data from τ decays gives [28]

$$(a_\mu)_{\rm SM} = (11659195.6 \pm 6.8) \times 10^{-10}, \tag{4.5}$$

which is only $\sim 1.4\sigma$ below the measurement (4.3). Since even the e^+e^- data lead to a less than 3σ discrepancy between the prediction for and measurement of a_μ, we do not want to claim evidence for a non–vanishing SUSY contribution. In order to be conservative, we construct the upper limit of the "2σ allowed" range for $(a_\mu)_{\rm SUSY} = (a_\mu)_{\rm exp} - (a_\mu)_{\rm SM}$ by using the lower value (4.4), reduced by two combined standard deviations, as our estimate of $(a_\mu)_{\rm SM}$. Similarly, the lower end of this "2σ range" is obtained when $(a_\mu)_{\rm SM}$ is estimated by adding two standard deviations to the higher value (4.5). This gives:

$$-5.7 \times 10^{-10} \leq (a_\mu)_{\rm SUSY} \leq 47.1 \times 10^{-10}. \tag{4.6}$$

The upper bound in (4.6) constrains the SUSY parameter space only for large values of $\tan\beta$, but the lower bound is significant also for moderate $\tan\beta$.

4.2 Analytical results

Figure 1: SUSY contributions to leptonic dipole operators

The supersymmetric one–loop contributions to lepton dipole moments are shown in Fig. 1. The left diagram depicts the neutralino contribution while the right one contains the chargino contribution. Using the interaction Lagrangians given in Section 3 we find for the chargino contribution to the electric dipole moment of the electron

$$\left(\frac{d_e}{e}\right)^{\tilde{\chi}^\pm}_{\rm SUSY} = \frac{1}{96\pi^2} \sum_{i=1}^{2} \frac{2}{m_{\tilde{\chi}_i^\pm}} f_1(x_i) \Im{\rm m}(c_{Li}^\star c_{Ri}). \tag{4.7}$$

The chargino loop contribution to the magnetic dipole moment of the muon is

$$(a_\mu)^{\tilde{\chi}^\pm}_{\rm SUSY} = \frac{1}{192\pi^2} \sum_{i=1}^{2} \left\{ \frac{8 m_\mu}{m_{\tilde{\chi}_i^\pm}} f_1(x_i) \Re{\rm e}(c_{Li} c_{Ri}^\star) + \frac{m_\mu^2}{m^2_{\tilde{\chi}_i^\pm}} f_3(x_i) (|c_{Li}|^2 + |c_{Ri}|^2) \right\}. \tag{4.8}$$

The corresponding results for the neutralino contribution read

$$\left(\frac{d_e}{e}\right)^{\tilde{\chi}^0}_{\rm SUSY} = \frac{-1}{96\pi^2}\sum_{i=1}^{4}\sum_{\alpha=1}^{2}\frac{1}{m_{\tilde{\chi}_i^0}} f_2(y_{i\alpha})\Im{\rm m}(n^\star_{Li\alpha}n_{Ri\alpha}); \tag{4.9}$$

$$(a_\mu)^{\tilde{\chi}^0}_{\rm SUSY} = \frac{-1}{192\pi^2}\sum_{i=1}^{4}\sum_{\alpha=1}^{2}\left\{\frac{4m_\mu}{m_{\tilde{\chi}_i^0}} f_2(y_{i\alpha})\Re{\rm e}(n^\star_{Li\alpha}n_{Ri\alpha}) + \frac{m_\mu^2}{m^2_{\tilde{e}_\alpha}} f_3(y_{i\alpha})(|n_{Li\alpha}|^2+|n_{Ri\alpha}|^2)\right\}. \tag{4.10}$$

The variables x_i and $y_{i\alpha}$ are defined as

$$x_i = \frac{m^2_{\tilde{\chi}_i^\pm}}{m^2_{\tilde{\nu}}}, \qquad y_{i\alpha} = \frac{m^2_{\tilde{l}_\alpha}}{m^2_{\tilde{\chi}_i^0}}, \tag{4.11}$$

and the loop functions f_i are

$$f_1(z) = \frac{3z}{2(z-1)^3}(z^2-4z+3+2\log z)\,; \tag{4.12a}$$

$$f_2(z) = \frac{3}{(z-1)^3}(z^2-1-2z\log z)\,; \tag{4.12b}$$

$$f_3(z) = \frac{2z}{(z-1)^4}(z^3-6z^2+3z+2+6z\log z)\,. \tag{4.12c}$$

These functions are normalized such that $f_i(1)=1,\ i=1,2,3$. Finally the coupling coefficients c_{Ai} and $n_{Ai\alpha}$ can be written as:

$$c_{Li} = -\frac{e}{\sin\theta_{\rm W}}\,(U_R)_{i1}\,; \tag{4.13a}$$

$$c_{Ri} = \frac{e}{\sin\theta_{\rm W}} Y_l\,(U_L)_{i2}\,; \tag{4.13b}$$

$$n_{Li\alpha} = \frac{e}{\sqrt{2}\sin\theta_{\rm W}}\left[(N_{2i}+\tan\theta_{\rm W}N_{1i})\,(U_{\tilde{l}})^\star_{L\alpha} - \sqrt{2}Y_l N_{3i}\,(U_{\tilde{l}})^\star_{R\alpha}\right]; \tag{4.13c}$$

$$n_{Ri\alpha} = -\frac{e}{\sqrt{2}\sin\theta_{\rm W}}\left[2\tan\theta_{\rm W}N^\star_{1i}\,(U_{\tilde{l}})^\star_{R\alpha} + \sqrt{2}Y_l N^\star_{3i}\,(U_{\tilde{l}})^\star_{L\alpha}\right]. \tag{4.13d}$$

Our results agree with those of refs. [11],[29]; the neutralino contribution in ref.[12] seems to have some misprints.

The analytic expressions of Sec. 2.2 can be used to rewrite both chargino contributions in terms of the loop functions f_i and the basic SUSY parameters:

$$\left(\frac{d_e}{e}\right)^{\tilde{\chi}^\pm}_{\rm SUSY} = -\frac{m_e}{48\pi^2}\frac{e^2}{\sin^2\theta_{\rm W}}\frac{\tan\beta|\mu|M_2\sin\phi_\mu}{\Delta_C}\sum_{i=1}^{2}(-1)^i\frac{f_1(x_i)}{m^2_{\tilde{\chi}_i^\pm}}, \tag{4.14}$$

$$(a_\mu)^{\tilde\chi^\pm}_{\rm SUSY} = -\frac{m_\mu^2}{96\pi^2}\frac{e^2}{\sin^2\theta_{\rm W}}\left\{2\sum_{i=1}^2 \frac{f_1(x_i)}{m^2_{\tilde\chi_i^\pm}} - \frac{1}{4}(1+Y_\mu^2)\sum_{i=1}^2\frac{f_3(x_i)}{m^2_{\tilde\chi_i^\pm}}\right.$$
$$+\ 2\left[M_2^2+|\mu|^2+2\tan\beta M_2|\mu|\cos\phi_\mu + 2M_W^2\cos 2\beta\right]\sum_{i=1}^2\frac{(-1)^i f_1(x_i)}{\Delta_C m^2_{\tilde\chi_i^\pm}} \qquad (4.15)$$
$$\left.-\ \frac{1}{4}\left[(M_2^2-|\mu|^2)(1-Y_\mu^2)+2M_W^2\cos 2\beta(1+Y_\mu^2)\right]\sum_{i=1}^2\frac{(-1)^i f_3(x_i)}{\Delta_C m^2_{\tilde\chi_i^\pm}}\right\},$$

where Δ_C has been defined in eq.(2.11). Together with eqs.(4.12) these expressions explicitly show that the chargino contributions to the leptonic dipole moments decouple like $1/m^2_{\tilde\chi^\pm}$ for $m^2_{\tilde\chi^\pm} \gg m^2_{\tilde\nu}$, and like $1/m^2_{\tilde\nu}$ in the opposite limit $m^2_{\tilde\nu} \gg m^2_{\tilde\chi^\pm}$. For completeness we have included terms $\propto Y_\mu^2$, even though eq.(3.14) shows that $Y_\mu^2 \ll 1$; if these terms are neglected, $(a_\mu)^{\tilde\chi^\pm}_{\rm SUSY} \propto m_\mu^2$, as advertised earlier.

Analogous statements also hold for the neutralino contributions, but because of the more complicated nature of neutralino mixing we were not able to find simple exact analytic expressions for these contributions. However, with the help of eqs.(2.17) and (2.18) one can derive an approximate expression for the neutralino loop contribution to d_e:

$$\left(\frac{d_e}{e}\right)^{\tilde\chi^0}_{\rm SUSY} \simeq -\frac{e^2 m_e}{96\pi^2}\left\{\frac{|A_e^* + \mu\tan\beta|}{\cos^2\theta_W|M_1|}\cdot\frac{f_2(m^2_{\tilde e_R}/|M_1|^2)-f_2(m^2_{\tilde e_L}/|M_1|^2)}{m^2_{\tilde e_L}-m^2_{\tilde e_R}}\cdot\sin(\phi_1-\phi_{\tilde e})\right.$$
$$+\frac{\tan\beta\sin(\phi_\mu+\phi_1)}{\cos^2\theta_W|M_1\mu|\,(|\mu|^2-|M_1|^2)}\left[|\mu|^2\left(f_2(m^2_{\tilde e_R}/|M_1|^2)-\frac{f_2(m^2_{\tilde e_L}/|M_1|^2)}{2}\right)\right.$$
$$\left.-|M_1|^2\left(f_2(m^2_{\tilde e_R}/|\mu|^2)-\frac{f_2(m^2_{\tilde e_L}/|\mu|^2)}{2}\right)\right]$$
$$\left.+\frac{\tan\beta\sin\phi_\mu\left[|\mu|^2 f_2(m^2_{\tilde e_L}/M_2^2)-M_2^2 f_2(m^2_{\tilde e_L}/|\mu|^2)\right]}{2\sin^2\theta_W M_2|\mu|\,(|\mu|^2-M_2^2)}\right\}. \qquad (4.16)$$

In the first line of eq.(4.16) we have used an approximate treatment of selectron mixing, which is quite sufficient for the given purpose.* The last line in eq.(4.16), which involves the $SU(2)$ gauge interactions, has a very similar structure as the chargino loop contribution (4.14); however, the overall factor in front of the neutralino contribution is four times smaller than that of the chargino contribution. Note also that eq.(4.16) does not contain contributions $\propto \sin\phi_1$, which in our convention measures the relative phase between M_1 and M_2; only the phase of M_1 relative to either the phase $\phi_{\tilde e}$ in selectron mixing or to the phase of μ is relevant.

*The electric dipole moment is chirality violating and hence proportional to the Yukawa coupling. Therefore slepton mixing, which is proportional to the Yukawa coupling, cannot be neglected.

4.3 Numerical analysis

As well known [30, 31, 32, 11, 10], the experimental bound (4.1) on d_e provides stringent constraints on MSSM parameter space. For example, the chargino contribution (4.14) to d_e can be estimated to be

$$(d_e)^{\tilde{\chi}^\pm}_{\rm SUSY} \sim 3 \cdot 10^{-24} \cdot \tan\beta \sin\phi_\mu \cdot \left(\frac{100\,{\rm GeV}}{m_{\rm SUSY}}\right)^2 e \cdot {\rm cm}, \tag{4.17}$$

where $m_{\rm SUSY}$ stands for the relevant sparticle (sneutrino or chargino, whichever is heavier) mass scale. The chargino contribution by itself can therefore satisfy the experimental constraint (4.2) only for very small phase ϕ_μ and/or very large sparticle masses. For sparticle masses not much above 100 GeV, one would need phases of order 10^{-3} (10^{-2}) or less in the chargino (neutralino or slepton) mass matrices; if $\tan\beta \gg 1$, this constraint would become even stronger. Such small phases are unlikely to lead to measurable effects in high–energy collider experiments [16, 17]. Alternatively one can postulate that sparticle masses are very large [32]. Since gaugino masses are coupled to parameters in the Higgs sector via one–loop renormalization group equations, whereas a similar coupling between first generation sfermion masses and the Higgs sector only exists at two–loop level [33], naturalness arguments favor models with large slepton masses and relatively modest gaugino masses. The estimate (4.17) indicates that first generation slepton masses well above 1 TeV would be required if the relevant phases are $\mathcal{O}(1)$. In that case these sleptons would be beyond the reach of the next linear e^+e^- collider, which will have center–of–mass energy $\sqrt{s} \lesssim 1$ TeV. Moreover, since FCNC constraints would then also indicate very large masses for second generation sleptons (recall that we assume them to be exactly degenerate with the first generation), a possible excess in a_μ could not be accommodated within the MSSM.

We therefore focus on the third possibility for satisfying the constraint (4.2), where the different contributions to d_e largely cancel [10, 11]; that is, the neutralino contribution must cancel the chargino contribution. Here we quantitatively analyze this possibility for three scenarios; later we will analyze high–energy observables that are sensitive to phases within the same scenarios.

In all cases we assume that the ratio of M_2 and $|M_1|$ is similar to that in models with gaugino mass unification at the GUT scale, which predicts [33] $|M_1| \simeq 0.5 M_2$ at the weak scale. Similarly, we take values for the soft breaking masses of $SU(2)$ singlet and doublet sleptons that are consistent with the assumption of universal scalar masses at the GUT scale. Recall that we assume degenerate first and second generation soft breaking parameters in the slepton sector:

$$m_{\tilde{e}_L} = m_{\tilde{\mu}_L} \equiv m_{\tilde{l}_L}; \tag{4.18a}$$

$$m_{\tilde{e}_R} = m_{\tilde{\mu}_R} \equiv m_{\tilde{l}_R}; \tag{4.18b}$$

$$A_e = A_\mu \equiv A. \tag{4.18c}$$

The assumption of universal scalar masses at the GUT scale implies [33] that

$$m^2_{\tilde{l}_L} \simeq m^2_{\tilde{l}_R} + 0.46 M_2^2 \tag{4.19}$$

at the weak scale. Finally, we are interested in scenarios where at least $\tilde{l}_R$, $\tilde{l}_L$, $\tilde{\chi}_1^\pm$ and $\tilde{\chi}_2^0$ can be pair–produced at a "first stage" linear collider operating at $\sqrt{s} = 500$ GeV.

This leads us to consider three different scenarios, which we call B1, B2 and B3. Scenario B1 has $|\mu| = M_2$, i.e. is characterized by strong mixing between $SU(2)$ gauginos and Higgsinos; this will occur in both the chargino and neutralino sector. Contrariwise, B2 has $|\mu|^2 \gg M_2^2$, i.e. all Higgsino–gaugino mixing is suppressed. In these two cases we take a relatively large value of $|A|$, which enhances slepton $L - R$ mixing for small $\tan\beta$; we will see shortly that this increases the possibility of cancellations between the chargino and neutralino contributions to d_e. On the other hand, $\tilde{e}_L - \tilde{e}_R$ mixing, while important for the calculation of d_e, in all cases remains negligible as far as selectron production at high energies is concerned. Case B3, which is almost[†] identical to the much–studied Snowmass "benchmark point SPS1A" [34], has intermediate gaugino–Higgsino mixing, as well as slightly reduced slepton masses. In all three cases we take four different values of $\tan\beta$. Moreover, we allow the three relevant phases ϕ_1, ϕ_μ and ϕ_A to float freely, i.e. we pick random values for these phases. (Recall that we work in a phase convention where M_2 is real and positive.) These three scenarios are summarized in Table 1. Of course, we respect all relevant limits from direct searches for superparticles at colliders, in particular at LEP2 [22].

	$\lvert M_1\rvert$	M_2	$m_{\tilde{l}_L}$	$m_{\tilde{l}_R}$	$\lvert A\rvert$	$\lvert\mu\rvert$	$\tan\beta$	ϕ_1, ϕ_μ, ϕ_A
B1	100	200	235	180	500	200	3, 6,9, 12	$\in [-\pi, \pi]$
B2	100	200	235	180	500	500	3, 6, 9, 12	$\in [-\pi, \pi]$
B3	102.2	191.8	198.7	138.2	255.5	343.2	5, 10, 15, 20	$\in [-\pi, \pi]$

Table 1: The three scenarios studied in this paper. All dimensionful parameters are in GeV.

For simplicity and limited space of representation we only show results for two choices of $\tan\beta = 3$ or 12 in scenarios B1 and B2, and for $\tan\beta = 10$ or 20 in case B3. Results for the other cases are qualitatively similar and can be obtained by extrapolation from these extreme cases. Note that the numerical results shown below are projections of a three–dimensional parameter space onto two–dimensional planes. Hence it should be kept in mind that each correlation in the $\phi_x - \phi_y$ plane has been obtained by scanning over the entire allowed range for ϕ_z. By far the strongest restriction on parameter space comes from d_e: at least 99.4% of all randomly chosen points in a given run violate the constraint (4.2); the success rate at large $\tan\beta$ is even smaller.[*] In the following we will quote upper bounds on $|\phi_\mu|$ that result from the constraint (4.2). A similar band around $\phi_\mu = \pi$ exists for small $\tan\beta$ and large $|\mu|$.

Fig. 2 shows allowed combinations of the phases ϕ_μ and ϕ_1. We observe very strong constraints on ϕ_μ in scenario B1, which become stronger as $\tan\beta$ increases. Scenario B2 allows

[†]The agreement becomes exact for the "benchmark value" $\tan\beta = 10$ and vanishing phases.

[*]This indicates that rather severe fine-tuning is required [17] to obtain the necessary cancellations if all phases are indeed independent quantities. To put it differently, one faces the challenge to construct models that "naturally" explain the required correlations between these phases. We will not attempt to do this here.

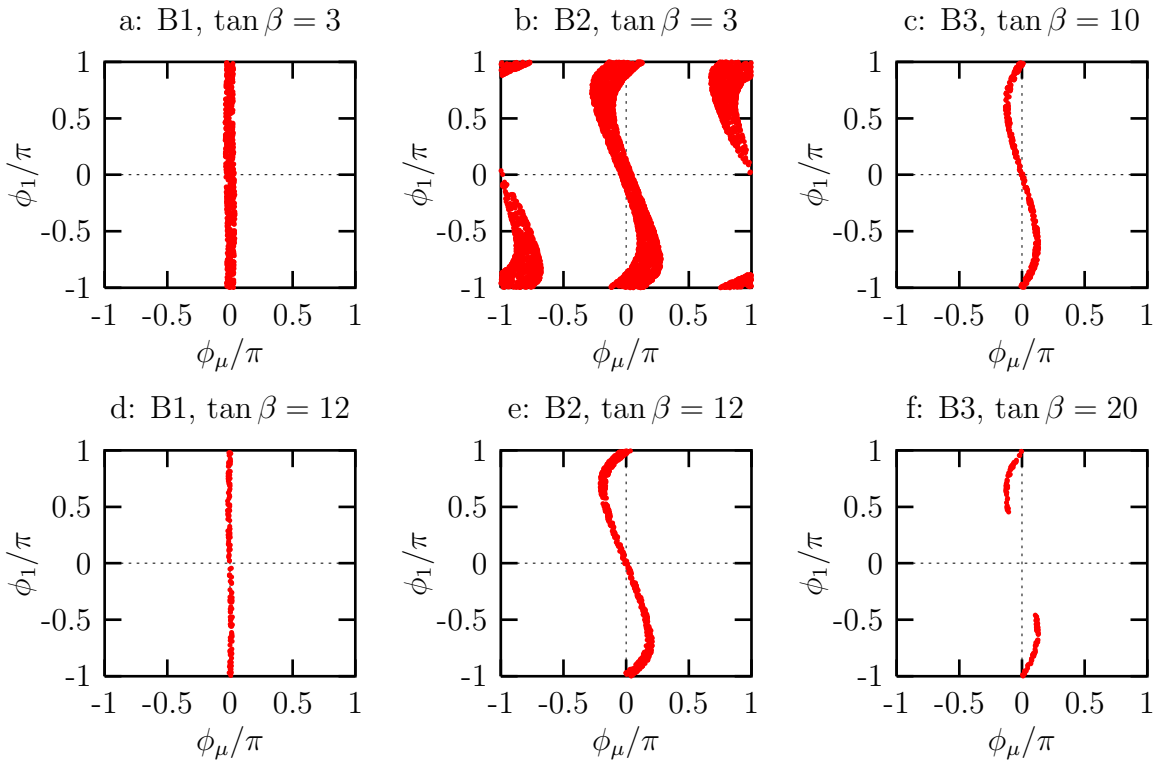

Figure 2: Combinations of ϕ_μ and ϕ_1 that are allowed for at least one $\phi_A \in [-\pi, \pi]$.

much larger values of $|\phi_\mu|$, which moreover do not decrease much with increasing $\tan\beta$, while scenario B3 is intermediate between these two. This behavior can be understood from eqs.(4.14) and (4.16). We saw that the contributions involving $SU(2)$ gauge interactions have very similar structure in both cases, but the chargino loop contribution is bigger by a factor ~ 4 than this part of the neutralino contribution. The potentially most important cancellation therefore occurs between the chargino contribution [more exactly: the total contribution involving $SU(2)$ interactions, which is however always dominated by the chargino contribution] and the neutralino contributions involving $U(1)_Y$ interactions.

Scenario B1 has $|\mu| = M_2$, i.e. very strong mixing between Higgsinos and $SU(2)$ gauginos. Eq.(4.16) no longer gives an accurate estimate of the neutralino contribution in this limit, but we expect it to remain qualitatively correct; note that it gives a finite answer (involving the derivative of the function f_2) in this case. In particular, the contributions involving the $SU(2)$ gauge coupling would be much bigger than those involving $U(1)_Y$ interactions if the relevant phases had similar magnitude; in other words, a significant cancellation can only occur if $|\phi_\mu|$ is well below $|\phi_1|$. Furthermore, for this choice of parameters a strong internal cancellation occurs between the two contributions from $U(1)_Y$ interactions that grow $\propto \tan\beta$, i.e. between the first line and the following two lines on the r.h.s. of eq.(4.16). As a result we find $|\phi_\mu| \leq \pi/30$ even for $\tan\beta = 3$. Moreover, the dominant contribution from $U(1)_Y$ interactions in this scenario involves A, i.e. is independent of $\tan\beta$, whereas the contribution

from $SU(2)$ interactions increases $\propto \tan\beta$. The upper bound on $|\phi_\mu|$ therefore scales essentially like $\cot\beta$. The importance of ϕ_A in this scenario also explains why there is almost no correlation between the allowed values of ϕ_μ and ϕ_1. Moreover, in this scenario values of ϕ_μ near π are excluded by the lower bound (4.6) on $(a_\mu)_{\rm SUSY}$.

Eq.(4.14) shows that increasing $|\mu|$ while keeping all other parameters the same decreases the chargino contribution to d_e; according to eq.(4.16) it also decreases the neutralino contributions that involve $SU(2)$ interactions, but it actually *increases* the neutralino contribution that is sensitive to $\tilde{e}_L - \tilde{e}_R$ mixing, i.e. the first line in eq.(4.16).[†] Much larger values of $|\phi_\mu|$ therefore now become possible. For the given choice of parameters the coefficient of the neutralino contribution $\propto \sin(\phi_1 - \phi_{\tilde{e}})$ is still about 5 times smaller than the coefficient of $\sin\phi_\mu$ in the chargino contribution, leading to an upper limit of $\sim \pi/4$ on $|\phi_\mu|$. Since these two coefficients have the same sign, cancellations obtain only if $\phi_1 + \phi_\mu$ and ϕ_μ have opposite signs. Note that both of these contributions are (essentially) $\propto \tan\beta$. The upper bound on $|\phi_\mu|$ is therefore now almost independent of $\tan\beta$. However, one needs increasingly more perfect cancellations as $\tan\beta$ increases; moreover, the relative importance of the phase ϕ_A diminishes with increasing $\tan\beta$, since its contribution to $\tilde{e}_L - \tilde{e}_R$ mixing is not enhanced in this limit. These two considerations explain why the width of the allowed band decreases essentially like $\cot\beta$ for large $\tan\beta$.

The increase of $|\mu|$ when going from scenario B1 to B2 also reduces the supersymmetric contribution to a_μ. For $\tan\beta = 3$ we therefore now also find an allowed band with $\phi_\mu \simeq \pi$; however, this band disappears at $\tan\beta \sim 10$. Note that the phase ϕ_1 enters a_μ mostly in the combination[‡] $\cos(\phi_1 + \phi_\mu)$. This means that $\phi_1 \simeq 0$ will give positive (negative) contributions to a_μ if $\phi_\mu \simeq 0$ (π). In other words, for values of ϕ_1 near zero the $U(1)_Y$ interactions contributes with equal sign to a_μ as the (usually leading) $SU(2)$ interactions do, whereas $\phi_1 \simeq \pi$ leads to a partial cancellation between $U(1)_Y$ and $SU(2)$ contributions. $\phi_\mu \simeq \pi$ therefore remains allowed to slightly higher values of $\tan\beta$ if $\phi_1 \simeq \pi$ as well.

If $|\mu|$ is increased by another factor of $\sim \sqrt{5}$, chargino and neutralino loop contributions to d_e can be of the same size, in which case no upper limit can be given on either $|\phi_1 + \phi_\mu|$ or $|\phi_\mu|$ separately [11], although a strong (anti–)correlation between these two phases still has to hold. If $|\mu|$ is increased even further, the neutralino contribution becomes dominant. In that case ϕ_μ could take any value (after scanning over the other phases), but significant absolute constraints on the combination $\phi_1 + \phi_\mu$ would emerge that hold even after scanning over all ϕ_A and ϕ_μ. However, most models of supersymmetry breaking prefer [33] values of $|\mu|$ that are not much larger than M_2. We therefore do not discuss scenarios with $|\mu| \gg M_2$ any further.

Scenario B3 has a significantly smaller value of $|\mu|$ than scenario B2, although it is larger than in B1. The absolute upper bound on $|\phi_\mu|$ is therefore reduced to $\sim \pi/8$. The allowed bands in figs. 2c,f are narrower than in 2b,e due to the larger values of $\tan\beta$ and slightly smaller slepton masses; both effects tend to increase the SUSY contributions to d_e, requiring

[†]In principle one can therefore have large cancellations between chargino and neutralino contributions even for $M_2 \simeq |\mu|$, if $M_2 \simeq m_{\tilde{\nu}} \gg |M_1|, m_{\tilde{e}_R}$. However, if M_2 and $m_{\tilde{\nu}}$ are as in scenario B1, this would require values of $m_{\tilde{e}_R}$ well below the direct search limit of ~ 100 GeV.

[‡]For $|\mu|\tan\beta \gg |A|$, $\cos(\phi_1 - \phi_{\tilde{\ell}}) \simeq \cos(\phi_1 + \phi_\mu)$ as well.

correspondingly more perfect cancellations. Note also that for $\tan\beta = 20$ values of ϕ_1 near zero give a_μ above the range (4.6), i.e. in this case neutralino and chargino contributions to a_μ must not add constructively. Parameter sets with ϕ_μ near π are only allowed for $\tan\beta \lesssim 5$.

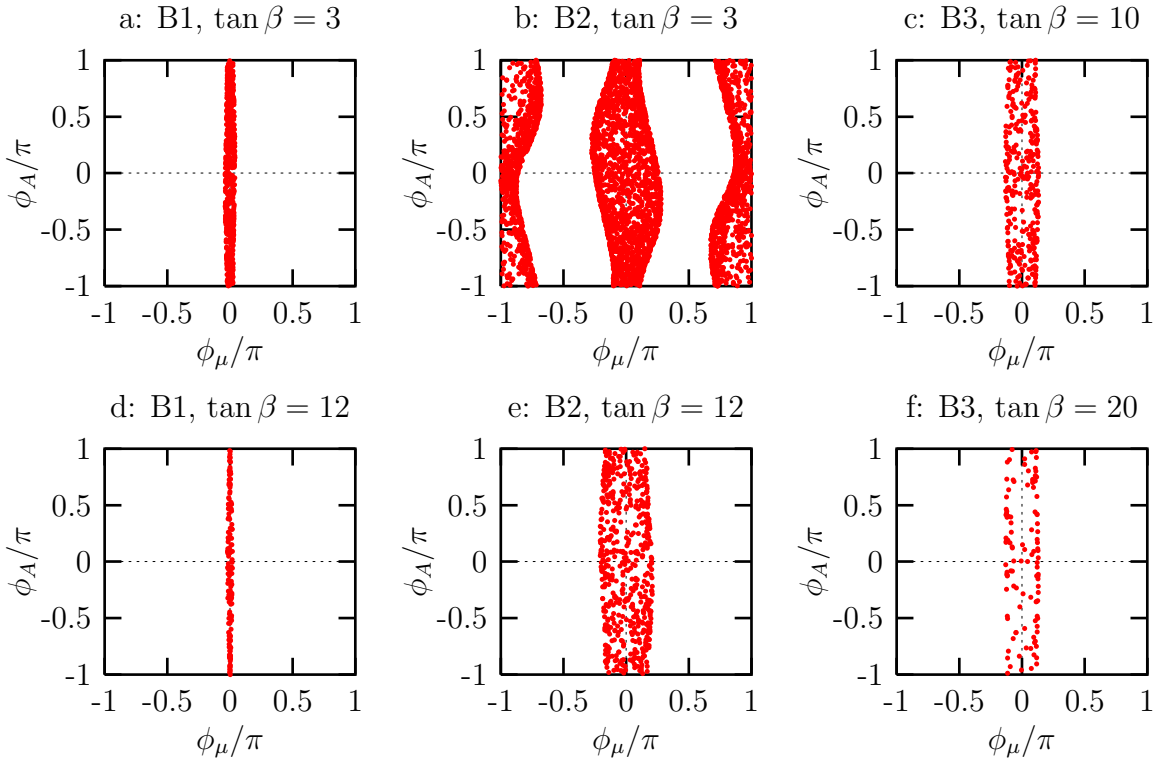

Figure 3: Combinations of ϕ_μ and ϕ_A that are allowed for at least one value of $\phi_1 \in [-\pi, \pi]$.

The allowed regions in the $(\phi_\mu, \phi_A)-$plane are shown in Fig. 3. Most of our scenarios have $|\mu \tan\beta|$ significantly above $|A|$, in which case the value of ϕ_A is not very important. Even if ϕ_A is important, as in scenario B1, there is little correlation between ϕ_A and ϕ_μ, since ϕ_A only enters in the combination $\phi_{\tilde{e}} - \phi_1$, and ϕ_1 is scanned in Fig. 3. In all cases the bound on $|\phi_\mu|$ is slightly weaker for $\phi_A \simeq 0$ than for $\phi_A \simeq \pm\pi$, since in the former case A and μ add (mostly) constructively to the mixing of selectrons, thereby increasing the first line on the r.h.s. of eq.(4.16).

We see from figs. 2 and 3 that in all cases the entire range of values of ϕ_A and ϕ_1 is allowed by the d_e constraint for some combinations of the other phases. Fig. 4 shows that there is little correlation between the allowed ranges of these two phases. Indeed, the d_e constraint allows all combinations of these two phases, for some value of ϕ_μ. On the other hand, in case B3 with $\tan\beta = 20$ the a_μ constraint (4.6) excludes $|\phi_1| \lesssim \pi/2$, see Fig. 2f.

In Sec. 7.3 we will study correlations between low– and high–energy observables. To that end it is instructive to see how the low–energy observables correlate with the SUSY phases in the experimentally allowed region of parameter space. We saw above that ϕ_μ is tightly

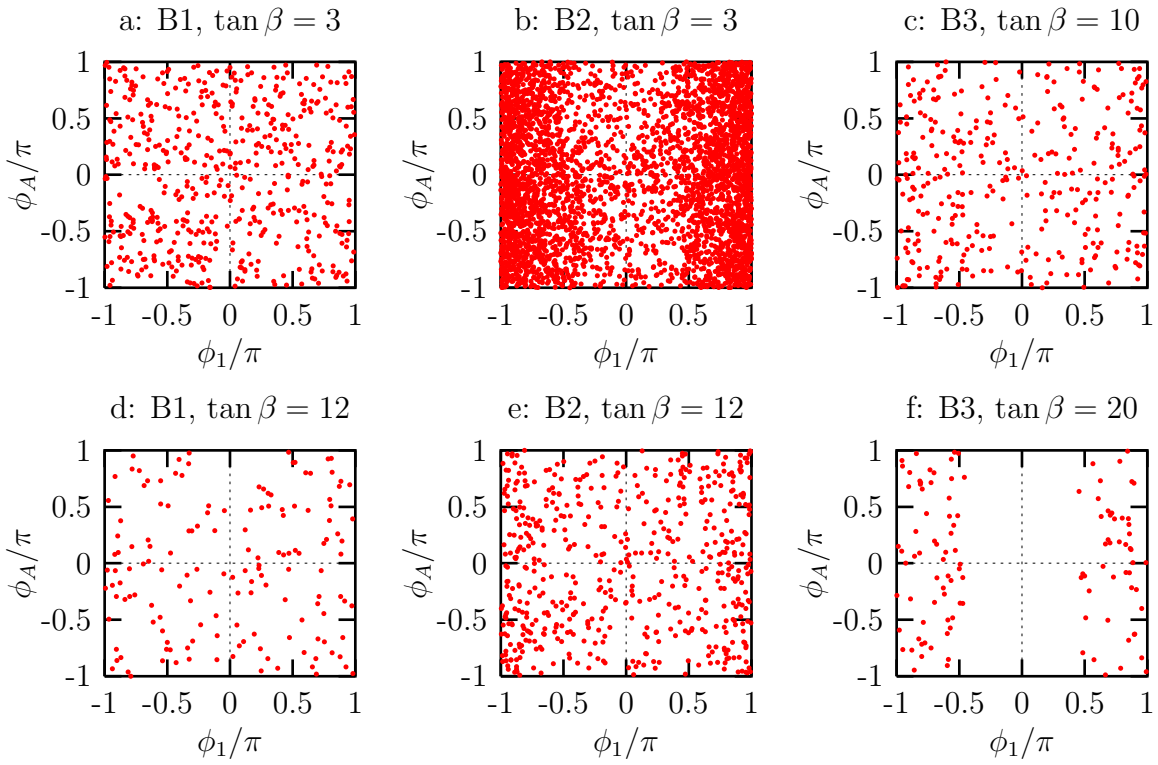

Figure 4: Combinations of ϕ_1 and ϕ_A that are allowed for at least one value of $\phi_\mu \in [-\pi, \pi]$.

constrained, whereas ϕ_A and ϕ_1 are not. Since ϕ_A does not affect high–energy observables, the most interesting correlations are those between low–energy observables and ϕ_1, after scanning over ϕ_A and ϕ_μ.

We find that there is no correlation between d_e and ϕ_1 (not shown), whereas in scenarios B2 and B3 a_μ shows a behavior $\propto a \cos\phi_1 + b$ with a finite scatter, see Fig. 5. This difference originates from the requirement of very strong cancellations in d_e discussed above. In particular, the phases ϕ_1 and ϕ_μ have to be correlated such that the leading terms $\propto \sin(\phi_1 + \phi_\mu)$ and $\propto \sin\phi_\mu$ cancel each other, to an accuracy determined by the size of (subleading) terms $\propto \sin\phi_A$ as well as by the experimental error on d_e. This completely removes the correlation between d_e and $\sin\phi_1$ that one might naively expect from eq.(4.16). The phase–dependent neutralino loop contributions to $(a_\mu)_{\rm SUSY}$ can be read off from eq.(4.16) by replacing m_e by $2m_\mu^2$ in the overall factor, and all sin by cos; in addition, there are phase–independent contributions of comparable size. Since for our examples ϕ_μ is constrained to be small (or near π), $|\cos\phi_\mu| \simeq 1$ and one finds a $\cos-$like dependence of a_μ on ϕ_1, as already stated. The crucial observation is that the ϕ_1–dependent and ϕ_μ–dependent terms do *not* cancel in this case, so the 'naive' dependence of a_μ on ϕ_1 survives. We note in passing that $(a_\mu)_{\rm SUSY} = 0$ can usually not be achieved for a given choice of the absolute values of the SUSY parameters once we have required large cancellations in d_e, i.e. we cannot choose the phases such that there are large cancellations in both d_e and $(a_\mu)_{\rm SUSY}$. A better measurement of, and more accurate SM prediction for, a_μ therefore has

higher potential to further constrain the SUSY phases than improved measurements of d_e.[§]

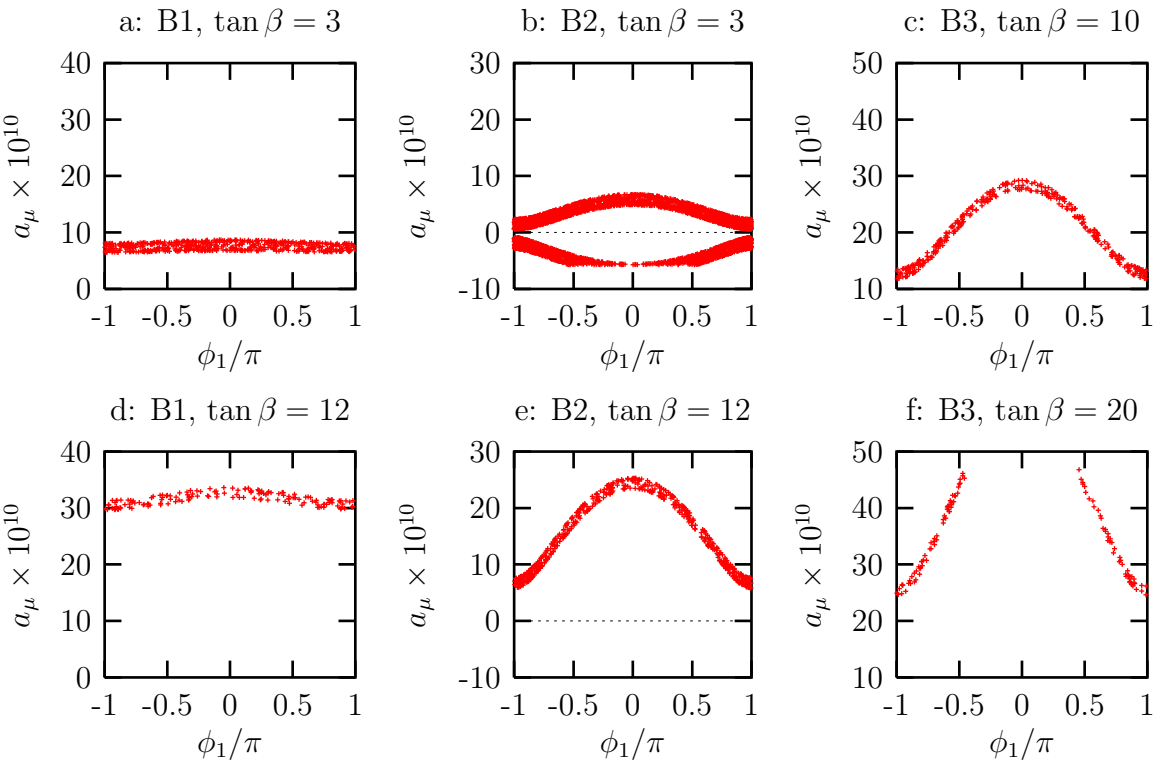

Figure 5: $(a_\mu)_{\rm SUSY}$ vs. ϕ_1 after scanning over ϕ_μ and ϕ_A.

5 High Energy Observables

We are now ready to analyze the impact of SUSY phases on high energy observables. After defining the relevant kinematical quantities for the $2 \to 2$ processes under consideration, we briefly present the calculation of the corresponding unpolarized total cross sections. All these processes have already been discussed in the literature: results for $\tilde{e}^-\tilde{e}^+$ and $\tilde{e}^-\tilde{e}^-$ production results can be found in [35, 36, 37, 38] and [39], whereas results for $\tilde{\chi}_i^-\tilde{\chi}_j^+$ and $\tilde{\chi}_i^0\tilde{\chi}_j^0$ production are given in [40, 36, 19] and [41]. We nevertheless list our results here in order to provide a self–contained presentation and to illustrate consistency with previous works.

[§]Of course, experimentally establishing a nonvanishing value of d_e would be of the greatest importance, since it would require physics beyond the SM. However, while it would require some SUSY phase to be non–zero, it would not further reduce the allowed ranges of any one of these phases after scanning over the other two phases.

5.1 Kinematics

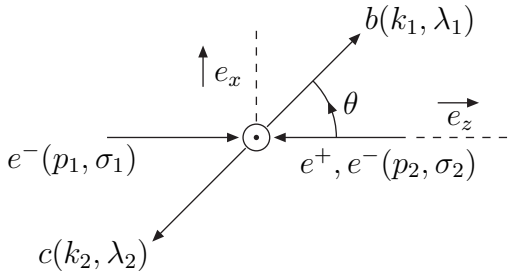

Figure 6: Kinematical situation

The kinematical situation is illustrated by Fig. 6. The momenta and helicities of the incoming (first) electron and positron (second electron) are denoted by p_1^μ and σ_1, and p_2^μ and σ_2, respectively. The momenta of the produced superparticles, generically labeled by b and c, are denoted by k_1^μ and k_2^μ. In case of fermions being produced their helicities are denoted by λ_1 and λ_2.

Working in the center of mass (CMS) frame, we define the $z-$axis of the coordinate system such that $\vec{p}_1$ points in $+z$ direction. The event plane is then completed by the momentum $\vec{k}_1$ of particle b and defines the (x, z) plane of the coordinate system. The scattering angle θ is defined as the angle between $\vec{p}_1$ and $\vec{k}_1$. The nominal range for θ, which we use when going from the differential to the total cross section, extends from 0 to π. However, if the final state consists of two identical particles, physically θ has to be $\leq \pi/2$; we therefore have to multiply the cross section for the production of identical particles with a factor of $1/2$. Notice that our convention implies vanishing azimuthal angle ϕ. This definition of the (x, z) plane is convenient since we are only interested in total cross sections for unpolarized $e^\pm$ beams.* Of course, the phase space integration, which should be performed in a lab–fixed coordinate system, still gives a factor of 2π from the integration over the azimuthal angle. Explicit expressions for the momenta p_i^μ and k_i^μ can be found in Appendix A.

5.2 Cross section for $e^-e^+ \to \tilde{e}_i^- \tilde{e}_j^+$

Fig. 7 shows the s- and t-channel diagram contributing to selectron pair production. By introducing a dimensionless Z boson propagator

$$D_Z = \frac{s}{s - M_Z^2 + iM_Z\Gamma_Z}, \tag{5.1}$$

*A nontrivial dependence on the azimuthal angle would arise only if we considered transversely polarized $e^\pm$ beams, and/or were interested in the kinematical distribution of the decay products of the produced superparticles b and c.

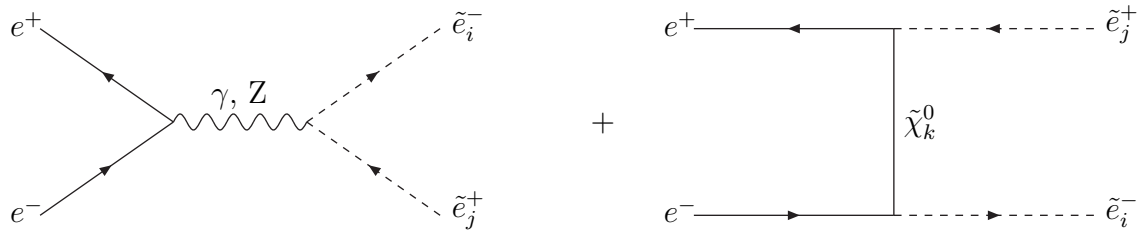

Figure 7: Diagrams for $e^+e^- \to \tilde{e}_i^- \tilde{e}_j^+$

and bilinear charges $Z_{ij}^{\pm}$

$$Z_{LL}^- = 1 + \frac{(\sin^2\theta_{\rm W} - \frac{1}{2})^2}{\sin^2\theta_{\rm W}\cos^2\theta_{\rm W}} D_Z, \quad Z_{RR}^- = 1 + \frac{\sin^2\theta_{\rm W} - \frac{1}{2}}{\cos^2\theta_{\rm W}} D_Z, \tag{5.2a}$$

$$Z_{LL}^+ = 1 + \frac{\sin^2\theta_{\rm W} - \frac{1}{2}}{\cos^2\theta_{\rm W}} D_Z, \qquad Z_{RR}^+ = 1 + \frac{\sin^2\theta_{\rm W}}{\cos^2\theta_{\rm W}} D_Z, \tag{5.2b}$$

$$Z_{LR}^{\pm} = Z_{RL}^{\pm} = 0, \tag{5.2c}$$

the gauge contribution to the helicity amplitudes can be written as

$$\mathcal{M}_{ij}^{\sigma_1\sigma_2,G} = \frac{e^2}{s} \bar{v}(p_2,\sigma_2) Z_{ij}^{\alpha} P_{\alpha} u(p_1,\sigma_1)(k_i - k_j)^{\mu}. \tag{5.3}$$

The neutralino contribution is

$$\mathcal{M}_{ij}^{\sigma_1\sigma_2,\tilde{\chi}_k^0} = -\bar{v}(p_2,\sigma_2) K_{-\alpha k}^{j\star} P^{\alpha} (\not{p}_1 - \not{k}_1 + m_{\tilde{\chi}_k^0}) D_t^k K_{\beta k}^i P^{\beta} u(p_1,\sigma_1). \tag{5.4}$$

The coefficients $K_{\alpha k}^i$ are given by

$$K_{Lk}^L = \frac{e}{\sqrt{2}\cos\theta_{\rm W}\sin\theta_{\rm W}} (\cos\theta_{\rm W} N_{2k} + \sin\theta_{\rm W} N_{1k}), \tag{5.5a}$$

$$K_{Rk}^R = \frac{-2e}{\sqrt{2}\cos\theta_{\rm W}} N_{1k}^{\star}, \tag{5.5b}$$

$$K_{Lk}^R = K_{Rk}^L = 0, \tag{5.5c}$$

and the neutralino propagators are

$$D_{t,u}^k = \frac{1}{(t,u) - m_{\tilde{\chi}_k^0}^2}, \tag{5.6}$$

where $t = (p_1 - k_1)^2$ and $u = (p_1 - k_2)^2$. By introducing a shorthand notation for the helicity amplitudes

$$\langle \sigma_1\sigma_2 \rangle_{ij} = \mathcal{M}_{ij}^{\sigma_1\sigma_2,G} + \mathcal{M}_{ij}^{\sigma_1\sigma_2,\tilde{\chi}_k^0}, \tag{5.7}$$

and using the explicit expressions for helicity amplitudes given in Appendix B and the definition of the neutralino functions in Eqs.(C.2) we find six non-vanishing helicity amplitudes (θ is the angle between the momenta of the incident e^- and the produced $\tilde{e}^-$):

$$\langle ++\rangle_{RL} = -2e^2 M^{\star}_{LR}(s,t); \tag{5.8a}$$

$$\langle --\rangle_{LR} = 2e^2 M_{RL}(s,t); \tag{5.8b}$$

$$\langle +-\rangle_{RR} = -e^2 \lambda^{\frac{1}{2}}_{RR} \sin\theta \left(N_{RR}(s,t) + Z^{+}_{RR}\right); \tag{5.8c}$$

$$\langle +-\rangle_{LL} = -e^2 \lambda^{\frac{1}{2}}_{LL} \sin\theta Z^{+}_{LL}; \tag{5.8d}$$

$$\langle -+\rangle_{RR} = -e^2 \lambda^{\frac{1}{2}}_{RR} \sin\theta Z^{-}_{RR}; \tag{5.8e}$$

$$\langle -+\rangle_{LL} = -e^2 \lambda^{\frac{1}{2}}_{LL} \sin\theta \left(N_{LL}(s,t) + Z^{-}_{LL}\right). \tag{5.8f}$$

Here, the kinematical factors $\lambda^{\frac{1}{2}}_{ij} \equiv \lambda^{\frac{1}{2}}_{\tilde{e}_i \tilde{e}_j}$ are as in eqs.(A.3). As usual, the unpolarized cross section can be obtained by averaging over initial helicities. After integrating over the azimuthal angle, we obtain

$$\frac{d\sigma_{LL}}{d\cos\theta} = \frac{\lambda^{\frac{1}{2}}_{LL}}{128\pi s}\left(|\langle +-\rangle_{LL}|^2 + |\langle -+\rangle_{LL}|^2\right); \tag{5.9a}$$

$$\frac{d\sigma_{RR}}{d\cos\theta} = \frac{\lambda^{\frac{1}{2}}_{RR}}{128\pi s}\left(|\langle +-\rangle_{RR}|^2 + |\langle -+\rangle_{RR}|^2\right); \tag{5.9b}$$

$$\frac{d\sigma_{LR}}{d\cos\theta} = \frac{\lambda^{\frac{1}{2}}_{LR}}{128\pi s}|\langle --\rangle_{LR}|^2; \tag{5.9c}$$

$$\frac{d\sigma_{RL}}{d\cos\theta} = \frac{\lambda^{\frac{1}{2}}_{RL}}{128\pi s}|\langle ++\rangle_{RL}|^2. \tag{5.9d}$$

Finally, for these and all following reactions the total, unpolarized cross sections may be obtained by performing the remaining integration over the scattering angle:

$$\sigma_{ij} = \int_{-1}^{1} d\cos\theta \left(\frac{d\sigma_{ij}}{d\cos\theta}\right). \tag{5.10}$$

5.3 Cross section for $e^-e^- \to \tilde{e}^-_i \tilde{e}^-_j$

The t- and u-channel diagrams contributing to $\tilde{e}^-_i \tilde{e}^-_j$ pair production are shown in Fig. 8. The corresponding invariant amplitude can be written as

$$\begin{aligned}\mathcal{M}^{\sigma_1\sigma_2}_{ij} \;&= -K^j_{\alpha k} K^i_{\beta k} \bar{v}(p_2,\sigma_2)\times \\ &\left\{\delta_{\beta,-\alpha}\left[\frac{\not{p}_1 - \not{k}_1}{t - m^2_{\tilde{\chi}^0_k}} + \frac{\not{p}_1 - \not{k}_2}{u - m^2_{\tilde{\chi}^0_k}}\right] P_\alpha + \delta_{\alpha\beta} m_{\tilde{\chi}^0_k}\left[\frac{1}{t - m^2_{\tilde{\chi}^0_k}} + \frac{1}{u - m^2_{\tilde{\chi}^0_k}}\right] P_\alpha\right\} u(p_1,\sigma_1).\end{aligned} \tag{5.11}$$

Figure 8: Diagrams for $e^-e^- \to \tilde{e}_i^-\tilde{e}_j^-$

Using the results of Appendix B we evaluate the helicity amplitudes and find

$$\begin{aligned}\mathcal{M}_{ij}^{\sigma_1\sigma_2} = \langle\sigma_1\sigma_2\rangle_{ij} = -\frac{s}{2}\sin\theta\lambda_{ij}^{\frac{1}{2}}\delta_{\sigma_2,-\sigma_1}\left(K^i_{\sigma_1 k}K^j_{-\sigma_1 k}D^k_t - K^i_{-\sigma_1 k}K^j_{\sigma_1 k}D^k_u\right)\\ + m_{\tilde{\chi}_k^0}\sqrt{s}K^i_{\sigma_1 k}K^j_{\sigma_1 k}\sigma_1\delta_{\sigma_1\sigma_2}\left(D^k_t + D^k_u\right).\end{aligned} \tag{5.12}$$

Rewriting these results in terms of neutralino functions as defined in Eqs.(C.2) we find four non–vanishing helicity amplitudes (θ is the angle between the momenta of an incident e^- and a produced $\tilde{e}^-$; it does not matter which initial and final state particles are chosen, since the cross section is invariant under $\theta \to \pi - \theta$):

$$\langle++\rangle_{RR} = 2e^2\left[M^\star_{RR}(s,t) + M^\star_{RR}(s,u)\right]; \tag{5.13a}$$

$$\langle--\rangle_{LL} = -2e^2\left[M_{LL}(s,t) + M_{LL}(s,u)\right]; \tag{5.13b}$$

$$\langle-+\rangle_{LR} = e^2\lambda_{LR}^{\frac{1}{2}}\sin\theta N_{LR}(s,t); \tag{5.13c}$$

$$\langle+-\rangle_{RL} = -e^2\lambda_{LR}^{\frac{1}{2}}\sin\theta N_{LR}(s,u). \tag{5.13d}$$

After calculating the polarization averaged squared matrix elements and including the phase space factor, the differential cross sections are:

$$\frac{d\sigma_{LL}}{d\cos\theta} = \frac{\lambda_{LL}^{\frac{1}{2}}}{256\pi s}|\langle--\rangle_{LL}|^2; \tag{5.14a}$$

$$\frac{d\sigma_{RR}}{d\cos\theta} = \frac{\lambda_{RR}^{\frac{1}{2}}}{256\pi s}\langle++\rangle_{RR}|^2; \tag{5.14b}$$

$$\frac{d\sigma_{LR}}{d\cos\theta} = \frac{\lambda_{LR}^{\frac{1}{2}}}{128\pi s}\left(|\langle-+\rangle_{LR}|^2 + |\langle+-\rangle_{RL}|^2\right). \tag{5.14c}$$

Note that σ_{LR} and σ_{RL} are not physically distinguishable in this case, unlike for e^+e^- annihilation.

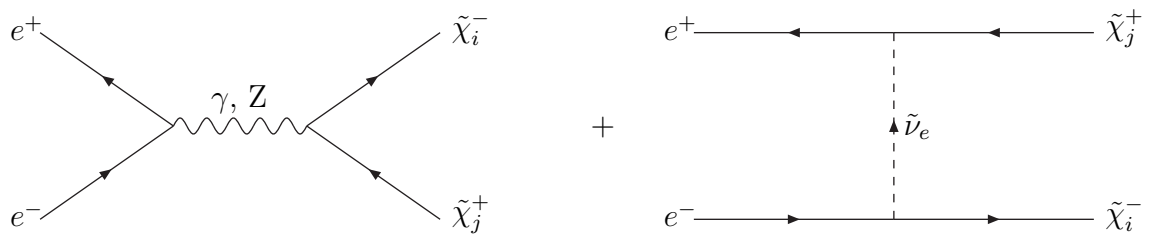

Figure 9: Diagrams for $e^-e^+ \to \tilde{\chi}_i^- \tilde{\chi}_j^+$

5.4 Cross section for $e^-e^+ \to \tilde{\chi}_i^- \tilde{\chi}_j^+$

Fig. 9 shows the s- and t-channel contributions to $\tilde{\chi}_i^- \tilde{\chi}_j^+$ pair production. After a Fierz–rearrangement of the $\tilde{\nu}$ contribution, the invariant amplitude can be written as

$$\mathcal{M}^{ij}_{\sigma_1\sigma_2;\lambda_1\lambda_2} = \frac{-e^2}{s}\bar{v}(p_2,\sigma_2)\gamma_\mu P^\alpha u(p_1,\sigma_2) Q^{ij}_{\alpha\beta}\bar{u}_i(k_1,\lambda_1)\gamma^\mu P^\beta v_j(k_2,\lambda_2), \tag{5.15}$$

where we introduced the bilinear charges (with $x = \sin^2\theta_{\rm W}$)

$$Q^{11}_{LL} = 1 + \frac{D_Z(2x-1)}{2x(1-x)}\left(x - \frac{3}{4} - \frac{1}{4}\cos 2\phi_L\right), \tag{5.16a}$$

$$Q^{11}_{RR} = 1 + \frac{D_Z}{1-x}\left(x - \frac{3}{4} - \frac{1}{4}\cos 2\phi_R\right), \tag{5.16b}$$

$$Q^{11}_{LR} = 1 + \frac{D_Z(2x-1)}{2x(1-x)}\left(x - \frac{3}{4} - \frac{1}{4}\cos 2\phi_R\right) + \frac{sD^{\tilde{\nu}}_t}{4x}(1+\cos 2\phi_R), \tag{5.16c}$$

$$Q^{11}_{RL} = 1 + \frac{D_Z}{1-x}\left(x - \frac{3}{4} - \frac{1}{4}\cos 2\phi_L\right); \tag{5.16d}$$

$$Q^{22}_{LL} = 1 + \frac{D_Z(2x-1)}{2x(1-x)}\left(x - \frac{3}{4} + \frac{1}{4}\cos 2\phi_L\right), \tag{5.17a}$$

$$Q^{22}_{RR} = 1 + \frac{D_Z}{1-x}\left(x - \frac{3}{4} + \frac{1}{4}\cos 2\phi_R\right), \tag{5.17b}$$

$$Q^{22}_{LR} = 1 + \frac{D_Z(2x-1)}{2x(1-x)}\left(x - \frac{3}{4} + \frac{1}{4}\cos 2\phi_R\right) + \frac{sD^{\tilde{\nu}}_t}{4x}(1-\cos 2\phi_R), \tag{5.17c}$$

$$Q^{22}_{RL} = 1 + \frac{D_Z}{1-x}\left(x - \frac{3}{4} + \frac{1}{4}\cos 2\phi_L\right); \tag{5.17d}$$

$$Q^{12}_{LL} = \left(Q^{21}_{LL}\right)^\star = \frac{D_Z(2x-1)}{8x(1-x)}\sin 2\phi_L e^{-i\beta_L}, \tag{5.18a}$$

$$Q^{12}_{RR} = \left(Q^{21}_{RR}\right)^\star = \frac{D_Z}{4(1-x)} \sin 2\phi_R e^{i(\gamma_1-\beta_R-\gamma_2)}, \tag{5.18b}$$

$$Q^{12}_{LR} = \left(Q^{21}_{LR}\right)^\star = \left(\frac{D_Z(2x-1)}{8x(1-x)} - \frac{sD^{\tilde\nu}_t}{4x}\right) \sin 2\phi_R e^{i(\gamma_1-\beta_R-\gamma_2)}, \tag{5.18c}$$

$$Q^{12}_{RL} = \left(Q^{21}_{RL}\right)^\star = \frac{D_Z}{4x(1-x)} \sin 2\phi_L e^{-i\beta_L}. \tag{5.18d}$$

Here the sneutrino propagator $D^{\tilde\nu}_t$ is defined analogously to the neutralino propagators (5.6). Using the results of Appendix B we find for a generic helicity amplitude (θ is the angle between the momenta of the incident e^- and the produced $\tilde\chi^-$):

$$\begin{aligned}\langle\sigma_1,-\sigma_1;\lambda_1\lambda_2\rangle_{ij} = \frac{-e^2}{2}\sum_\beta Q^{ij}_{\sigma_1\beta}\Big\{&\lambda_1\delta_{\lambda_1\lambda_2}\sqrt{1-\eta^2_{\beta\lambda_1}}\sin\theta \\ &+ \delta_{\lambda_1,-\lambda_2}\sqrt{(1+\beta\lambda_1\eta_{\beta\lambda_1})(1+\beta\lambda_1\eta_{-\beta\lambda_1})}\,(\cos\theta+\lambda_1\sigma_1)\Big\},\end{aligned} \tag{5.19}$$

where the kinematical quantities $\eta_\pm$ are defined in eq.(B.3). The unpolarized cross sections can be computed from eq.(5.19) by averaging over initial helicities and summing over the final ones:

$$\frac{d\sigma_{ij}}{d\cos\theta} = \frac{\pi\alpha^2}{8s}\lambda^{\frac12}_{ij}\left\{\left[(1-\Delta^2_{ij})+\lambda_{ij}\cos^2\theta\right]Q^{ij}_1 + 8\mu_i\mu_j Q^{ij}_2 + 2\lambda^{\frac12}_{ij}\cos\theta Q^{ij}_3\right\}, \tag{5.20}$$

where $4\pi\alpha = e^2$, $\mu_i = m_{\tilde\chi_i}/\sqrt{s}$ and $\Delta_{ij} = \mu^2_i - \mu^2_j$. The new quartic charges Q^{ij}_n are given by:

$$Q^{ij}_1 = |Q^{ij}_{++}|^2 + |Q^{ij}_{+-}|^2 + |Q^{ij}_{-+}|^2 + |Q^{ij}_{--}|^2; \tag{5.21a}$$

$$Q^{ij}_2 = \Re\mathrm{e}\left(Q^{ij}_{++}Q^{ij\star}_{+-} + Q^{ij}_{--}Q^{ij\star}_{-+}\right); \tag{5.21b}$$

$$Q^{ij}_3 = |Q^{ij}_{++}|^2 - |Q^{ij}_{+-}|^2 - |Q^{ij}_{-+}|^2 + |Q^{ij}_{--}|^2. \tag{5.21c}$$

5.5 Cross section for $e^-e^+ \to \tilde\chi^0_i\tilde\chi^0_j$

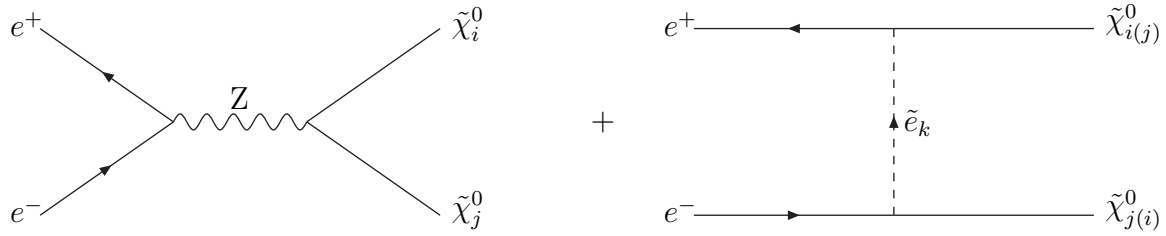

Figure 10: Diagrams for $e^-e^+ \to \tilde\chi^0_i\tilde\chi^0_j$

In Fig. 10 the $s-$ and $t-$channel contributions to $\tilde\chi^0_i\tilde\chi^0_j$ production are shown; the additional, destructively interfering $u-$channel diagram is indicated by the exchanged indices in

parentheses. Applying a Fierz rearrangement on both the $t-$ and $u-$channel diagram, and re–ordering the $u-$channel amplitude, we obtain the invariant amplitude

$$\mathcal{M}^{ij}_{\sigma_1\sigma,\lambda_1\lambda_2} = \frac{-e^2}{s}\bar{v}(p_2,\sigma_2)\gamma_\mu P^\alpha u(p_1,\sigma_2)Q^{ij}_{\alpha\beta}\bar{u}(k_1,\lambda_1)\gamma^\mu P^\beta v(k_2,\lambda_2). \tag{5.22}$$

Here, the bilinear charges $Q^{ij}_{\alpha\beta}$ are given by ($x = \sin^2\theta_{\rm W}$)

$$Q^{ij}_{LL} = \frac{D_Z}{2x(1-x)}(2x-1)Z^\star_{ij} - sD^L_u g_{Lij}, \tag{5.23a}$$

$$Q^{ij}_{RR} = -\frac{D_Z}{1-x}Z_{ij} - sD^R_u g^\star_{Rij}, \tag{5.23b}$$

$$Q^{ij}_{LR} = -\frac{D_Z}{2x(1-x)}(2x-1)Z_{ij} + sD^L_t g^\star_{Lij}, \tag{5.23c}$$

$$Q^{ij}_{RL} = \frac{D_Z}{1-x}Z^\star_{ij} + sD^R_t g_{Rij}, \tag{5.23d}$$

with

$$g_{Lij} = \frac{1}{4x}\left(N^\star_{2i} + \tan\theta_{\rm W}N^\star_{1i}\right)\left(N_{2j} + \tan\theta_{\rm W}N_{1j}\right), \tag{5.24a}$$

$$g_{Rij} = \frac{1}{1-x}N^\star_{1i}N_{1j}. \tag{5.24b}$$

The selectron propagators are defined as

$$D^{L,R}_{t,u} = \frac{1}{(t,u) - m^2_{\tilde{e}_{L,R}}}. \tag{5.25}$$

Since this amplitude has the same structure as the amplitude for $\tilde{\chi}^-_i\tilde{\chi}^+_j$ production, eq. (5.15), we can directly translate the result (5.19) from this calculation; we just have to replace the bilinear charges. We can also use the result (5.20) for the unpolarized, differential cross section, but we have to include a statistical factor:

$$\frac{d\sigma_{ij}}{d\cos\theta} = 2^{-\delta_{ij}}\frac{\pi\alpha^2}{8s}\lambda^{\frac{1}{2}}_{ij}\left\{\left[(1-\Delta^2_{ij}) + \lambda_{ij}\cos^2\theta\right]Q^{ij}_1 + 8\mu_i\mu_j Q^{ij}_2 + 2\lambda^{\frac{1}{2}}_{ij}\cos\theta Q^{ij}_3\right\}. \tag{5.26}$$

Of course, now the bilinear charges of eqs.(5.23) have to be used when evaluating the quartic charges defined in eqs.(5.21).

5.6 P_N for 2 fermion production

We will see in Sec. 7 that some of the cross sections calculated in the previous subsections depend quite sensitively on the CP–violating phases ϕ_1 and/or ϕ_μ. Nevertheless, if measurements of these cross sections establish a deviation from the CP–conserving MSSM, one will need

to measure some CP–violating asymmetries in order to convince oneself that the observed deviation is indeed due to non–vanishing phases, rather than due to some extension of the MSSM. We will see that this is possible only for the production of fermionic final states. Consider

$$e^-(\vec{p}_1,\vec{s}_1)e^+(\vec{p}_2,\vec{s}_2) \to \tilde{\chi}_i(\vec{k}_1,\vec{\tilde{s}}_1)\bar{\tilde{\chi}}_j(\vec{k}_2,\vec{\tilde{s}}_2)\,. \tag{5.27}$$

The momenta $\vec{p}_{1,2}$ and $\vec{k}_{1,2}$ have been defined in Fig. 6, and $\vec{s}_{1,2}$ and $\vec{\tilde{s}}_{1,2}$ are the spin vectors in the initial and final state, respectively. A CP transformation on reaction (5.27) gives the CP–conjugate process

$$\mathrm{CP}:\ e^+(-\vec{p}_1,\vec{s}_1)e^-(-\vec{p}_2,\vec{s}_2) \to \bar{\tilde{\chi}}_i(-\vec{k}_1,\vec{\tilde{s}}_1)\tilde{\chi}_j(-\vec{k}_2,\vec{\tilde{s}}_2)\,. \tag{5.28}$$

In the center–of–mass system, $\vec{p}_1 = -\vec{p}_2$ and $\vec{k}_1 = -\vec{k}_2$. The initial state will therefore be self–conjugate if $\vec{s}_1 = \vec{s}_2$, in particular for unpolarized beams. Comparing reactions (5.27) and (5.28) one can introduce two CP–odd asymmetries even after summing over the spins in the final state. One can define a rate asymmetry for chargino production, essentially $\sigma(\tilde{\chi}_1^-\tilde{\chi}_2^+) - \sigma(\tilde{\chi}_2^-\tilde{\chi}_1^+)$, as well as an angular asymmetry for the production of two different neutralinos, proportional to $d\sigma(\tilde{\chi}_i^0\tilde{\chi}_j^0,\theta) - d\sigma(\tilde{\chi}_i^0\tilde{\chi}_j^0,\pi-\theta)$. However, far from the Z pole, both these asymmetries vanish identically at the tree level. The reason is that they are odd under a combined CP$\widetilde{\mathrm{T}}$ transformation, where the "naive time reversal" $\widetilde{\mathrm{T}}$ reverses the direction of all 3–momenta, but does *not* exchange initial and final state. Quantities that are odd under CP$\widetilde{\mathrm{T}}$ can be non–zero only in the presence of absorptive phases, which can come from nearly resonant $s-$channel propagators, or from loop corrections if the kinematics allows the particles in the loop to be on–shell.

A CP–odd quantity can therefore only be non–zero in the absence of absorptive phases, if it is also $\widetilde{\mathrm{T}}-$odd. This is true for triple products of momentum and spin vectors. In general, the spin of the final state fermions in (5.27) can be decomposed in three components: $P_L^{i,ij}$ is the component of $\vec{\tilde{s}}_i$ in direction of $\vec{k}_i$, averaged over many events (with fixed θ); $P_T^{i,ij}$ is orthogonal to $\vec{k}_i$, but lies *in* the event plane; and $P_N^{i,ij}$ is orthogonal to $\vec{k}_i$ *and* orthogonal to the event plane. The first two of these quantities are $\widetilde{\mathrm{T}}-$even; however, since

$$P_N^{i,ij} = \langle \vec{\tilde{s}}_i \cdot (\vec{p_1} \times \vec{k}_i)\rangle,\ i = 1,2, \tag{5.29}$$

$P_N^{i,ij}$ is indeed $\widetilde{\mathrm{T}}-$odd; here $\langle\ldots\rangle$ denotes averaging over many events with fixed scattering angle θ.* We will comment on the measurability of this quantity when we present numerical results.

The normal components of the polarizations of $\tilde{\chi}_i$ and $\tilde{\chi}_j$ can be computed using results of ref.[42]:

$$P_N^{i,ij} = \frac{-2\Im\mathrm{m}\left\{\sum_{\sigma_1\sigma_2}\left[\langle\sigma_1\sigma_2;++\rangle\langle\sigma_1\sigma_2;-+\rangle^\star + \langle\sigma_1\sigma_2;+-\rangle\langle\sigma_1\sigma_2;--\rangle^\star\right]\right\}}{\sum_{\sigma_1\sigma_2}|\langle\sigma_1\sigma_2;++\rangle|^2 + |\langle\sigma_1\sigma_2;+-\rangle|^2 + |\langle\sigma_1\sigma_2;-+\rangle|^2 + |\langle\sigma_1\sigma_2;--\rangle|^2}; \tag{5.30a}$$

*Strictly speaking, P_N^i is CP–odd only for self–conjugate final states (any two neutralinos, or $\tilde{\chi}_i^-\tilde{\chi}_i^+$). However, since at tree–level and away from $s-$channel resonances T and $\widetilde{\mathrm{T}}$ transformations are essentially the same, a non–vanishing P_N^i in $\tilde{\chi}_1^-\tilde{\chi}_2^+$ production can also be considered evidence for CP–violation.

$$P_N^{j,ij} = \frac{2\Im\mathrm{m}\left\{\sum_{\sigma_1\sigma_2}\left[\langle\sigma_1\sigma_2;++\rangle\langle\sigma_1\sigma_2;+-\rangle^\star + \langle\sigma_1\sigma_2;-+\rangle\langle\sigma_1\sigma_2;--\rangle^\star\right]\right\}}{\sum_{\sigma_1\sigma_2}\left[|\langle\sigma_1\sigma_2;++\rangle|^2 + |\langle\sigma_1\sigma_2;+-\rangle|^2 + |\langle\sigma_1\sigma_2;-+\rangle|^2 + |\langle\sigma_1\sigma_2;--\rangle|^2\right]}. \quad (5.30b)$$

After introducing a fourth quartic charge,

$$Q_4^{ij} = \Im\mathrm{m}\left(Q_{++}^{ij}Q_{+-}^{ij\star} + Q_{--}^{ij}Q_{-+}^{ij\star}\right), \quad (5.31)$$

and using eq.(5.19), eqs.(5.30) simplify to

$$P_N^{i,ij} = \frac{4\sin\theta\mu_j\lambda_{ij}^{\frac{1}{2}}Q_4^{ij}}{\left[1-\Delta_{ij}^2+\lambda_{ij}\cos^2\theta\right]Q_1^{ij} + 8\mu_i\mu_jQ_2^{ij} + 2\lambda_{ij}^{\frac{1}{2}}\cos\theta Q_3^{ij}}; \quad (5.32a)$$

$$P_N^{j,ij} = \frac{-4\sin\theta\mu_i\lambda_{ij}^{\frac{1}{2}}Q_4^{ij}}{\left[1-\Delta_{ij}^2+\lambda_{ij}\cos^2\theta\right]Q_1^{ij} + 8\mu_i\mu_jQ_2^{ij} + 2\lambda_{ij}^{\frac{1}{2}}\cos\theta Q_3^{ij}} = -P_N^{i,ij}\frac{\mu_i}{\mu_j}. \quad (5.32b)$$

We see that $P_N^{i(j),ij}$ vanishes both at threshold (where $\lambda_{ij}\to 0$) and far above threshold (where $\mu_{j,i}\to 0$). Eqs.(5.16) and (5.17) show that all bilinear charges describing $\tilde{\chi}_i^-\tilde{\chi}_i^+$ production are real. Likewise, eqs.(5.2) and (5.24) show that the couplings appearing in the expressions (5.23) of the bilinear charges for neutralino pair production are real for final states consisting of two identical neutralinos. We thus see that Q_4^{ij} and hence $P_N^{i(j),ij}$ can only be non–vanishing for off–diagonal production modes ($i\neq j$). Moreover, the second identity in eq.(5.32b) shows that there is only one independent P_N for each distinct $\tilde{\chi}_i\tilde{\chi}_j$ production channel, for a total of 7 independent CP–odd observables.

5.7 Approximate results

The results presented in the previous sections allow the exact (tree–level) calculation of the phase dependences of the selectron and neutralino production cross sections, and of P_N. However, it is useful to get a qualitative understanding of where one can expect strong sensitivity to the fundamental phases in the supersymmetric Lagrangian. To this end we here discuss the behavior of the relevant cross sections and polarization components using the approximate diagonalization of the neutralino mass matrix described by eqs.(2.17)–(2.19).

We begin with the cross sections for selectron pair production. All modes receive $\mathcal{O}(M_Z^0)$ contributions from the exchange of the bino–like neutralino; in case of $\tilde{e}_L$ pair production the exchange of the wino–like neutralino also contributes at order M_Z^0. The $\tilde{e}_L^-\tilde{e}_L^-$ mode is the only one which has a phase sensitivity to order M_Z^0, where the cross section is sensitive to the relative phase between M_1 and M_2. The other cross sections show phase sensitivity only at order M_Z^2. This is due to both the exchange of heavier, Higgsino–like neutralinos which develop gaugino components at $\mathcal{O}(M_Z)$, and due to the $\mathcal{O}(M_Z^2)$ corrections to the gaugino components of the gaugino–like neutralinos; the importance of these latter contributions explains why we included the $\mathcal{O}(M_Z^2)$ quantities δ_{12} and δ_{21}, and included the normalization factors $N_{1,2}$, in eqs.(2.17) and (2.18). The $\mathcal{O}(M_Z^2)$ shifts $\delta m_{1,2}$ of the masses of the gaugino–like neutralinos also affect the

selectron production cross sections, either directly (if the physical masses are allowed to vary with the phases), or indirectly (if physical masses are kept fixed, in which case the absolute values of the input parameters have to be varied along with the phases); since $\mathcal{O}(M_Z^2)$ shifts of $|M_1|$, M_2 and $|\mu|$ change the eigenstates $\tilde{\chi}_i^0$ only at $\mathcal{O}(M_Z^3)$, we will ignore such indirect effects in the following. Since $\tilde{e}_R$ does not have $SU(2)$ interactions, $\sigma(\tilde{e}_R^-\tilde{e}_R^\pm)$ are at $\mathcal{O}(M_Z^2)$ only sensitive to the phase combination $\phi_1 + \phi_\mu$, whereas the other modes are also sensitive to* ϕ_1 and ϕ_μ. One should also bear in mind that the phase sensitivity of the diagonal $\tilde{e}^+\tilde{e}^-$ production channels is further diluted by the presence of large $s-$channel (γ and Z exchange) contributions, which do not depend on any phase.

	$\cos(\phi_\mu + \phi_1)$	$\cos\phi_\mu$	$\cos\phi_1$
$\tilde{e}_L^-\tilde{e}_L^+$	$\sin 2\beta \frac{M_Z^2\lvert M_1\rvert}{M_2^2\lvert\mu\rvert}$	$\sin 2\beta \frac{M_Z^2}{M_2\lvert\mu\rvert}$	$\frac{M_Z^2\lvert M_1\rvert}{M_2\lvert\mu\rvert^2}$
$\tilde{e}_L^-\tilde{e}_R^+$	$\sin 2\beta \frac{M_Z^2}{\lvert M_1\mu\rvert}$	$\sin 2\beta \frac{M_Z^2}{M_2\lvert\mu\rvert}$	$\frac{M_Z^2 M_2}{\lvert M_1\rvert\lvert\mu\rvert^2}$
$\tilde{e}_R^-\tilde{e}_R^+$	$\sin 2\beta \frac{M_Z^2\lvert M_1\rvert}{\lvert\mu\rvert^3}$	none	none
$\tilde{e}_L^-\tilde{e}_L^-$	$\sin 2\beta \frac{M_Z^2}{M_2\lvert\mu\rvert}$	$\sin 2\beta \frac{M_Z^2}{M_2\lvert\mu\rvert}$	$\frac{\lvert M_1\rvert}{M_2}$
$\tilde{e}_L^-\tilde{e}_R^-$	$\sin 2\beta \frac{M_Z^2\lvert M_1\rvert}{M_2^2\lvert\mu\rvert}$	$\sin 2\beta \frac{M_Z^2}{M_2\lvert\mu\rvert}$	$-\frac{M_Z^2\lvert M_1\rvert}{M_2\lvert\mu\rvert^2}$
$\tilde{e}_R^-\tilde{e}_R^-$	$\sin 2\beta \frac{M_Z^2}{\lvert M_1\mu\rvert}$	none	none

Table 2: Phase dependence of the cross sections for selectron pair production in e^+e^- as well as e^-e^- annihilation for fixed physical neutralino masses. Each entry gives the dependence of the coefficient of the indicated (combination of) phase(s) on the supersymmetric parameters relative to the leading (phase–independent) contribution to this cross section, under the assumption $|M_1|^2 < M_2^2 \ll |\mu|^2$. "None" means that the corresponding term does not exist to $\mathcal{O}(M_Z^2)$. The cross section for $\tilde{e}_L^-\tilde{e}_L^-$ production also has terms $\propto \cos(2\phi_1 + \phi_\mu)$ and $\propto \cos(\phi_\mu - \phi_1)$, but with small coefficients $\propto \sin 2\beta M_Z^2/(|\mu|^3)$.

The phase dependence of the selectron production cross sections for fixed physical neutralino masses is summarized in Table 2. Here we show the coefficients of the various phase–dependent terms that can appear, relative to the leading (phase–independent) contribution to this cross section. We have omitted numerical factors, including factors involving the weak mixing angle. Nevertheless we can draw some conclusions from this table. First, we notice that the dependence on the phase ϕ_μ shown in the second and third columns vanishes like $1/\tan\beta$ for $\tan\beta \gg 1$. The reason is that the dependence on this phase in the neutralino mass matrix could be rotated†

*Recall that $\phi_2 \equiv 0$ in our convention.

†This rotation does not introduce any phase in those parts of $f\tilde{f}\tilde{\chi}$ vertices that come from gauge interactions, but *does* introduce a phase in the Yukawa contribution to these vertices. Recall that these Yukawa contributions can be ignored when calculating cross sections, but have to be kept when computing leptonic dipole moments. This explains why the ϕ_μ dependence of d_e and a_μ is not suppressed at large $\tan\beta$.

into the off–diagonal gaugino–Higgsino mixing entries $\propto \cos\beta$. However, the dependence on the relative phase between the two soft gaugino masses does not vary with $\tan\beta$.

Second, with the exception of the $\tilde{e}^-_L\tilde{e}^-_L$ mode, all phase dependence vanishes as $|\mu| \to \infty$, but the $|\mu|$ dependence varies for different modes. In particular, the phase dependence of the diagonal mode $\tilde{e}^-_R\tilde{e}^+_R$ vanishes $\propto 1/|\mu|^3$ for large $|\mu|$, whereas all other cross sections receive phase–dependent contributions that only fall like $1/|\mu|$; however, for $\tan\beta \to \infty$ the $|\mu|-$dependence of the total phase sensitivity becomes stronger, as can be seen in the last column. In most cases the leading phase dependence comes from the exchange of the lighter, gaugino–like, neutralinos. The exception is the $\tilde{e}^-_R\tilde{e}^-_R$ mode, where the the exchange of the heavier, Higgsino–like states contributes at the same order.

Clearly the LL mode will have the strongest phase dependence of all $\tilde{e}^-\tilde{e}^-$ channels [38], and indeed of all selectron production channels, since it already occurs at $\mathcal{O}(M_Z^0)$, as noted earlier. The phase–dependent terms in $\tilde{e}^-_L\tilde{e}^+_L$ and $\tilde{e}^-_L\tilde{e}^+_R$ production are of similar size. For our choice of parameters the second mode is preferable, since it is accessible at lower energies, and since the cross section near threshold scales like $\sqrt{\lambda}$, rather than like $\lambda^{3/2}$. Finally, the relative importance of phase–sensitive and phase–insensitive terms in most selectron production cross sections does not depend strongly on the beam energy. We therefore expect the best statistical accuracy for the determination of the relevant phases when the beam energy is chosen such that the cross section being investigated is maximal.

So far we have kept the physical neutralino masses fixed, which means that $|M_1|$, M_2 and $|\mu|$ have to be varied along with the phases; we saw above that this affects the cross sections only at $\mathcal{O}(M_Z^2)$ relative to the leading term. If instead these input parameters are held fixed, the physical neutralino masses will vary at $\mathcal{O}(M_Z^2)$. Of particular interest are the masses of the gaugino–like states, whose exchange gives much bigger contributions to the matrix elements than that of the Higgsino–like neutralinos. The relevant mass shifts are given in eqs.(2.19). We see that these effects also vanish $\propto 1/\tan\beta$ for large $\tan\beta$. However, they only scale like $1/|\mu|$ for large $|\mu|$. They will therefore dominate the total phase dependence of the $\tilde{e}^+_R\tilde{e}^-_R$ production cross section. For the other modes, the dependence on $\cos(\phi_1+\phi_\mu)$ and on $\cos\phi_\mu$ that comes from the variation of the masses of the gaugino–like neutralinos is qualitatively the same as shown in Table 2, if we ignore factors $|M_1|/M_2$. A more detailed analysis is therefore required to decide which source of phase dependence dominates. However, in case of $\tilde{e}^-_L\tilde{e}^-_L$ production the total phase dependence is still dominated by the $\mathcal{O}(M_Z^0)$ term from bino–wino interference.

We now turn to the cross sections for neutralino pair production in e^+e^- annihilation, $\sigma_{ij} \equiv \sigma(e^+e^- \to \tilde{\chi}^0_i\tilde{\chi}^0_j)$. We first note that of the 10 distinct cross sections, only four receive $\mathcal{O}(M_Z^0)$ contributions: the cross sections σ_{11}, σ_{12} and σ_{22} describing the production of two gaugino–like neutralinos receive large contributions from selectron exchange in the $t-$ or $u-$channel, while σ_{34} receives large contributions from Z exchange in the $s-$channel. The cross sections σ_{33} and σ_{44} describing the production of two equal Higgsino–like states receive non–vanishing contributions only at $\mathcal{O}(M_Z^4)$, whereas the cross sections for the production of one Higgsino–like and one gaugino–like state start at $\mathcal{O}(M_Z^2)$.

Only σ_{12} has sensitivity to some phase (in this case, ϕ_1) at order M_Z^0. All other cross sections are sensitive to phases only at order M_Z^2 or even M_Z^4. The strong phase sensitivity of

σ_{12} can be traced to the Q_2-term in eq.(5.26). It comes from the fact [31] that the production of two Majorana fermions is $P-$wave suppressed near threshold if they have the same relative CP–phase, whereas any difference in this phase leads to an $S-$wave contribution to the cross section. This effect can be probed with optimal statistical significance rather close to threshold, in this case for $\sqrt{s}$ not too much above $|M_1| + M_2$.

The $\mathcal{O}(M_Z^2)$ phase–dependent terms in the neutralino production cross sections should be most easily observable in the mixed "gaugino–Higgsino" final states, since here the cross sections also only start at $\mathcal{O}(M_Z^2)$, as remarked above. Note that the two Higgsino–like neutralinos are closely mass–degenerate in the limit $|\mu^2| \gg M_Z^2$. This makes it very difficult to experimentally distinguish between the production of $\tilde{\chi}_3^0$ and $\tilde{\chi}_4^0$. In the following discussion we therefore always sum over these two Higgsino–like states. Once this has been done, we again find that all terms involving ϕ_μ come with a factor $\sin 2\beta$, and are thus suppressed at large $\tan\beta$. These cross sections also contain terms $\propto \cos(\phi_1 - \phi_\mu)$ and $\cos(2\phi_1 + \phi_\mu)$, which result from the rephasing–invariant combinations of phases $\pm(\phi_1 - \phi_2) - (\phi_{2,1} + \phi_\mu)$ in our convention $\phi_2 = 0$. Altogether we find the following phase–dependent terms in these two cross sections:

$$\sigma_{1\tilde{h}} \equiv \sigma_{13} + \sigma_{14} \,:\, \cos(\phi_\mu + \phi_1) \left(\frac{\sin 2\beta |M_1|}{|\mu|}, \, \frac{\sin 2\beta |\mu M_1|}{s} \right); \, \cos\phi_\mu \left(\frac{\sin 2\beta M_2}{|\mu|}, \, \frac{\sin 2\beta |M_1|^2 M_2}{|\mu| s} \right); \\ \cos(\phi_1 - \phi_\mu) \frac{\sin 2\beta |M_1| M_2^2}{|\mu| s}; \, \cos\phi_1 \left(\frac{|M_1| M_2}{|\mu|^2}, \, \frac{|M_1| M_2}{s} \right); \tag{5.33a}$$

$$\sigma_{2\tilde{h}} \equiv \sigma_{23} + \sigma_{24} \,:\, \cos(\phi_\mu + \phi_1) \left(\frac{\sin 2\beta |M_1|}{|\mu|}, \, \frac{\sin 2\beta |M_1| M_2^2}{|\mu| s} \right); \, \cos\phi_\mu \left(\frac{\sin 2\beta M_2}{|\mu|}, \, \frac{\sin 2\beta |\mu| M_2}{s} \right); \\ \cos(2\phi_1 + \phi_\mu) \frac{\sin 2\beta |M_1|^2 M_2}{|\mu| s}; \, \cos\phi_1 \left(\frac{|M_1| M_2}{|\mu|^2}, \, \frac{|M_1| M_2}{s} \right). \tag{5.33b}$$

A common factor $\propto \alpha^2 M_Z^2/(|\mu|^2 s)$, characterizing the size of the leading phase–independent contributions, has been factored out. Here we have listed the $s-$dependent contributions coming from the terms $\propto Q_2$ separately, where present. Note that they usually have a different dependence[‡] on $|\mu|$ than the terms that survive for $s \to \infty$. We conclude from eqs.(5.33) that $\sigma_{1\tilde{h}}$ might show a somewhat stronger overall phase dependence in the region of parameter space allowed by low–energy data, since it depends on the potentially large phase $\phi_1 + \phi_\mu$ through terms with fewer powers of $|\mu|$ in the denominator than $\sigma_{2\tilde{h}}$ does, whereas the dependence on $\cos\phi_1$ is parametrically the same in both cases. This is fortunate, since the $1\tilde{h}$ mode is accessible at lower energies. Finally, note that the phase dependence of the neutralino masses affects these cross sections only at $\mathcal{O}(M_Z^4)$.

We do not list the $\mathcal{O}(M_Z^2)$ phase dependent terms of the cross sections that receive $\mathcal{O}(M_Z^0)$ contributions, since these will clearly be much more difficult to measure.

The situation concerning chargino pair production is rather similar. Here both diagonal modes start at $\mathcal{O}(M_Z^0)$, but receive phase–dependent contributions only at $\mathcal{O}(M_Z^2)$. In case

[‡]In some cases these threshold terms seem to grow with increasing $|\mu|$. However, $\sigma_{1\tilde{h}}$ ($\sigma_{2\tilde{h}}$) is accessible only for $\sqrt{s} > |M_1| + |\mu|$ ($\sqrt{s} > M_2 + |\mu|$), i.e $|\mu|^2/s < 1$ in the physical region.

of the off–diagonal mode[§] both the cross section and the phase dependence starts at $\mathcal{O}(M_Z^2)$; indeed, the phase dependence is very similar to that in eq.(5.33b) with $\phi_1 \to 0$, since the $U(1)_Y$ gaugino mass does not appear in the chargino mass matrix.

Finally the results for perturbative neutralino mixing may be applied to the polarization vector components of the neutralinos produced in $e^+e^- \to \tilde{\chi}_i^0 \tilde{\chi}_j^0$ as calculated in Sec. 5.6. Here we only discuss the normal component as it is the only CP–odd quantity available if neutralino decays are not included explicitly. Recall that a non–vanishing P_N can only occur for final states consisting of two *different* neutralinos. We find that the numerators in eqs.(5.32) receive $\mathcal{O}(M_Z^0)$ contributions only for the (12) mode; in case of the $(1\tilde{h})$ and $(2\tilde{h})$ modes the numerator starts at $\mathcal{O}(M_Z^2)$, just like the corresponding total cross sections, and hence the denominators in (5.32). In all these cases P_N will therefore receive $\mathcal{O}(M_Z^0)$ contributions. On the other hand, P_N for the $\tilde{h}\tilde{h}$ [or (34)] mode vanishes to $\mathcal{O}(M_Z^2)$; this final state is therefore of little interest in the present context. Explicitly, for (12) production we find to $\mathcal{O}(M_Z^0)$:[¶]

$$P_N^{2,12} = \frac{-4\sqrt{\lambda_{12}}\frac{|M_1|}{\sqrt{s}}\sqrt{1-z^2}\sin\phi_1}{(1-\Delta_{12}^2+\lambda_{12}z^2)\frac{\left(D_t^L\right)^2+\left(D_u^L\right)^2}{D_t^L D_u^L} - 8\frac{|M_1|M_2}{s}\cos\phi_1 + 2\sqrt{\lambda_{12}}z\frac{\left(D_t^L\right)^2-\left(D_u^L\right)^2}{D_t^L D_u^L}}, \tag{5.34}$$

where $z = \cos\theta$. As expected for a CP–odd quantity the dominant dependence on ϕ_1 is through a sine function, while the denominator (basically the differential cross section discussed above) contains a CP–even dependence on ϕ_1 through a cosine.

Due to their mass degeneracy we have to average P_N for the mixed gaugino–Higgsino modes over the production of both Higgsino–like neutralinos. Using the event numbers N as weights, we obtain:

$$P_N^{i,i\tilde{h}} = \frac{N_{i3}P_N^{i,i3} + N_{i4}P_N^{i,i4}}{N_{i3}+N_{i4}}, \quad i = 1,2. \tag{5.35}$$

This amounts to replacing the quartic charges in eq. (5.32) by:

$$Q_k^{i\tilde{h}} = Q_k^{i3} + Q_k^{i4}. \tag{5.36}$$

The calculation of the relevant quartic charges $Q_4^{i\tilde{h}}$ to $\mathcal{O}(M_Z^2)$ is now straightforward, if somewhat tedious. We find the following terms, factoring out $\alpha^2 M_Z^2/|\mu|^2$:

$$Q_4^{1\tilde{h}} \;:\; \sin(\phi_1+\phi_\mu)\sin 2\beta;\; \sin\phi_\mu\frac{\sin 2\beta|M_1|M_2}{|\mu|^2};\; \sin(\phi_1-\phi_\mu)\frac{\sin 2\beta M_2^2}{|\mu|^2};\; \sin\phi_1\frac{M_2}{|\mu|}; \tag{5.37a}$$

$$Q_4^{2\tilde{h}} \;:\; \sin(\phi_1+\phi_\mu)\frac{\sin 2\beta|M_1|M_2}{|\mu|^2};\; \sin\phi_\mu\sin 2\beta;\; \sin(\phi_\mu+2\phi_1)\frac{\sin 2\beta|M_1|^2}{|\mu|^2};$$
$$\sin\phi_1\frac{|M_1|}{|\mu|}. \tag{5.37b}$$

[§]In principle $\tilde{\chi}_1^-\tilde{\chi}_2^+$ production is now distinguishable from $\tilde{\chi}_1^+\tilde{\chi}_2^-$ production. However, the two cross sections differ only in the presence of an absorptive phase, i.e. after including loop corrections.

[¶]Eqs.(5.32) show that $|P_N^{1,12}|$ is larger than $|P_N^{2,12}|$ by a factor $M_2/|M_1| \simeq 2$. However, we assume that $\tilde{\chi}_1^0$ is the LSP, and hence stable (if R–parity is conserved), so that its spin cannot be measured.

The terms in eqs.(5.37) directly correspond to terms in P_N, up to an additional factor of $|M_1|/\sqrt{s}$ ($|\mu|/\sqrt{s}$) for $P_N^{\tilde{h},1\tilde{h}}$ ($P_N^{2,2\tilde{h}}$), since the dependence of the leading term in the denominator in eq.(5.32) on SUSY parameters has already been factored out. As expected, the phase dependence is through sine functions here, and all terms that are sensitive to ϕ_μ are suppressed at large $\tan\beta$. The first term in $Q_4^{1\tilde{h}}$ gives rise to a contribution to $P_N^{\tilde{h},1\tilde{h}}$ that remains finite as $|\mu| \to \infty$, but vanishes $\propto 1/\tan\beta$ for large $\tan\beta$. On the other hand, in the $(2\tilde{h})$ mode we can measure the polarization of the lighter gaugino–like neutralino, giving rise to an extra factor $|\mu|/\sqrt{s}$. We thus see that (as long as $\sqrt{s} > |\mu| + M_2$) the second term in eq.(5.37b) gives a contribution to $P_N^{2,2\tilde{h}}$ that *rises* with increasing $|\mu|$. However, for the range of $|\mu|$ of interest to us, this term is suppressed by the stringent upper limit on $|\sin\phi_\mu|$, see Sec. 4.3; only in scenario B2 with small $\tan\beta$ can it reach comparable magnitude as the last term in eq.(5.37b). This last term leads to a contribution to $P_N^{2,2\tilde{h}}$ that approaches a constant for large $|\mu|$, *and* remains finite for large $\tan\beta$. We therefore conclude that $(2\tilde{h})$ production should allow a somewhat more sensitive direct probe of CP violation than $(1\tilde{h})$ production. Finally, the normal components of the polarization vectors in $\tilde{\chi}_1^\pm\tilde{\chi}_2^\mp$ production have similar structure as eq.(5.37b) with $\phi_1 \to 0$, but receive additional contributions from the Z coupling to the gaugino component of the heavy chargino state $\tilde{\chi}_2^\pm$.

6 Significances

Our aim in this Section is to introduce objects quantifying the impact of CP–odd phases on total cross sections, which are CP–even quantities. To this end we compare the difference in counting rates between a CP–conserving point in parameter space (CPC: all phases $\phi_i = 0$ or π) and a CP–violating one (CPV: identical absolute values, but $\phi_i \neq 0$ and low–energy compatible) to the statistical error at the CPC point. This determines the significance $\mathcal{S}$ with which a deviation from the cross section predicted for the CPC point can be measured. It can be written as

$$\mathcal{S} = \frac{\Delta N_{\rm CPC-CPV}}{\delta N_{\rm CPC}} = \frac{N_{\rm CPC} - N_{\rm CPV}}{\sqrt{N_{\rm CPC}}}. \tag{6.1}$$

Since there are two CP–conserving values $(0, \pi)$ for each phase, we have to deal with eight CPC points for each set of absolute values, and hence the same number of significances is available for each kinematical accessible cross section. The smallest of these evidently determines the statistical significance with which the presence of CP–violating phases can be inferred from this cross section for given values of the absolute values of all SUSY parameters. We therefore define as our final measure of the sensitivity of a given cross section to phases the significance

$$\mathcal{S}\left(f_i f_j\right) = \min_n \left(\frac{|\sigma_{f_i f_j}^{\rm CPV} - \sigma_{f_i f_j}^{{\rm CPC}_n}|}{\sqrt{\sigma_{f_i f_j}^{{\rm CPC}_n}}} \right) \times \sqrt{\mathcal{L}}, \tag{6.2}$$

where $\sigma_{f_i f_j}$ is the total cross section for $e^- e^\pm \to f_i f_j$, and $n = 1, \ldots, 8$; we only include CPC points which are low–energy compatible.† Finally, $\mathcal{L}$ is the integrated luminosity, which is expected to be different for the e^+e^- and e^-e^- options.

In the procedure outlined so far, the CPC and CPV points have the same absolute values of M_1, M_2 and μ. This means that these points will in general have *different* physical neutralino and chargino masses [43]. Recall that the phase dependence of the $\tilde{\chi}$ masses is suppressed by $M_Z^2/(|\mu| m_{\tilde{\chi}})$, see eq.(2.19). Nevertheless, changes of several percent are possible, in particular in the neutralino sector. This could lead to similar changes in the cross sections through kinematical factors (in $\tilde{\chi}$ production) or through neutralino propagator factors (in $\tilde{e}$ production). Moreover, these masses are often more easily measurable than the cross sections which are the focus of this analysis.

We therefore introduce a second set of significances $\bar{\mathcal{S}}$ where CPC and CPV points have the same physical masses for $\tilde{\chi}_1^0, \tilde{\chi}_3^0$ and $\tilde{\chi}_1^\pm$; in the limit of large $\tilde{\chi}$ masses and for our choice $|\mu| \geq M_2 > |M_1|$, these three masses essentially fix $|M_1|$, $|\mu|$ and M_2, respectively. Note that we only have three (dimensionful) absolute values that can be adjusted in the neutralino and chargino mass matrices. We can therefore not guarantee that all chargino and neutralino masses are the same in the CPC and CPV points. However, after ensuring that these three $\tilde{\chi}$ masses are the same in both points, the remaining variation of the other three $\tilde{\chi}$ masses between the CPC and CPV points is quite small. For technical reasons we keep $|M_1|$, M_2 and $|\mu|$ fixed (at the values listed in Table 1) for the CPC points, and adjust them at the CPV points. Since the eight CPV points have four different $\tilde{\chi}$ mass spectra, a given set of phases now also produces several different CPC points. The new significance can thus be written as

$$\bar{\mathcal{S}}\,(f_i f_j) = \min_n \left(\frac{|\sigma_{f_i f_j}^{\overline{\mathrm{CPV}}_n} - \sigma_{f_i f_j}^{\mathrm{CPC}_n}|}{\sqrt{\sigma_{f_i f_j}^{\mathrm{CPC}_n}}} \right) \times \sqrt{\mathcal{L}}. \tag{6.3}$$

Our algorithm for calculating the significances can be summarized as follows:

- Select a CPV point. For a set of the absolute values of the relevant SUSY parameters, as listed in Table 1 for our three scenarios B1, B2 and B3, this amounts to randomly choosing values for the phases ϕ_A, ϕ_μ and ϕ_1. Repeat this step until a point that is compatible with the low–energy constraints has been found.

- For each process, find the low–energy allowed CPC point that minimizes $\mathcal{S}(f_i f_j)$ as defined in eq.(6.2). Note that there are only eight CPC points for each scenario B1, B2 and B3 if $\tan\beta$ is kept fixed; however, this procedure in general selects different CPC points for different processes. This completes the calculation of the $\mathcal{S}$.

- Define four new CPV points $\overline{\mathrm{CPV}}_n$ by adjusting $|M_1|$, M_2 and $|\mu|$ such that $m_{\tilde{\chi}_1^0}$, $m_{\tilde{\chi}_1^\pm}$ and $m_{\tilde{\chi}_3^0}$ are the same in points $\overline{\mathrm{CPV}}_n$ and CPC_n.

†Since $\sigma_{f_i f_j}$ does not depend on ϕ_A, there are only four different values of $\sigma_{f_i f_j}^{\mathrm{CPC}_n}$ for a given CPV point. However, occasionally both $\phi_A = 0$ and $\phi_A = \pi$ have to be checked to find a CPC point that is compatible with the bound on a_μ. Of course, the bound on d_e is trivially satisfied by all CPC points.

- Calculate the $\bar{\mathcal{S}}\,(f_i f_j)$ as in eq.(6.3).

Note that $\mathcal{S}$ and $\bar{\mathcal{S}}$ only measure *statistical* significances. In addition there will be systematic uncertainties, both from experiment and theory. We have little to say about experimental systematic errors, except that we hope that they will be small. A theoretical error is introduced since our cross sections can only be predicted with finite precision. At tree–level these cross sections are determined uniquely by the parameters listed in Table 1, plus a few SM parameters that are already now known with high precision. However, explicit calculations for $\tilde{\chi}_1^\pm$ pair production show that quantum corrections can easily amount to $\mathcal{O}(10\%)$ [44]. Some of these corrections can be calculated unambiguously once the parameters listed in Table 1 are specified, but the remaining corrections can still amount to several percent. In particular, the lepton–slepton–gaugino "gauge couplings" depend (logarithmically) on the squark mass scale [45]. The production of Higgsino–like charginos [44] and, presumably, neutralinos also depends on the parameters appearing in third generation sfermion masses. These corrections will only be calculable once the parameters of the (presumably quite heavy) squark sector have been determined. Until this has happened, out of two processes with roughly equal significances as defined above, the process with a *smaller* cross section should be preferred, since here a given significance corresponds to a *larger* relative variation of the cross section with the phases.

7 Numerical Analysis

We are now ready to present numerical results for our high–energy observables. We will first discuss the impact of the CP–phases on the (CP–even) cross sections, before turning to the (T–odd) normal components of $\tilde{\chi}$ polarization vectors. Finally, in Sec. 7.3 we will study correlations between phase–sensitive quantities.

7.1 Cross sections

As discussed in Sec. 4.3, we chose our SUSY parameters such that selectron pair production as well as the production of two lighter neutralinos or charginos is possible already at the first stage of a future linear e^+e^- collider (LC) operating at $\sqrt{s} = 500$ GeV, which is our default choice. However, in scenario B2 the Higgsino–like states are not accessible at this energy. In this scenario we therefore take $\sqrt{s} = 800$ GeV when discussing reactions where at least one $\tilde{\chi}_3^0$, $\tilde{\chi}_4^0$ or $\tilde{\chi}_2^\pm$ state is produced; note that all current LC designs foresee an upgrade to at least that energy. A similar treatment is used in scenario B3, except for the $\tilde{\chi}_1^0\tilde{\chi}_{3,4}^0$ final state, which is already accessible at $\sqrt{s} = 500$ GeV in this case.

In Table 3 we show the maximal allowed cross sections for the 19 different production channels discussed in Sec. 5, for our three scenarios B1, B2 and B3, and the same choices of $\tan\beta$ employed in Sec. 4.3. Only combinations of phases that are allowed by the low–energy constraints on d_e and a_μ have been included in the maximization. These cross sections have been calculated at tree–level, as described in Secs. 5.2–5.5. We have also ignored corrections due to initial–state radiation and beamstrahlung. These effects are often larger than the dependence

on CP–violating phases; they should therefore certainly be included in any future experimental analysis (along with radiative corrections, which will likely be known well before the first LC commences operations). However, they are largely independent of CP–phases, and should therefore not affect our conclusions.

	B1		B2		B3	
$\tan\beta$	3	12	3	12	10	20
$\tilde{e}^-_R\tilde{e}^-_R$	378	371	398	390	513	512
$\tilde{e}^-_L\tilde{e}^-_R$	79.8	79.0	80.3	75.1	181	182
$\tilde{e}^-_L\tilde{e}^-_L$	272	261	281	270	523	378
$\tilde{e}^-_R\tilde{e}^+_R$	180	172	182	176	296	293
$\tilde{e}^-_L\tilde{e}^+_R$	106	104	96.5	94.5	168	160
$\tilde{e}^-_L\tilde{e}^+_L$	8.3	7.2	8.0	6.9	60.9	60.3
$\tilde{\chi}^-_1\tilde{\chi}^+_1$	250	212	144	126	175	170
$\tilde{\chi}^-_1\tilde{\chi}^+_2$	179	173	16.0*	7.5*	43.6*	38.7*
$\tilde{\chi}^-_2\tilde{\chi}^+_2$	–	–	–	–	85.9*	89.4*
$\tilde{\chi}^0_1\tilde{\chi}^0_1$	201	197	236	231	271	271
$\tilde{\chi}^0_1\tilde{\chi}^0_2$	130	120	140	132	159	161
$\tilde{\chi}^0_1\tilde{\chi}^0_3$	46.8	41.2	6.4*	5.7*	20.1	19.7
$\tilde{\chi}^0_1\tilde{\chi}^0_4$	52.8	53.7				
$\tilde{\chi}^0_2\tilde{\chi}^0_2$	74.6	49.6	58.5	49	76.2	68.9
$\tilde{\chi}^0_2\tilde{\chi}^0_3$	73.6	77.7	5.1*	5.2*	22.3*	21.4*
$\tilde{\chi}^0_2\tilde{\chi}^0_4$	27.1	22.8				
$\tilde{\chi}^0_3\tilde{\chi}^0_3$	0.26	0.43	–	–	38.3*	38.6*
$\tilde{\chi}^0_3\tilde{\chi}^0_4$	36.6	36.0				
$\tilde{\chi}^0_4\tilde{\chi}^0_4$	–	–				

Table 3: Maximal values of the total cross sections [in fb] for unpolarized $e^\pm$ beams, for the scenarios defined in Table 1. "–" means that the corresponding mode is not accessible. In scenarios B2 and B3 we have summed over the production of the heavy Higgsino–like neutralinos, as described in the text. The beam energy is 500 GeV in most cases, but has been raised to 800 GeV for the production of $\tilde{\chi}^\pm_2$ and $\tilde{\chi}^0_{3,4}$ states in scenarios B2 and B3, as indicated by the asterisk. Note that the charge–conjugate mode is included, if it is distinct from the listed one.

We saw in Secs. 2.3 and 5.7 that the two heaviest, Higgsino–like neutralinos are close in mass if $|\mu| > M_2$ and $|\mu|^2 \gg M_Z^2$; the degeneracy between these states is only lifted at

$\mathcal{O}(M_Z^2/[|\mu|^2 - M_2^2])$ (as well as by radiative corrections, which however are sizable only in the presence of large $A-$terms in the stop sector [46]). Numerically, we find that the relative difference between $m_{\tilde{\chi}_4^0}$ and $m_{\tilde{\chi}_3^0}$ ranges from 24 to 35% in scenario B1, but only from 0.2 to 3.5% (0.1 to 7.5%) in B2 (B3). Since the production of nearly degenerate particles is difficult to distinguish experimentally, we simply sum over the production of $\tilde{\chi}_3^0$ and $\tilde{\chi}_4^0$ in scenarios B2 and B3; in particular, we only give results for a single process of heavy Higgsino–like neutralino pair production in these cases. Recall that we used the same treatment in Sec. 5.7, eqs.(5.33) and (5.35)–(5.37).

As well known [39, 41] many of our cross sections can be enhanced by factors of a few if both beams are polarized. Moreover, the discussion of Sec. 5.7 indicates that the greatest sensitivity to phases comes (through ϕ_1) from the interference of $SU(2)$ and $U(1)_Y$ interactions; these contributions will be suppressed if one chooses e_R^- beams, since e_R^- is a singlet under $SU(2)$. However, the sensitivity to other combinations of phases is enhanced for different choices of beam polarizations. We therefore only show results for unpolarized beams, with the understanding that in many cases the cross section (phase sensitivity) could be enhanced by up to a factor of 4 (2) if fully polarized beams were available.

We see from Table 3 that the cross sections for selectron pair production are generically bigger at e^-e^- colliders than at e^+e^- colliders [37]. This difference is only partially compensated by the higher e^+e^- luminosity; we assume $\int \mathcal{L}dt = 500$ (100) fb^{-1} for e^+e^- (e^-e^-) collisions. We use these relatively conservative values since we do not include efficiency factors. These are expected to reduce the actually available event samples by factors of a few, the precise values depending on both the process under consideration and the sparticle spectrum. Moreover, at e^-e^- colliders the diagonal, chirality–conserving modes have higher cross section than the off–diagonal, chirality–violating mode; recall that the latter is $P-$wave suppressed near threshold, and vanishes for vanishing gaugino masses. At e^+e^- colliders the diagonal selectron production modes are $P-$wave suppressed; this explains the rather small cross sections for $\tilde{e}_L^+\tilde{e}_L^-$ production. Finally, the selectron production cross sections are highest in scenario B3, since the selectron masses are somewhat smaller than in the other two cases; this effect is particularly significant for $\tilde{e}_L^-\tilde{e}_L^+$ production, which is a $P-$wave process quite close to threshold. The strong $\tan\beta$ dependence of the maximal $\tilde{e}_L^-\tilde{e}_L^-$ production cross section in this scenario follows from the fact that the region near $\phi_1 = \phi_\mu = 0$ is excluded by the a_μ constraint for $\tan\beta = 20$, see Fig. 2f.

The biggest cross sections at e^+e^- collisions are those for $\tilde{e}_R^+\tilde{e}_R^-$, $\tilde{\chi}_1^+\tilde{\chi}_1^-$ and $\tilde{\chi}_1^0\tilde{\chi}_1^0$ production. However, the latter leads to an invisible, and hence undetectable, final state if $\tilde{\chi}_1^0$ is a stable LSP; we will therefore not analyze it any further. The cross sections for producing two heavy charginos or neutralinos are suppressed both by phase space and by their Higgsino–like nature. However, the production of one light and one heavy $\tilde{\chi}$ state is possible in all three cases. Since, as discussed in Sec. 5.7, these cross sections are non–vanishing only in the presence of gaugino–Higgsino mixing, they fall with increasing $|\mu|$. However, even in scenario B2 one will have several thousand events containing these Higgsino–like states. For the other channels, typically several tens of thousands of events will be available, meaning that the cross sections could be measured with statistical uncertainty of 1% or less.

The maximal possible values of the significances $\mathcal{S}$ and $\bar{\mathcal{S}}$ of eqs.(6.2) and (6.3) that can be

found in our three scenarios are summarized in Table 4. The $\tilde{e}_L^- \tilde{e}_L^-$ mode shows the strongest phase dependence of all selectron production channels, i.e. the highest significance, largely independent of $|\mu|$ and $\tan\beta$; the $\tan\beta$ dependence of $\mathcal{S}$ in scenario B3 is due to the fact that the point $\phi_1 = \phi_\mu = 0$ is excluded by the a_μ constraint at $\tan\beta = 20$, but still allowed at $\tan\beta = 10$, as shown in Fig. 2c. The mixed $\tilde{e}_L^- \tilde{e}_R^+$ mode is the for our purposes most promising selectron production mode at e^+e^- colliders. It would allow to unambiguously detect (at more than five statistical standard deviations) the presence of CP–violating phases over much of the allowed parameter space, although the effect diminishes with increasing $|\mu|$ and increasing $\tan\beta$ (except in case B3, for the reason given above). For both these modes $\mathcal{S}$ and $\bar{\mathcal{S}}$ give very similar results. Except for scenario B1 with strong Higgsino–gaugino mixing, $\tilde{e}_R$ pair production at both e^+e^- and e^-e^- colliders is much less promising, especially if the physical masses of $\tilde{\chi}_1^0$, $\tilde{\chi}_1^\pm$ and $\tilde{\chi}_3^0$ are held fixed, i.e. for $\bar{\mathcal{S}}$. All these features can be understood from the discussion of Table 2 in Sec. 5.7.

The small phase sensitivity of the $\tilde{e}_L^- \tilde{e}_L^+$ mode relative to the $\tilde{e}_L^- \tilde{e}_R^+$ mode can partly be explained by the smaller cross section of the former mode; recall that the significances scale with the square root of the number of events. In addition, closer inspection of the matrix elements shows that in case of $\tilde{e}_L^- \tilde{e}_L^+$ production, the terms $\propto \cos\phi_1$ and $\propto \cos(\phi_1 + \phi_\mu)$ are suppressed by extra factors $\sin^2\theta_W$ and $\sin^4\theta_W$ relative to the leading phase–independent terms; for the $\tilde{e}_L^- \tilde{e}_R^+$ mode the corresponding relative factors are 1 and $\sin^2\theta_W$, respectively.

Turning to chargino modes, we observe that they are sensitive to phases only in scenario B2, with large $|\mu|$, and for small $\tan\beta$. The only relevant phase here is ϕ_μ. Recall from the discussion of Sec. 4.3 that the maximal allowed value of this phase scales like $|\mu|^2$. This means that the maximal deviation of $|\cos\phi_\mu|$ from unity scales like $|\mu|^4$. In case of $\tilde{\chi}_1^+ \tilde{\chi}_1^-$ production the main phase sensitivity comes from $m_{\tilde{\chi}_1^\pm}$, which gives an extra factor $\sin 2\beta/|\mu|$. Altogether the maximal $\mathcal{S}(\tilde{\chi}_1^+ \tilde{\chi}_1^-)$ therefore scales like $|\mu|^3 \sin 2\beta$; this reproduces the numerical behavior in scenarios B2 and B3, with small gaugino–Higgsino mixing. A similar argument also holds for the mixed $\tilde{\chi}_1^- \tilde{\chi}_2^+$ mode. However, in this case the cross section itself vanishes in the absence of gaugino–Higgsino mixing. This means that now the phase–dependent terms are of the same order in M_W as the phase–independent ones. Moreover, significant phase dependence now also comes from the $Z\tilde{\chi}_1^- \tilde{\chi}_2^+$ coupling, not only from the chargino masses. Hence both definitions of the significance now give very similar results. Finally, the very strong $\tan\beta$ dependence of these significances in case B2 is due to the fact that values of ϕ_μ near π are only allowed for small $\tan\beta$ in this case, see Fig. 2b.

In contrast to the chargino modes, some neutralino modes are promising for all scenarios we considered. This is true in particular for the (12) mode. We saw in Sec. 5.7 that in this case both the total cross section and the phase dependence (on ϕ_1) already start at $\mathcal{O}(M_Z^0)$, i.e. they are *not* suppressed for large $|\mu|$ or large $\tan\beta$. Indeed, we find that this mode often allows somewhat better sensitivity than the celebrated $\tilde{e}_L^- \tilde{e}_L^-$ mode. The mixed gaugino–Higgsino modes also do well, especially for not too large values of $|\mu|$. As expected from the discussion of eqs.(5.33), the $(1\tilde{h})$ mode is somewhat more promising than the $(2\tilde{h})$ mode. The rather good phase sensitivity of the (22) mode at first seems surprising, given that the phase dependence only enters at $\mathcal{O}(M_Z^2)$, whereas the cross section is $\mathcal{O}(M_Z^0)$. However, closer inspection of the

sensitivities for the (22) and $(1\tilde{h})$ modes shows that the relative factor between them is in fact $\mathcal{O}(|M_1|/M_Z)$, which is close to unity in our case. Note that the relatively large size of the (22) cross section facilitates its precise measurements and therefore increases the significances. However, as remarked at the end of Sec. 6 we still consider the mixed $(1\tilde{h})$ final state to be more promising, since it will be less sensitive to systematic uncertainties.

	B1				B2				B3			
$\tan\beta$	3		12		3		12		10		20	
	$\mathcal{S}$	$\bar{\mathcal{S}}$	$\mathcal{S}$	$\bar{\mathcal{S}}$	$\mathcal{S}$	$\bar{\mathcal{S}}$	$\mathcal{S}$	$\bar{\mathcal{S}}$	$\mathcal{S}$	$\bar{\mathcal{S}}$	$\mathcal{S}$	$\bar{\mathcal{S}}$
$\tilde{e}_R^-\tilde{e}_R^-$	3.7	17.0	0.8	5.0	2.9	1.0	0.8	0.4	0.5	1.1	0.3	0.8
$\tilde{e}_L^-\tilde{e}_R^-$	3.0	10	2.8	4.7	0.9	2.5	0.8	1.3	2.7	4.2	2.9	4.1
$\tilde{e}_L^-\tilde{e}_L^-$	61	60	61	60	59	57	59	59	90	90	136	136
$\tilde{e}_R^-\tilde{e}_R^+$	10	27	2.2	7.8	6.7	1.1	1.8	0.5	4.3	2.6	3.0	2.1
$\tilde{e}_L^-\tilde{e}_R^+$	43	68	32	39	16	16	11	12	20	23	22	24
$\tilde{e}_L^-\tilde{e}_L^+$	1.9	3.3	1.5	0.9	1.2	1.3	0.5	0.7	3.3	4.0	3.5	3.8
$\tilde{\chi}_1^-\tilde{\chi}_1^+$	0.4	0.9	< 0.1	2.5	25	1.6	2.8	0.2	1.3	0.3	0.6	0.6
$\tilde{\chi}_1^-\tilde{\chi}_2^+$	< 0.1	1.8	< 0.1	6.4	$70^\star$	$70^\star$	$3.5^\star$	$3.5^\star$	$2.4^\star$	$1.7^\star$	$1.4^\star$	$2.9^\star$
$\tilde{\chi}_2^-\tilde{\chi}_2^+$	–	–	–	–	–	–	–	–	$1.4^\star$	$1.6^\star$	$0.7^\star$	$1.5^\star$
$\tilde{\chi}_1^0\tilde{\chi}_2^0$	41	46	34	32	81	81	92	92	100	100	94	94
$\tilde{\chi}_1^0\tilde{\chi}_3^0$	56	73	30	29	$9.9^\star$	$10.5^\star$	$6.2^\star$	$6.2^\star$	21.5	23.8	21.1	23.2
$\tilde{\chi}_1^0\tilde{\chi}_4^0$	92	104	82	89								
$\tilde{\chi}_2^0\tilde{\chi}_2^0$	74	90	56	66	11	8.2	5.2	5.2	17	18	18	19
$\tilde{\chi}_2^0\tilde{\chi}_3^0$	16	37	7.0	2.9	$6.0^\star$	$6.2^\star$	$2.9^\star$	$2.8^\star$	$1.9^\star$	$1.1^\star$	$3.1^\star$	$2.0^\star$
$\tilde{\chi}_2^0\tilde{\chi}_4^0$	20	14	5.5	5.6								
$\tilde{\chi}_3^0\tilde{\chi}_3^0$	6.3	5.4	8.4	9.3	–	–	–	–	$2.4^\star$	$3.1^\star$	$2.6^\star$	$3.4^\star$
$\tilde{\chi}_3^0\tilde{\chi}_4^0$	9.3	11	9.3	10								
$\tilde{\chi}_4^0\tilde{\chi}_4^0$	–	–	–	–								

Table 4: The maximal significances $\mathcal{S}$ of eq.(6.2) and $\bar{\mathcal{S}}$ of eq.(6.3) that can be found for choices of phases which are compatible with all low–energy constraints. The scenarios B1, B2 and B3 have been defined in Table 1. Notation and calculational procedures are as in Table 3.

7.2 Polarizations

As emphasized earlier, the significances $\mathcal{S}$ and $\bar{\mathcal{S}}$ strictly speaking only measure deviations from the CP–conserving MSSM; they do not directly measure CP violation. Direct evidence for CP

violation could come from the measurement of the T–odd normal component of $\tilde{\chi}$ polarization vectors introduced in Sec. 5.6. The maximal possible absolute values of these "polarization asymmetries" for scattering angle $\theta = \pi/2$ are summarized in Table 5. Recall that a nonzero asymmetry can emerge only in the production of two *different* $\tilde{\chi}$ states, and that the asymmetry will be larger for the *lighter* of the two final–state particles. However, the polarization can only be measured through the $\tilde{\chi}$ decay products; we therefore do not consider the polarization of $\tilde{\chi}_1^0$, which is probably the LSP.

	i	B1		B2		B3	
$\tan\beta$		3	12	3	12	10	20
$\tilde{\chi}_1^- \tilde{\chi}_2^+$	$\tilde{\chi}_1^-$	1.4	0.2	$57^\star$	$5.2^\star$	$1.6^\star$	$0.9^\star$
$\tilde{\chi}_1^0\tilde{\chi}_2^0$	$\tilde{\chi}_2^0$	6.4	7.8	34	33	31	31
$\tilde{\chi}_1^0\tilde{\chi}_3^0$	$\tilde{\chi}_3^0$ $(\tilde{h})$	22	27	$7.2^\star$	$2.4^\star$	6.3	6.8
$\tilde{\chi}_1^0\tilde{\chi}_4^0$	$\tilde{\chi}_4^0$ $(\tilde{h})$	5.5	6.6				
$\tilde{\chi}_2^0\tilde{\chi}_3^0$	$\tilde{\chi}_2^0$	5.5	6.4	$23^\star$	$7.8^\star$	$9.7^\star$	$9.9^\star$
$\tilde{\chi}_2^0\tilde{\chi}_4^0$	$\tilde{\chi}_2^0$	45	30				
$\tilde{\chi}_3^0\tilde{\chi}_4^0$	$\tilde{\chi}_3^0$ $(\tilde{h})$	4.9	6.8	–	–	$1.9^\star$	$1.8^\star$

Table 5: Maximal absolute values of $P_N^{i,ij}$ in percent. The scattering angle θ is set to $\frac{\pi}{2}$. Notations and conventions are as in Table 3.

We see that the chargino polarization is likely too small to be useful, except in scenario B2 with large $|\mu|$ and small $\tan\beta$. Recall from the discussion at the end of Sec. 5.6 that this asymmetry (for the lighter chargino) scales like $|\mu| \sin 2\beta \sin\phi_\mu$; we saw in Sec. 4.3 that the upper bound on $|\sin\phi_\mu|$ scales like $|\mu|^2$. Altogether the maximal value of P_N of the lighter chargino therefore scales like $|\mu|^3$. The very rapid decrease of this polarization with increasing $\tan\beta$ is partly due to the explicit $\sin 2\beta$ dependence, and partly due to the disappearance of the band around $\phi_\mu \simeq \pi$, see Fig. 2b.

In scenarios with large $|\mu|$ (B2, B3) the $\tilde{\chi}_1^0\tilde{\chi}_2^0$ mode again proves most sensitive to CP–violating phases. Eq.(5.34) shows that in this case a nonzero P_N already emerges at $\mathcal{O}(M_Z^0)$, and remains finite both for large $|\mu|$ and large $\tan\beta$. This describes well the behavior seen in cases where the perturbative diagonalization of the neutralino mass matrix is reliable. Moreover, recall from Table 3 that this mode has a fairly high cross section. This is important, since even for perfect (100%) analyzing power one needs nearly 1,000 events to detect a 10% asymmetry at the 3σ level.

As expected from our earlier discussion of eqs.(5.37), the mixed gaugino–Higgsino modes also have sizable asymmetries even for large $|\mu|$, the heavier $(2\tilde{h})$ mode being more promising. However, the relatively small cross sections of these modes imply that one would need a very large luminosity for a meaningful measurement of polarization asymmetries in these modes,

except in scenario B1 with strong wino–Higgsino mixing. Indeed, in this last case the (13) and (24) modes are far more promising than the (12) mode.

As noted earlier, the spin of the produced $\tilde{\chi}$ particles can only be determined on a statistical basis by (partly) reconstructing their decays. We find it encouraging that recent dedicated studies demonstrated sensitivity to phases in the neutralino mass matrix using T–odd variables constructed in $e^+e^- \to \tilde{\chi}_1^0\tilde{\chi}_i^0$ with $\tilde{\chi}_i^0 \to \tilde{\chi}_1^0\ell^+\ell^-$ [47], $\tilde{\chi}_i^0 \to \tilde{\tau}_1^\pm\tau^\mp \to \tau^+\tau^-\tilde{\chi}_1^0$ [48], and $\tilde{\chi}_i^0 \to \tilde{\chi}_1^0 Z$ [49].

7.3 Correlations between observables

In addition to their absolute sizes, the correlations between various phase–sensitive quantities are also of interest. Such correlations can provide stringent tests of the MSSM, since they are a consequence of the limited number of parameters affecting these leptonic observables in the MSSM. Recall that all our "high–energy" variables (cross sections and polarizations) depend on the phase ϕ_μ; most of them also depend on ϕ_1, the exception being observables related to chargino pair production. We saw in Sec. 4.3 that ϕ_μ is tightly constrained by the "low–energy" observables a_μ and (especially) d_e, while ϕ_1 in most scenarios can take any value (for some combination of the other phases). Moreover, the d_e constraint enforces a tight correlation between ϕ_μ and ϕ_1, see Fig. 2.

In Fig. 11 we compare high– and low–energy quantities. We see that the phase–sensitive high–energy quantities are *not* correlated at all with d_e. This is true both for T–even variables (Fig. 11a) and T–odd ones (b); in scenarios with strong gaugino–Higgsino mixing (a) and in scenarios where this mixing is suppressed (b); and for quantities that depend on both ϕ_1 and ϕ_μ (a) as well as those that depend only on ϕ_μ (b). This can be explained from the observation made at the end of Sec. 4.3 that d_e itself is not correlated with any of the phases after scanning over the other two phases; recall that the low–energy observables also depend on ϕ_A. For example, except at the very edges of the allowed range of ϕ_μ, d_e can still take any value within its experimentally allowed range even after ϕ_μ is fixed; this is due to the variation of ϕ_1 and ϕ_A.

On the other hand, in some cases we do observe significant correlations between high–energy observables and a_μ. We saw in Fig. 5 that in scenarios B2 and B3 a_μ shows a $\cos -$like dependence on ϕ_1; in some cases (e.g. B2 at small $\tan\beta$) two separate bands of a_μ values exist, corresponding to $\cos\phi_\mu \simeq \pm 1$. However, in scenario B1 a_μ shows very little correlation with ϕ_1, see Fig. 5a,d. Correspondingly, Fig. 11c shows no correlation for scenario B1, while Figs. 11d–f show significant correlations for scenario B2. Comparison of panels d and e shows that this correlation becomes stronger at larger $\tan\beta$. This is due to the diminished role of ϕ_A and the reduced width of the allowed band in the (ϕ_μ, ϕ_1) plane; the overall size of $|a_\mu|$ also increases with increasing $\tan\beta$, see eq.(4.15). Finally, Fig. 11f shows that high–energy quantities whose only phase sensitivity is through ϕ_μ also correlate with a_μ. Note in particular that $\mathcal{S}(\tilde{\chi}_1^+\tilde{\chi}_2^-)$ is much bigger for $a_\mu < 0$, which corresponds to $\phi_\mu \simeq \pi$, than for $a_\mu > 0$, which corresponds to $|\phi_\mu| \ll 1$. This confirms the explanation we gave in the discussion of Table 4 for the very strong $\tan\beta$ dependence of this quantity. For this class of observables the correlation with a_μ

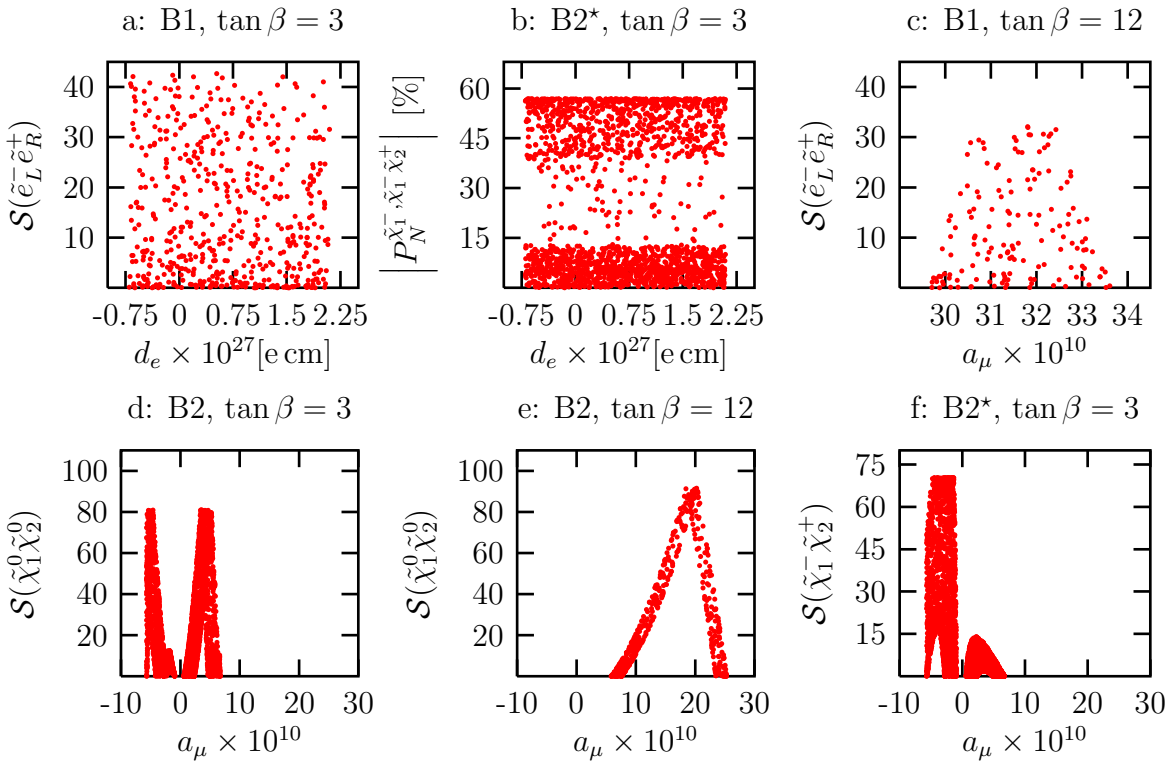

Figure 11: Correlations between low– and high–energy quantities. Most high–energy observables have been computed at $\sqrt{s} = 500$ GeV, except for panels b) and f), which are for $\sqrt{s} = 800$ GeV. The parameter sets B1 and B2 have been defined in Table 1, and the significance $\mathcal{S}$ is defined via eq.(6.2).

also becomes stronger with increasing $\tan\beta$; however, as remarked in Sec. 5.7, the sensitivity to ϕ_μ disappears $\propto \sin 2\beta$ at least.

In most cases different phase sensitive high–energy observables are strongly correlated with each other. This is illustrated by Fig. 12, where we plot the two usually most promising significances, for the $\tilde{e}_L^- \tilde{e}_L^-$ and $\tilde{\chi}_1^0 \tilde{\chi}_2^0$ final states, against each other. The simplest correlation obtains for scenario B3 for $\tan\beta = 20$, shown in panel f. In this case the a_μ constraint excludes values of ϕ_1 near 0 as well as ϕ_μ near π, see Fig. 2f. Hence the minimization in the definition (6.2) of $\mathcal{S}$ only goes over the single CPC point $\phi_\mu = 0$, $\phi_1 = \pi$. The strong correlation observed in Fig. 12f then follows from the fact that both significances shown here are essentially $\propto \cos\phi_1$ to leading order in M_Z, as explained in Sec. 5.7.

The next simplest situation obtains if both $\phi_1 = 0$ and $\phi_1 = \pi$ are allowed, but $\phi_\mu = \pi$ is still forbidden, and $\tan\beta$ is not small [panels c), d) and e)]. Now the minimization in eq.(6.2) goes over two CPC points. Recall that this minimization is performed *independently* for the two significances shown in Fig. 12. The upper (lower) branch connected to the origin is populated by combinations of phases where both minimizations pick the CPC point $\phi_1 = 0$ ($\phi_1 = \pi$). These two bands are connected by sets of points where our algorithm picks the CPC point

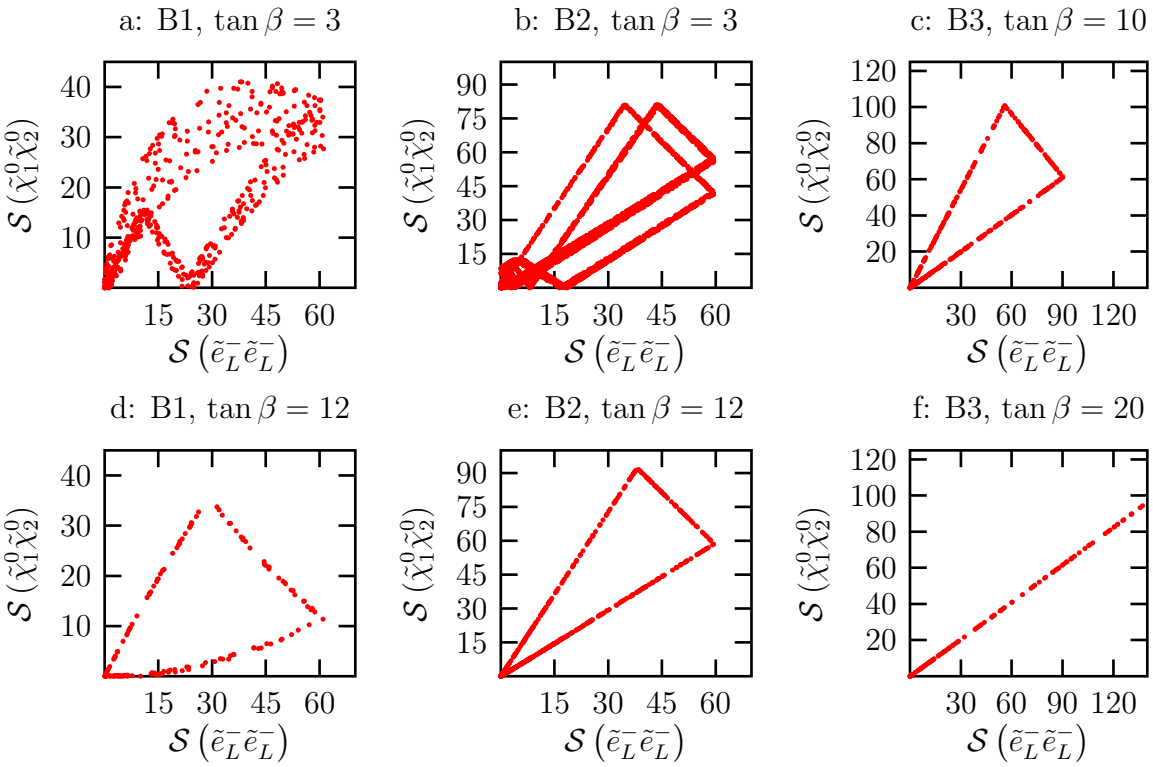

Figure 12: Correlations between the significances, defined as in eq.(6.2), for the processes $e^-e^- \to \tilde{e}_L^-\tilde{e}_L^-$ and $e^+e^- \to \tilde{\chi}_1^0\tilde{\chi}_2^0$, both taken at $\sqrt{s} = 500$ GeV.

$\phi_1 = 0$ for $\mathcal{S}(\tilde{e}_L^-\tilde{e}_L^-)$, but chooses the point $\phi_1 = \pi$ for $\mathcal{S}(\tilde{\chi}_1^0\tilde{\chi}_2^0)$.

Fig. 12a shows that in scenario B1 the correlations get weaker at smaller $\tan\beta$. To understand this, recall that scenario B1 has strong wino–Higgsino mixing, and hence a relatively strong dependence on ϕ_μ through the combination $\cos(\phi_1 + \phi_\mu)$, which depends linearly on ϕ_μ when $|\phi_1|$ and $|\phi_1 - \pi|$ are sizable. In contrast, $\cos\phi_\mu$ depends only quadratically on ϕ_μ for small $|\phi_\mu|$, and can therefore to good approximation be set to 1 in scenario B1, see Fig. 2a,d. This dependence on ϕ_μ will be numerically different for the two modes present, loosening the correlation. This effect is important only at small $\tan\beta$ for two reasons. First, all contributions to our cross sections that are sensitive to ϕ_μ are suppressed by a factor $\sin 2\beta$ at large $\tan\beta$. Secondly, we saw that in scenario B1 the upper bound on $|\phi_\mu|$ decreases with $\tan\beta$.

Fig.12a shows another new effect on the lower branch, where both significances are evaluated with the CPC point $\phi_1 = \pi$, $\phi_\mu = 0$. The cross section for $\tilde{\chi}_1^0\tilde{\chi}_2^0$ production in this case shows a non–monotonous dependence on $\cos\phi_1$. As expected from the expansion of the result (5.26) in powers of M_Z using eqs.(2.17)–(2.19), this cross section reaches its absolute minimum at $\cos\phi_1 = +1$, where the $S-$wave contribution vanishes. However, $\cos\phi_1 = -1$ is also a (local) minimum, the maximum being reached at $\cos\phi_1 \simeq -0.8$; recall that the expansion in powers of M_Z is not reliable in this case, since $M_2 = |\mu|$. As a result of this non–monotonous behavior, the cross section at $\cos\phi_1 \simeq -0.6$ becomes identical to that at $\cos\phi_1 = -1$. Since $\sigma(\tilde{e}_L^-\tilde{e}_L^-)$

does decrease monotonically with $\cos\phi_1$, values of $\cos\phi_1 \simeq -0.6$ give rise to scenarios with very small $\mathcal{S}(\tilde{\chi}_1^0\tilde{\chi}_2^0)$ but sizable $\mathcal{S}(\tilde{e}_L^-\tilde{e}_L^-)$.

The comparison of Figs. 12b and e shows that the correlation becomes weaker for smaller $\tan\beta$ also in scenario B2. This is partly because the width of the allowed band in the (ϕ_μ, ϕ_1) plane decreases with increasing $\tan\beta$, see Fig. 2. In addition, in scenario B2 with $\tan\beta = 3$ the low–energy constraints also allow values of ϕ_μ near π. One can then find values of ϕ_1 not far from π where $\sigma(\tilde{\chi}_1^0\tilde{\chi}_2^0)$ for CPV points with $|\phi_\mu| \ll 1$ is very close to this cross section at the CPC point $\phi_\mu = \phi_1 = \pi$. This again leads to scenarios where $\mathcal{S}(\tilde{\chi}_1^0\tilde{\chi}_2^0)$ is very small, but $\mathcal{S}(\tilde{e}_L^-\tilde{e}_L^-)$ is sizable. The existence of four different allowed CPC points also explains the occurrence of additional bands in Fig. 12b.

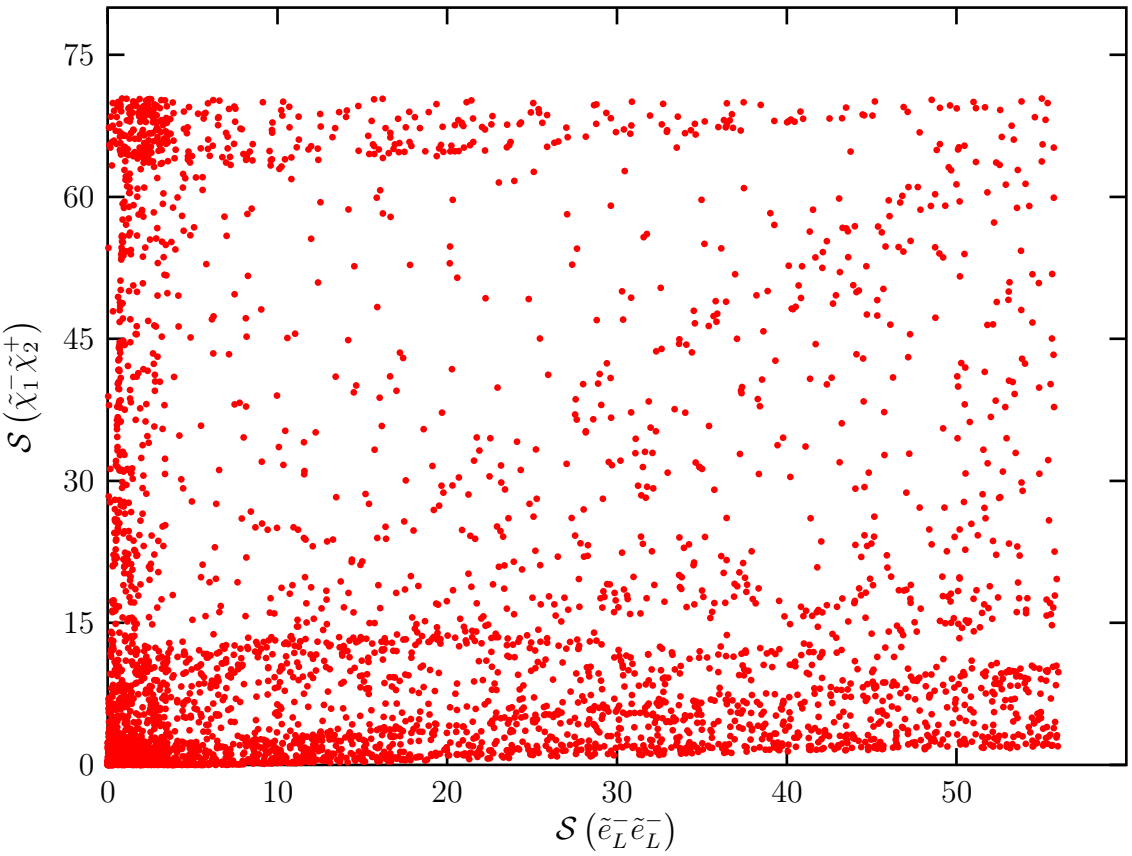

Figure 13: Correlation between the significances for the processes $e^-e^- \to \tilde{e}_L^-\tilde{e}_L^-$ and $e^+e^- \to \tilde{\chi}_1^-\tilde{\chi}_2^+$, both taken at $\sqrt{s} = 800$ GeV, for scenario B2 with $\tan\beta = 3$.

In some cases the correlations between different significances are quite weak. The most extreme case we found is shown in Fig. 13, and occurs for scenario B2 at $\tan\beta = 3$. We saw in Table 4 that here (and only here) $\sigma(\tilde{\chi}_1^-\tilde{\chi}_2^+)$ allows a significant probe of the phase ϕ_μ, whereas $\mathcal{S}(\tilde{e}_L^-\tilde{e}_L^-)$ is always mostly determined by ϕ_1. Moreover, Fig. 2b shows that in the allowed band with $\phi_\mu \simeq \pi$, the deviation $|\phi_\mu - \pi|$ becomes maximal for ϕ_1 quite close to $\pm\pi$. This leads to

scenarios with large $\mathcal{S}(\tilde{\chi}_1^- \tilde{\chi}_2^+)$, but very small $\mathcal{S}(\tilde{e}_L^- \tilde{e}_L^-)$. Conversely, $\big||\cos\phi_1| - 1\big|$ can be quite large for small $|\phi_\mu|$, leading to scenarios with $\mathcal{S}(\tilde{e}_L^- \tilde{e}_L^-) \gg \mathcal{S}(\tilde{\chi}_1^- \tilde{\chi}_2^+)$, although the latter cannot be strictly zero if the former is bigger than 10. However, we saw earlier that other combinations of parameters do not allow meaningful probes of ϕ_μ using high–energy quantities. We therefore conclude that in most cases, significances that can be large are also fairly strongly correlated.

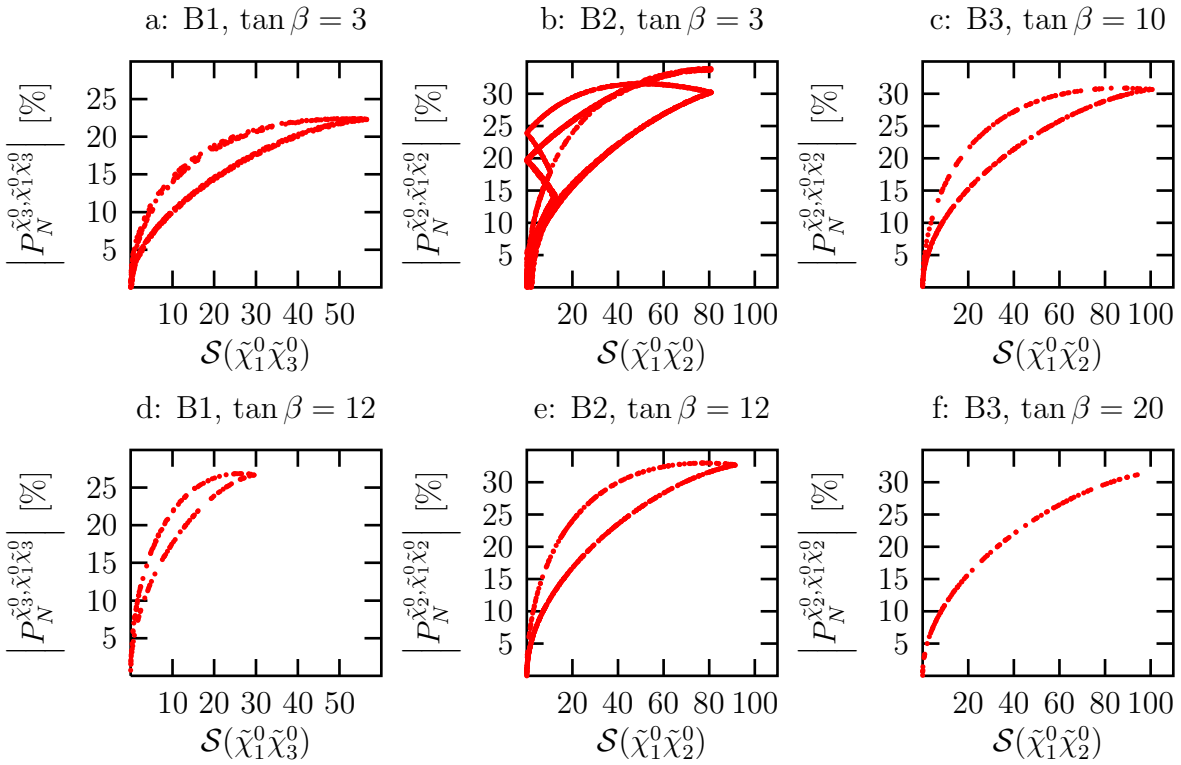

Figure 14: Correlation between the significance $\mathcal{S}$ and the absolute value of normal polarization P_N, measured at scattering angle $\theta = \pi/2$, for mixed neutralino pair production at $\sqrt{s} = 500$ GeV. We consider $\tilde{\chi}_1^0 \tilde{\chi}_2^0$ production for scenarios B2 and B3, but switch to the $\tilde{\chi}_1^0 \tilde{\chi}_3^0$ final state for scenario B1.

Finally, in Fig. 14 we compare the normal component of the polarization vector of the heavier neutralino in mixed neutralino pair production with the significance of the same mode. We consider $\tilde{\chi}_1^0 \tilde{\chi}_2^0$ production in scenarios B2 and B3, but switch to $\tilde{\chi}_1^0 \tilde{\chi}_3^0$ production in scenario B1, where this final state is far more promising, see Tables 4 and 5. These figures look somewhat simpler than those in Fig. 12, since now the existence of two allowed CPC points only leads to two bands, as compared to three in Fig. 12. Of course, scenarios with a single allowed CPC point (Fig. 14f) again only yield a single band. In panel b) we again find scenarios with sizable phases, hence sizable $|P_N^{\tilde{\chi}_2^0, \tilde{\chi}_1^0 \tilde{\chi}_2^0}|$, and yet vanishing $\mathcal{S}(\tilde{\chi}_1^0 \tilde{\chi}_2^0)$; we saw analogous behavior in Fig. 12b.

More importantly, Fig. 14 shows that the polarization $|P_N|$ increases much more quickly as the (relevant) phase ϕ_1 is moved away from 0 or π than the significance $\mathcal{S}$ does. The reason is

that $|P_N|$, being T–odd, has a sin–like dependence on ϕ_1, i.e. grows linearly with $|\phi_1|$ or $|\phi_1 - \pi|$. In contrast, the T– and CP–even quantity $\mathcal{S}$ has cos–like dependence on all phases, and thus only grows $\propto |\phi_1|^2$ or $|\phi_1 - \pi|^2$ as ϕ_1 is moved away from a CPC point. T–odd observables like P_N are therefore in principle better suited to probe small phases.

8 Summary and Conclusions

In this article we have discussed to what extent the phases of dimensionful parameters in the SUSY Lagrangian can be determined from leptonic observables. Since we assumed universal soft breaking parameters for the first two generations of sleptons and did not discuss processes involving third generation (s)particles, we only have to deal with three phases: those of the Higgsino mass parameter μ, of the $U(1)_Y$ gaugino mass M_1, and of the leptonic trilinear soft breaking parameter A_l, in all cases measured relative to M_2 which we took to be real and positive by convention.

Our main focus was on quantities that can be measured at future high–energy e^+e^- and e^-e^- colliders, but we first analyzed the constraints that follow from the present measurements of the leptonic dipole moments d_e and a_μ. We worked in a scenario with moderately heavy sparticles; as well known, in this case sizable CP–odd phases are possible only if neutralino and chargino loop contributions to d_e cancel to good approximation. In agreement with earlier work [10, 11], we found that, unless $|\mu| \gg M_2$, $m_{\tilde{l}}$, the phases of M_1 and A_l can take any value (for some combination of the other phases), whereas the phase of μ is tightly constrained, the maximal allowed deviation from 0 or π scaling like $|\mu|^2$. Our analysis of Sec. 4 also gave the perhaps surprising result that in this case improved measurements of d_e will not significantly reduce the allowed range for any one of the three relevant phases after scanning over the other two. This is true independently of whether this measurement leads to improved upper bounds on $|d_e|$ or finds a non–vanishing result. On the other hand, improved measurements of a_μ do have the potential to further restrict the allowed ranges of these phases; however, here improved measurements have to be combined with improved SM predictions for the hadronic contributions to a_μ.

Turning to high–energy observables, we first analyzed in detail the phase sensitivity of total cross sections of various final states. To that end we introduced "significances" that determine the statistical significance with which the presence of non–trivial phases could be determined in a given production channel. As pointed out in ref. [38], the cross section for $\tilde{e}_L^-\tilde{e}_L^-$ production depends very strongly on the relative phase between M_1 and M_2; we found that a deviation of ~ 60 to 90 standard deviations from the predictions of the CP–conserving MSSM is possible in this channel. However, this does not necessarily argue in favor of constructing an e^-e^- collider, since certain neutralino production channels – in particular, $\tilde{\chi}_1^0\tilde{\chi}_2^0$ production for $|\mu| > M_2$ – have comparable or better sensitivity to the same phase. We also found a somewhat lower, but still promising, sensitivity in the $\tilde{e}_L^-\tilde{e}_R^+$ final state. For our choice $m_{\tilde{l}} \sim 200$ GeV, chargino pair production can show significant phase dependence over the experimentally allowed parameter space only for $|\mu| \geq 2M_2$. Since the d_e–constraint on ϕ_μ becomes weaker for larger slepton

masses, the minimal ratio $|\mu|/M_2$ where chargino production channels can become useful for probing CP–violating phases should be smaller for larger $m_{\tilde{l}}$. However, these chargino modes will be useful only if $\tan\beta$ is quite small, since the relevant significances scale like $\sin 2\beta$.

A deviation of any of these cross sections from the prediction of the CP–conserving MSSM could perhaps also be explained by some extension of the model which does not introduce new CP–odd phases. We therefore also studied a CP–odd quantity: the component of the polarization of produced charginos and neutralinos that is normal to the production plane. We found that it can reach values exceeding 30% for the production of two different neutralinos; in scenarios with large $|\mu|$ and small $\tan\beta$ the polarization vector of the lighter chargino, produced in association with the heavier one, could have an even larger normal component. Recent studies [47, 48, 49] indicate that such large CP–odd polarizations might indeed lead to measurable CP–odd asymmetries in the phase space distribution of the $\tilde{\chi}$ decay products.

Finally, we studied correlations between the various phase–sensitive observables. We found that the high–energy observables are essentially not correlated at all with d_e. This is due to the required rather precise cancellation between different contributions to d_e; it implies that better measurements of d_e will not further restrict the possible ranges of phase–sensitive high–energy quantities. However, there is some correlation between these high–energy observables and a_μ. Moreover, most pairs of high–energy observables are quite strongly correlated with each other. This follows from the fact that most of them basically probe the phase of M_1, given the tight constraint on the phase of μ. Within the CP–violating MSSM the measurement of one phase sensitive high–energy observable therefore allows to greatly constrain the allowed range of other such quantities, thereby allowing stringent tests of the model. However, at large $|\mu|$ and small $\tan\beta$ the phase of μ can play an important role, in particular in chargino production. In that case phase–sensitive observables in the chargino sector correlate poorly with those in the selectron or neutralino sector. This underscores the importance of measuring as many phase–sensitive quantities as possible.

Total cross sections and CP–odd asymmetries offer complementary access to CP–odd phases, since they depend on these phases through cosine–like and sine–like functions, respectively. The former are rather insensitive to these phases if they are small (the perhaps most likely case). Measurements of, or bounds on, CP–odd asymmetries should then lead to better determinations or constraints on these phases. On the other hand, if some phase is near $\pi/2$, CP–odd asymmetries will be near maximal, which means that they are not well suited to precisely pinning down the value of this phase; precision measurements of some cross sections will then have the edge. Of course, there is also complementarity between high– and low–energy observables, since only the latter are sensitive to the phase of A_l.

We conclude that measurements at high energy colliders will be necessary to pin down the phases of dimensionful parameters in the SUSY Lagrangian. Both precision measurements of CP–even quantities like masses and cross sections, and searches for CP–violating asymmetries, are promising in certain regions of parameter space. Linear e^+e^- colliders seem to be ideally suited for performing these measurements.

Acknowledgments

The work of MD and BG was supported in part by the Deutsche Forschungsgemeinschaft, project number DR 263 as well via SFB 375. They would like to thank the KIAS school of physics and its members for hospitality. SYC was supported in part by the Korea Research Foundation (KRF-2002-070-C00022) and in part by KOSEF through CHEP at Kyungpook National University.

Appendix A Kinematics

Working in the CMS frame with total energy $\sqrt{s}$ and neglecting the electron mass, the first electron and positron (second electron) momenta can be written as

$$p_1^\mu = \frac{\sqrt{s}}{2}\,(1,0,0,1)\,; \tag{A.1a}$$

$$p_2^\mu = \frac{\sqrt{s}}{2}\,(1,0,0,-1)\,. \tag{A.1b}$$

The outgoing momenta of the produced superparticles b and c are:

$$k_1^\mu = \frac{\sqrt{s}}{2}\left(1+\frac{m_b^2-m_c^2}{s}, \lambda_{bc}^{\frac{1}{2}}\sin\theta, 0, \lambda_{bc}^{\frac{1}{2}}\cos\theta\right), \tag{A.2a}$$

$$k_2^\mu = \frac{\sqrt{s}}{2}\left(1-\frac{m_b^2-m_c^2}{s}, -\lambda_{bc}^{\frac{1}{2}}\sin\theta, 0, -\lambda_{bc}^{\frac{1}{2}}\cos\theta\right), \tag{A.2b}$$

where λ_{bc} denotes the usual two–body final state kinematical function:

$$\lambda_{bc} = \lambda\left(1, \frac{m_b^2}{s}, \frac{m_c^2}{s}\right); \tag{A.3a}$$

$$\lambda(1,x,y) = 1 + x^2 + y^2 - 2(x + y + xy). \tag{A.3b}$$

Furthermore the kinematical invariants (Mandelstam variables) are

$$s = (p_1 + p_2)^2; \tag{A.4a}$$

$$t = (p_1 - k_1)^2; \tag{A.4b}$$

$$u = (p_1 - k_2)^2. \tag{A.4c}$$

Appendix B Helicity amplitudes

We calculate the relevant helicity amplitudes using the formalism introduced in [50][†]. Using our definition of the kinematical situation, we find the following results for the scalar and vectorial

[†]Our convention for a momentum–dependent Weyl spinor for fermions going in the $-z$ direction differs by an overall sign from that of [50].

fermionic string associated with massless fermions:

$$\bar{v}(p_2,\sigma_2)P_\alpha u(p_1,\sigma_1) = -\alpha\sqrt{s}\delta_{\alpha\sigma_1}\delta_{\sigma_1\sigma_2}, \tag{B.1a}$$

$$\bar{v}(p_2,\sigma_2)\gamma^\mu P_\alpha u(p_1,\sigma_1) = \sqrt{s}\delta_{\alpha\sigma_1}\delta_{\sigma_2,-\sigma_1}(0,1,i\sigma_1,0), \tag{B.1b}$$

where the four choices in eq.(B.1b) correspond to $\mu = 0,\ 1,\ 2,\ 3$. In the case of neutralinos or charginos with non–negligible masses only the vectorial string is required. It can be written as

$$\begin{aligned}\bar{u}_i(k_1,\lambda_1)\gamma^\mu P_\beta v_j(k_2,\lambda_2) = \frac{\sqrt{s}}{2}\Big[&\sqrt{1-\eta^2_{\beta\lambda_1}}\,\delta_{\lambda_1\lambda_2}(\beta,\lambda_1\sin\theta,0,\lambda_1\cos\theta) \\ &+ \sqrt{(1+\beta\lambda_1\eta_{\beta\lambda_1})(1+\beta\lambda_1\eta_{-\beta\lambda_1})}\,\delta_{\lambda_1,-\lambda_2}(0,\cos\theta,-i\lambda_1,-\sin\theta)\Big],\end{aligned} \tag{B.2}$$

where

$$\eta_{\beta\lambda_1} = \lambda_{ij}^{\frac{1}{2}} + \beta\lambda_1\Delta_{ij}, \tag{B.3}$$

and

$$\Delta_{ij} = \frac{m_i^2 - m_j^2}{s}. \tag{B.4}$$

Appendix C Neutralino functions

After introducing two effective neutralino mixing coefficients

$$V_L^j = \frac{N_{1j}}{2\cos\theta_{\rm W}} + \frac{N_{2j}}{2\sin\theta_{\rm W}}, \tag{C.1a}$$

$$V_R^j = \frac{N_{1j}}{\cos\theta_{\rm W}}, \tag{C.1b}$$

we define two dimensionless neutralino functions for t- or u-channel exchanges:

$$M_{\alpha\beta}(s,t/u) = \sum_{k=1}^{4} m_{\tilde{\chi}_k^0}\sqrt{s}V_\alpha^k V_\beta^k D_{t,u}^k, \tag{C.2a}$$

$$N_{\alpha\beta}(s,t/u) = \sum_{k=1}^{4} sV_\alpha^k V_\beta^{k\star} D_{t,u}^k, \tag{C.2b}$$

the propagators D_t^k and D_u^k have been defined in eq.(5.6). Very similar neutralino functions were introduced in [37]; we saw in Sec. 5 that they allow to give very compact expressions for the slepton production amplitudes.

References

[1] J.H. Christenson, J.W. Cronin, V.L. Fitch and R. Turlay, Phys. Rev. Lett. **13**, 138 (1964).

[2] BELLE Collab., A. Abashian et al., Phys. Rev. Lett. **86**, 2509 (2001), hep–ex/0102018; BABAR Collab., B. Aubert et al., Phys. Rev. Lett. **86**, 2515 (2001), hep–ex/0102030.

[3] A.D. Sakharov, Zh. Eksp. Teor. Fiz. Pis'ma **5**, 32 (1967), JETP Lett. **91B**, 24 (1967).

[4] M. Kobayashi and T. Maskawa, Prog. Theor. Phys. **49**, 652 (1973).

[5] For a recent review, see e.g. S. Pakvasa and J.W.F. Valle, hep–ph/0301061.

[6] E. Witten, Nucl. Phys. **B188**, 513 (1981).

[7] C. Giunti, C.W. Kim and U.W. Lee, Mod. Phys. Lett. **A6**, 1745 (1991); U. Amaldi, W. de Boer and H. Fürstenau, Phys. Lett. **B260**, 447 (1991); P. Langacker and M. Luo, Phys. Rev. D **44**, 817 (1991); J. Ellis, S. Kelley and D.V. Nanopoulos, Phys. Lett. **B260**, 131 (1991).

[8] S. Dimopoulos and D. Sutter, Nucl. Phys. **B452** (1995) 496; H. Haber, Proceedings of the 5th International Conference on Supersymmetries in Physics (SUSY'97), May 1997, ed. M. Cvetić and P. Langacker, hep-ph/9709450.

[9] W. Hollik, J.I. Illana, S. Rigolin, C. Schappacher and D. Stockinger, Nucl. Phys. **B439**, 3 (1999); S. Pokorski, J. Rosiek and C.A. Savoy, Nucl. Phys. **B570**, 81 (2000), hep–ph/9906206; E. Accomando, R. Arnowitt, and B. Dutta, Phys. Rev. **D61**, 115003 (2000), hep–ph/9907446.

[10] T. Ibrahim and P. Nath, Phys. Lett. **B418**, 98 (1998); Phys. Rev. **D57**, 478 (1998); **D58**, 019901 (1998) (E); *ibid*, 111301 (1998); *ibid.* **D61**, 095008 (2000), hep–ph/9907555.

[11] M. Brhlik, G.J. Good and G.L. Kane, Phys. Rev. **D59**, 115004 (1999), hep–ph/9810457.

[12] A. Bartl, T. Gajdosik, W. Porod, P. Stockinger and H. Stremnitzer, Phys. Rev. **D60**, 073003 (1999), hep–ph/9903402.

[13] T. Falk and K.A. Olive, Phys. Lett. **B439**, 71 (1998), hep–ph/9806236.

[14] ECFA/DESY LC Physics Working Group, J.A. Aguilar-Saavedra et al., hep–ph/0106315; American Linear Collider Working Group, T. Abe et al., hep–ex/0106056; ACFA Linear Collider Working Group, K. Abe et al., hep–ph/0109166; J.L. Feng and M.M. Nojiri, hep–ph/0210390.

[15] T. Tsukamoto, K. Fujii, H. Murayama, M. Yamaguchi and Y. Okada, Phys. Rev. **D51**, 3153 (1995); J.L. Feng, M.E. Peskin, H. Murayama and X. Tata, Phys. Rev. **D52**, 1418 (1995), hep–ph/9502260.

[16] V. Barger, T. Han, T. Li and T. Plehn, Phys. Lett. **B475**, 342 (2000), hep–ph/9907425.

[17] V. Barger, T. Falk, T. Han, J. Jiang, T. Li and T. Plehn, Phys. Rev. **D64**, 056007 (2001), hep–ph/0101106.

[18] H.E. Haber and G.L. Kane, Phys. Rep. **117**, 75 (1985).

[19] S.Y. Choi, A. Djouadi, M. Guchait, J. Kalinowski, H.S. Song and P. M. Zerwas, Eur. Phys. J. **C14**, 535 (2000), hep–ph/0002033.

[20] S.Y. Choi, J. Kalinowski, G. Moortgat-Pick and P. M. Zerwas, Eur. Phys. J. **C22**, 563 (2001), Addendum-ibid. **C23**, 769 (2002), hep–ph/0108117.

[21] S. Abel, S. Khalil and O. Lebedev, Nucl. Phys. **B606**, 151 (2001), hep–ph/0103320.

[22] K. Hagiwara *et al.*, Particle Data Group, Phys. Rev. **D66**, 010001 (2002).

[23] M. Graesser and S. Thomas, Phys. Rev. **D65**, 075012 (2002), hep–ph/0104254.

[24] G.W. Bennett *et al.*, Muon $g-2$ Collab., Phys. Rev. Lett. **89**, 101804 (2002), Erratum-ibid. **89**, 129903 (2002), hep–ex/0208001; hep–ex/0401008.

[25] M. Davier, S. Eidelman, A. Höcker and Z. Zhang, Eur. Phys. J. **C27**, 497 (2003), hep–ph/0208177.

[26] M. Hayakawa and T. Kinoshita, Phys. Rev. **D57**, 465 (1998), Erratum-ibid. **D66**, 019902 (2002), hep–ph/9708227 and hep–ph/0112102.

[27] CDM–2 collab., R. Akhmetshin et al, Phys. Lett. **B578**, 285 (2004), hep–ex/0308008.

[28] M. Davier, S. Eidelman, A. Höcker and Z. Zhang, hep–ph/0308213; see also the similar analyses in K. Hagiwara, A.D. Martin, D. Nomura and T. Teubner, hep–ph/0312250; J. F. de Troconiz and F.J. Yndurain. hep–ph/0402285.

[29] S.P. Martin and J.D. Wells, Phys. Rev. **D64**, 035003 (2001), hep–ph/0103067.

[30] J.R. Ellis, S. Ferrara and D.V. Nanopoulos, Phys. Lett. **B114**, 231 (1982); F. del Aguila, M.B. Gavela, J.A. Grifols and A. Mendez, Phys. Lett. **B126**, 71 (1983), Erratum-ibid. **B129**, 473 (1983).

[31] S.T. Petcov, Phys. Lett. **B178**, 57 (1986).

[32] Y. Kizukuri and N. Oshimo, Phys. Rev. **D46**, 3025 (1992); P. Nath, Phys. Rev. Lett. **66**, 2565 (1991).

[33] M. Drees and S.P. Martin, in Barklow, T.L. (ed.) et al.: *Electroweak symmetry breaking and new physics at the TeV scale*, hep–ph/9504324; S.P. Martin, in Kane, G.L. (ed.): *Perspectives on supersymmetry*, hep–ph/9709356.

[34] B.C. Allanach *et al.*, Eur. Phys. J. **C25**, 113 (2002), hep–ph/0202233.

[35] G.R. Farrar and P. Fayet, Phys. Lett. **B89**, 191 (1980); M. Glück and E. Reya, Phys. Lett. **B130**, 423 (1983); A. Bartl, H. Fraas and W. Majerotto, Z. Phys. **C34**, 411 (1987).

[36] X. Tata and D.A. Dicus, Phys. Rev. **D35**, 2110 (1987); H. Baer, A. Bartl, D. Karatas and W. Majerotto, Int. J. Mod. Phys. **A4**, 4111 (1989).

[37] M.E. Peskin, Int. J. Mod. Phys. **A13**, 2299 (1998), hep–ph/9803279; J.L. Feng and M.E. Peskin, Phys. Rev. **D64**, 115002 (2001), hep–ph/0105100.

[38] S. Thomas, Int. J. Mod. Phys. **A13**, 2307 (1998), hep–ph/9803420.

[39] C. Blochinger, H. Fraas, G. Moortgat-Pick and W. Porod, Eur. Phys. J. **C24**, 297 (2002), hep–ph/0201282.

[40] J.R. Ellis, J.M. Frère, J.S. Hagelin, G.L. Kane and S.T. Petcov, Phys. Lett. **B132**, 436 (1983); V. Barger, R.W. Robinett, W.Y. Keung and R.J.N. Phillips, Phys. Lett. **B131**, 372 (1983); A. Bartl, H. Fraas and W. Majerotto, Nucl. Phys. **B278**, 1 (1986), and Z. Phys. **C30**, 441 (1986); A. Bartl, H. Fraas, W. Majerotto and B. Mösslacher, Z. Phys. **C55**, 257 (1992)

[41] S.Y. Choi, A. Djouadi, M. Guchait, J. Kalinowski, H.S. Song and P.M. Zerwas, Eur. Phys. J. **C14**, 535 (2000), hep–ph/0002033; S.Y. Choi, M. Guchait, J. Kalinowski and P.M. Zerwas, Phys. Lett. **B479**, 235 (2000), hep–ph/0001175.

[42] S.Y. Choi, A. Djouadi, H.K. Dreiner, J. Kalinowski and P.M. Zerwas, Eur. Phys. J. **C7**, 123 (1999), hep–ph/9806279.

[43] J.L. Kneur and G. Moultaka, Phys. Rev. **D61**, 095003 (2000), hep–ph/9907360.

[44] M.A. Diaz, S.F. King and D.A. Ross, Nucl. Phys. **B529**, 23 (1998), hep–ph/9711307, and Phys. Rev. **D64**, 017701 (2001), hep–ph/0008117.

[45] P. Chankowski, Phys. Rev. **D41**, 2877 (1990); H.–C. Cheng, J.L. Feng and N. Polonsky, Phys. Rev. **D56**, 6875 (1997), hep–ph/9706438, and ibid. **D57**, 152 (1998), hep–ph/9706467; M.M. Nojiri, D.M. Pierce and Y. Yamada, Phys. Rev. **D57**, 1539 (1998), hep–ph/9707244; S. Kiyoura, M.M. Nojiri, D.M. Pierce and Y. Yamada, Phys. Rev. **D58**, 075002 (1998), hep–ph/9803210.

[46] G.F. Giudice, and A. Pomarol, Phys. Lett. **B372**, 253 (1996), hep–ph/9512337; M. Drees, M.M. Nojiri, D.P. Roy and Y. Yamada, Phys. Rev. **D56**, 276 (1997), Erratum-ibid. **D64**, 039901 (2001), hep–ph/9701219.

[47] A. Bartl, H. Fraas, O. Kittel and W. Majerotto, hep–ph/0308141.

[48] A. Bartl, T. Kernreiter and O. Kittel, Phys. Lett. **B578**, 341 (2004), hep–ph/0309340; S.Y Choi, M. Drees, B. Gaissmaier and J. Song. hep–ph/0310284.

[49] A. Bartl, H. Fraas, O. Kittel, W. Majerotto, hep–ph/0402016.

[50] K. Hagiwara and D. Zeppenfeld, Nucl. Phys. **B274**, 1 (1986).